A STUDY OF SURFACE MODIFICATION EFFECT OF HEMP FIBERS ON THE BULK PROPERTIES OF HEMP-POLY (LACTIC ACID) COMPOSITES: THERMAL STABILITY, MECHANICAL, THERMO-MECHANICAL AND BIODEGRADABILITY

by

Shubhashini Oza

A dissertation submitted to the faculty of
The University of North Carolina at Charlotte
in partial fulfillment of the requirements
for the degree of Doctor of Philosophy in
Infrastructure and Environmental Systems

Charlotte

2013

Approved by:

_____
Dr. Na Lu

_____
Dr. Helene Hilger

_____
Dr. Miguel Pando

_____
Dr. Brett Tempest

_____
Dr. Ian Ferguson

ABSTRACT

SHUBHASHINI OZA. A study of surface modification effect of hemp fibers on the bulk properties of poly (lactic acid) composite: thermal stability, mechanical, thermo-mechanical, and biodegradability (Under the direction of DR. NA (LUNA) LU)

Biocomposites made with, natural fiber and bio-based polymers, have many advantages over their synthetic counterparts including low cost, low density, high strength and biodegradability. However, some biocomposites can present problems due to high moisture absorption, low thermal stability during processing, and poor adhesion between the fiber and polymer matrix. Recent studies have shown that surface modification of the fiber can improve its adhesion to the polymer matrix and enhance the bulk material properties. Nevertheless, the mechanisms by which such surface modifications exert their effects on bulk material properties have not been systematically studied. Therefore, the main goal of this study is to investigate the impact of surface modifications of hemp on the thermal stability, mechanical, thermo-mechanical, and biodegradability of biocomposites comprised of hemp and poly (lactic acid) (PLA). This pairing was selected because it offers superior mechanical properties. The three surface treatments tested were: alkali (mechanical interlocking), silane (coupling) and acetic anhydride (grafting). The latter was most effective at improving thermal stability, mechanical, and thermo-mechanical properties of hemp-PLA biocomposites, and all treatments improved these properties relative to untreated hemp-PLA controls. The thermal stability of the composites increased with an increase in fiber content up to 30% by fiber volume fraction for both silane and acetic anhydride modified hemp. However, thermal stability decreased with fiber content for alkali and untreated composites due to

hydrogen bonding and inferior fiber-matrix adhesion, respectively. The activation energy of thermal degradation was assessed by applying Flynn-Wall-Osawa kinetic modeling to understand the fiber-matrix interface. The model predictions were consistent with experimental results and suggested that the mechanism by which, acetic anhydride treatment yielded superior thermal properties was related to high energy bond formation (C=O) between the fiber and polymer matrix. When tensile and flexural properties of composites were assessed, 30% fiber volume fraction was optimal, and this ratio also improved stiffness and damping properties of the composites during thermo-mechanical study. A biodegradability study of the treated and untreated hemp-PLA biocomposites was undertaken. ASTM standard 5511-11 was modified to stimulate landfill disposal conditions. Degradation of all treatments as well as untreated biocomposites was negligible over 50 d, although visual inspection of SEM images showed greater evidence of cracking in the composite samples than in pure PLA controls.

From this study it can be concluded that higher bond energy at the fiber-matrix interface due to surface modification of natural fiber results in higher activation energy of thermal degradation resulting in enhanced bulk material properties of the biocomposites.

ACKNOWLEDGMENTS

The investigation of the truth is in one way hard, in another easy. An indication of this is found in the fact that no one is able to attain the truth adequately, while, on the other hand, no one fails entirely, but everyone says something true about the nature of all things, and while individually they contribute little or nothing to the truth, by the union of all a considerable amount is amassed – ***Aristotle***

Foremost, I would like to thank my advisor, Dr. Na (Luna) Lu for giving me the opportunity of being part of her research group. She has been encouragingly supportive throughout my entire time at UNCC with her guidance and keen-foresight.

I am indebted to Dr. Helene Hilger for being the Co-Chair, a mentor, a guide, and a friend throughout these past four years. I would not have started my doctoral studies without her support and guidance.

I am grateful to my other two committee member Dr. Miguel Pando and Dr. Brett Q. Tempest for their encouragement and insightful comments. Further, I would like to thank Dr. Ian Ferguson, for his valuable suggestions during my work.

I want to recognize the professors with whom I took the core courses that helped me to establish the foundation to pursue this research. I am deeply grateful to Dr. Craig Allan, Dr. Jy S. Wu, Dr. John Diemer, Dr. Vincent (Tobi) Ogunro, Dr. William L. Saunders, and Dr. James D. Bowen.

I specially thank Dr. Weaver at the Material Characterization Laboratory for helping me learn new analytical techniques and for always being there to discuss my analysis on any experimental results.

My sincere thanks also goes to IDEAS faculty and staff, Dr. Clinton, Dr. Watkins, Regina Guyer, Sara Watson, and Karyn for assisting me with internship opportunities at the center and providing me with various lab facilities over the past four years.

I thank all my lab mates at SMART laboratory and IDEAS center: John Larson, Carter Garris, Jon McGraw, Rachelle Mercure, Janaya Perry, Wesley Waterhouse, Andrew Carlson, Morteza Ghaempanah Tajabadi, Tracy Chouinard, Lucia Nathalia Queen, Bhargavi Golluru, Seon-Yi Han and, Fabien Besnard, for helping me with my experiments, working hard together before deadlines, for the brainstorming discussion and the fun filled parties we have had in the past years.

I specially thank the Chief Operator Tara Romine at Mallard Water Reclamation Facility, Charlotte for helping me obtain samples from the plant for this study

Last but not the least; I would like to thank my family, my mother who struggled to provide me the best education, my husband who made sure that my goals were his, and my son Dhruv, who has given perspective to my research and how important it is to strive for a better greener future.

DEDICATION

To my mom Shylaja, my husband Gautam, and my son Dhruv

TABLE OF CONTENTS

LIST OF TABLES

LIST OF FIGURES

CHAPTER 1: INTRODUCTION

1.1 Background

Non-biodegradability of plastics in the environment, reduction in landfill space, depletion of petroleum resources, and ever-increasing concern over environmental pollution are all drivers for the development of materials that can substitute for petroleum-based plastics. Extensive research is underway to evaluate the feasibility of using natural plant fiber and biopolymers as replacements for synthetic fibers and petroleum-based polymers for various applications in the automotive, construction, and building industries [1-3]. Natural fibers are being used in place of synthetic fibers as reinforcements due to their high specific strength, low cost, light weight, and easy processing. These fibers are derived from various parts of plants, such as stems, leaves, and seeds. The fibers derived from stem (bast fibers) such as flax, hemp, kenaf, and jute are more commonly used for reinforcing due to their high tensile strength and high cellulose content [4].

Biocomposites in this study are defined as those composites consisting of both reinforcing fibers and polymeric matrixes derived from renewable resources. The biopolymers used in such composite systems are often produced from starch, cellulose, soybeans, and other plant materials. To mention a few, biopolymers that are of commercial interests are poly lactic acid (PLA), poly caprolactone, poly hyrdoxybutyrate.

Although natural fibers provide sufficient mechanical properties in composites, their inherent low thermal stability and poor adhesion with the matrix remains a challenge. To improve upon these characteristics, these fibers are subjected to several types of surface modifications: physical [5], chemical [6, 7], and biological [8]. Among the three methods, chemical treatment in particular has proven to be the most cost- and performance-effective method to improve the fiber-matrix interface. However, previous studies on chemical surface modification of fibers lack the scientific explanation related to the cause and effect of microscopic changes that result in bulk properties of the biocomposites. In this study, an effort is made to correlate the chemical modification on fiber surface to bulk properties of the composites with the aid of bond energy changes.

1.2 Objective

The main objective of this research is to advance the fundamental understanding of surface functionalization of natural fibers on the composites bulk properties, including mechanical, thermo-mechanical, thermal stability, and biodegradability. In this study, PLA has been chosen as the matrix due to its favorable mechanical properties and biodegradability properties. Hemp has been selected as the reinforcing fiber due to its superior tensile strength, along with other advantages, such as low cost, light weight, and renewability. Further, the biodegradability studies will aid in understanding how this material might contribute to environmental burdens if landfilled at the end of its life cycle. The results of this research may provide scientific understanding to enable the design or manufacturing of biodegradable composites with comparative mechanical properties to conventional engineering materials.

To achieve the overall research objective, the following three questions will be systematically investigated in this study.

1) How would surface functionalization of hemp fiber affect the mechanical and thermo-mechanical properties of a PLA-hemp composite?
2) How would surface functionalization of hemp fiber affect the thermal stability of a PLA-hemp composite?
3) How would surface functionalization of hemp fiber affect the biodegradability of a PLA-hemp composite at the end of life cycle?

1.3 Scope

This research provides an integrated approach to answering important questions about the relationship between surface treatment of natural fibers used for reinforcement, and the ultimate bulk material properties - the thermal and mechanical behavior of a biocomposite in which that fiber is used. Three surface modifications of hemp fiber were studied: alkali, silane and acetic anhydride. Further, the research incorporates the biodegradability studies of the biocomposites.

1.4 Chapter Outline

Chapter 2 is titled, “Literature Review” and outlines biocomposites and types of biocomposites. It describes, the current state of art related to PLA based biocomposites, the advantages and challenges of hemp fiber and PLA composites and concludes with a summary.

Chapter 3 is titled, “Research Methodology”. It outlines the surface treatment methods tested, describes how the composites were manufactured, and it sets forth the

various characterization and testing methods used for hemp fiber, PLA polymer and hemp-PLA composites.

Chapter 4 is titled, “Effect of Surface Functionalization on Fiber Chemical and Mechanical Properties”. This chapter provides the results from various characterization techniques used for hemp as well as from tensile test of single fibers. A discussion of the results is offered and the chapter concludes with a comparison between untreated and treated hemp fibers.

Chapter 5 is titled, “Effect of Surface Functionalization on The Thermal Stability of Hemp-PLA Composites”. It describes the thermal study of hemp-PLA and elucidates the correlation between activation energy of thermal degradation, bond energy and surface functionalization.

Chapter 6 is titled, “Effect of Surface Functionalization on the Mechanical and Thermo-mechanical Properties of Hemp-PLA Composites”. It describes the results of tensile, flexural and dynamic mechanical testing of hemp-PLA composites and offers a discussion of the results.

Chapter 7 is titled, “Effect of Surface Functionalization on the Biodegradability of Hemp-PLA Composites”. It provides a literature review on the biodegradability of biocomposites as well as the methodology for the biodegradability study. The results of the biodegradability study are offered with an accompanying discussion of the findings.

Chapter 8 is titled “Conclusions and Recommendations for Future Work”. It provides a summary of the findings of this study and suggests directions for future work.

CHAPTER 2 : LITERATURE REVIEW

2.1 Biocomposites

Definition: There are various definitions of biocomposites depending on the type of fiber and polymer chosen for preparing them. Composites with synthetic fibers and a bio-based matrix, or natural fibers and a synthetic resin, or natural fibers and a bio-based matrix, are all called biocomposites. The classification of biocomposites based on these various definitions is depicted in Figure 2.1. In this study, we refer to “biocomposites” as those composites that have been manufactured with natural fibers and a matrix that is derived from a bio-based material. These composites are environmentally benign and, therefore, they are also referred to as green composites.

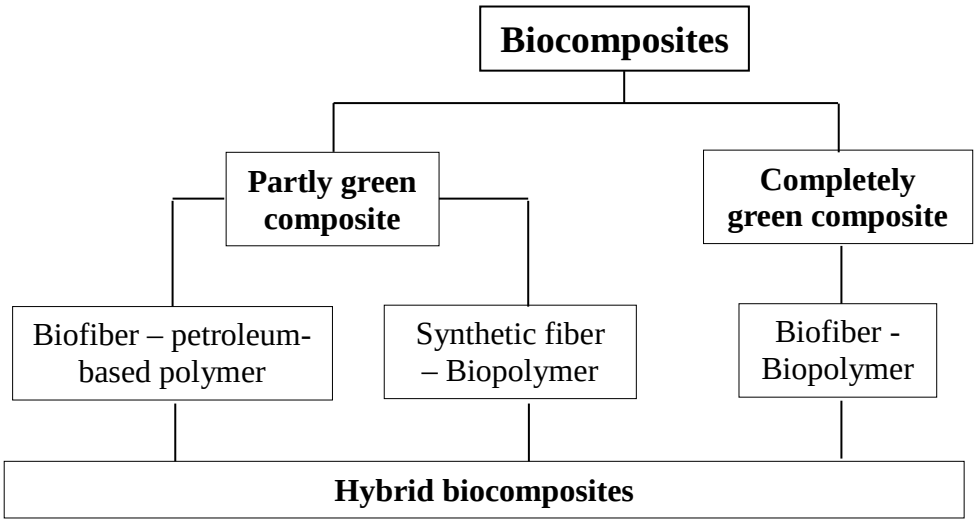

Figure 2.1: Classification of biocomposites [9].

2.2 Natural Fibers in Biocomposites

Depending on the source of origin, natural fibers can be obtained from plants, animals or minerals. Digital photographs of selected natural fibers and the classification of them with examples are presented in Figure 2.2 and Figure 2.3, respectively.

Figure 2.2: Digital photographs of selected natural fibers[1].

[1] www.hempspring.com, www.qrbiz.com, www.kalpataruproducts.com, www.tradekorea.com, nabilasamsudin.blogspot.com, pellets-wood.com, photo.net, yarnssilk.com, bonedryridge.com

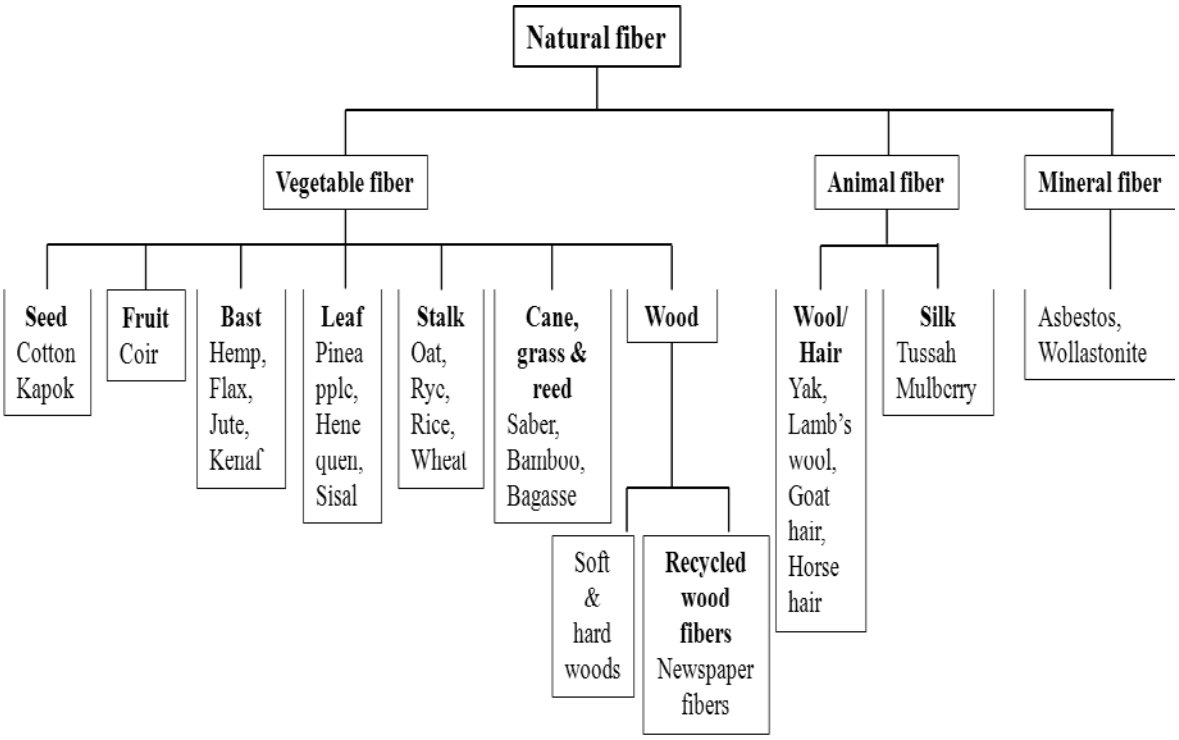

Figure 2.3: Classification of natural fibers [9, 10].

2.2.1 Chemical Composition of Natural Fibers

Although plants are mostly water, on a dry weight basis plant cell walls consists largely of carbohydrates with some amounts of extractives, proteins and inorganics. The relative proportions of those components vary slightly from plant to plant (Table 2.1).

Cell wall: Plant cell walls have three layers: a middle lamella, a primary wall, and a secondary wall (Figure 2.4b). The middle lamella constitutes the outer wall of the cell and is shared by the adjacent cell. It consists of pectin compounds and proteins. The primary wall is a rigid skeleton of cellulose microfibrils in a matrix of pectin compounds, hemicellulose and glycoproteins. The secondary wall is extremely rigid and is made up of three layers (S1, S2 and S3) consisting of cellulose, hemicellulose and lignin (Figure 2.4a). The thick middle layer in the secondary wall determines the mechanical strength of the fiber.

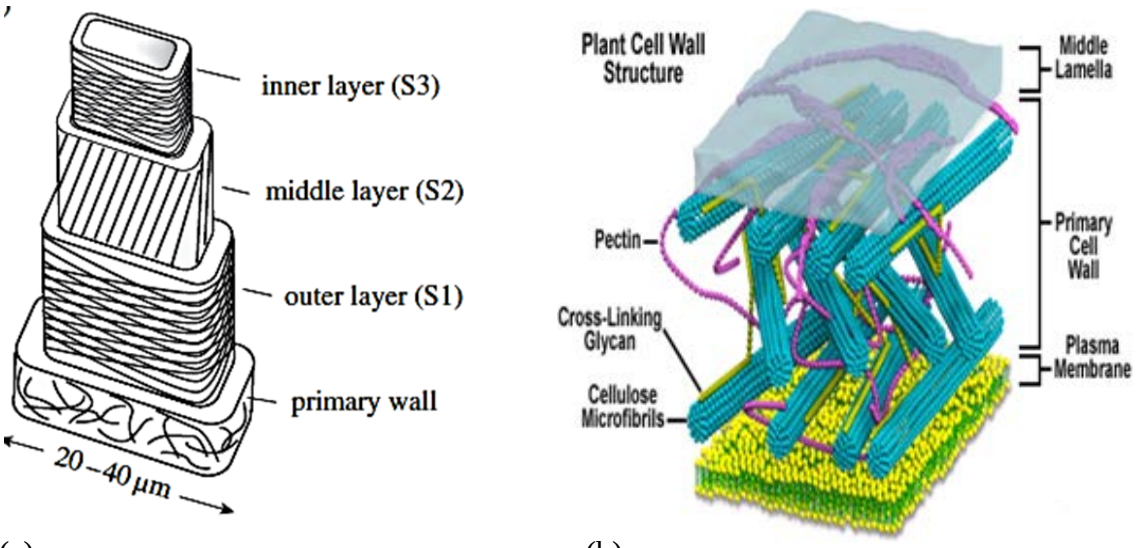

(a) (b)

Figure 2.4: (a) The cell wall of wood, made up of a primary layer and three secondary layers (S1, S2 and S3), with the cellulose microfibrils arranged in different orientations in each layer [12]. (b) Plant cell wall

Table 2.1: Chemical composition of some selected natural fibers [1, 11]

	Cellulose (%)	Lignin (%)	Hemicellulose (%)	Pectin (%)	Ash (%)
Flax	62-71	2.0-2.5	16-18	1.8-2.0	--
Kenaf	57-65	15-19	13-23	--	2-5
Jute	59-71	12-13	12-13	0.2-4.4	0.5-2
Hemp	62-75	2.9-3.3	16-18	0.8-0.9	0.8
Ramie	68-76	0.6-0.7	13-14	1.9-2.1	--
Sisal	47-78	7-11	10-24	10	0.6-1

Cellulose was first characterized by Anselme Payen in 1838, who concluded it had the empirical formula $C_6H_{10}O_5$ [12]. It is a homo-polysaccharide with a linear chain of 1, 4- β anhydro-glucose units that contain alcoholic hydroxyl groups (Figure 2.5). The hydroxyl groups in the molecule are responsible for inter and intra-molecular hydrogen bond formation. These hydroxyl groups are also responsible for plant fiber being hydrophilic. Though the cellulose structure is the same among different plant types, the degree of polymerization (DP) varies. In wood cellulose, the DP would be around 10,000,

but in cotton fibers it would be as high as 15,000 [13]. Cellulose has a very high Young's modulus of 138 GPa [14] and tensile strength of 1 GPa [15].

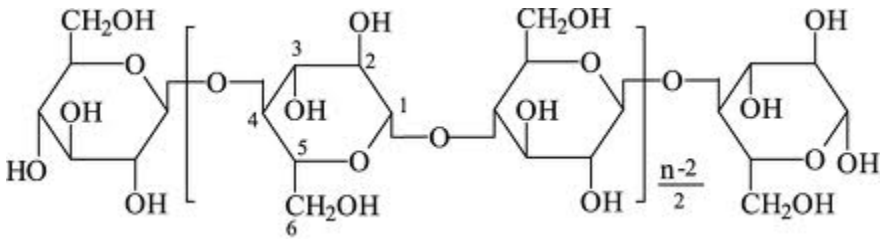

Figure 2.5: Cellulose structure [16]

Cellulose in the microfibrils exists as an amorphous lignin and hemicellulose matrix. Several hollow fibrils run the length of the fiber. In the S2 layer, these microfibrils are wound helically, with the angle between the fiber axis and the mcirofibril called microfiril angle. Fibers with a high microfibril angle, such as coir (~45°), show high elongation before breakage, while fibers such as hemp with, low microfibrile angle (~10°) and high cellulsoe content (~80%) tend to have high tensile strength but low tolerance for elongation before breakage [17].

Hemicellulose along with lignin forms the matrix for cellulose microfibrils. It is a group of complex polysaccharides with a combination of 5 and 6 ring carbon ring sugars such as, xyloglucans, xylans, mannans and glucomannans, and beta-glucans. Since hemicellulose are so heterogeneous they do not have a universal chemcial structure. The polymer chains are shorter compared to cellulose and have branching, which results in a lowed DP for hemicellulose than cellulose.

Lignin is the most abundant organic material on the earth. Although research indicates that lignin is produced by the polymerization reaction of alcohol molecules to yield a highly poly-disperse polymer [18], its molecular structure is not fully finalized. It

is thought to be a three-dimensional copolymer of aliphatic and aromatic constituents with high molecular weight. Its amorphous and hydrophobic nature is thought to make it resistant to microbial attack. The high carbon content and lower hydrogen content in lignin molecules provide rigidity to plants.

2.2.2 Bast Fibers

Bast is plant fiber obtained from the phloem/inner bark or bast of certain dicotyledonous plants (Figure 2.6). These fibers have high tensile strength and relatively low specific gravity. Some of the available bast fibers are flax, hemp, jute, kenaf, kudzu, nettle, okra, paper mulberry, ramie, rattan and wisteria, and they make up the majority of natural fibers used as reinforcement in composites because of their higher mechanical properties. Table 2.2 gives compares the mechanical properties of select bast fibers to those of E-glass, aramid and carbon fibers [19].

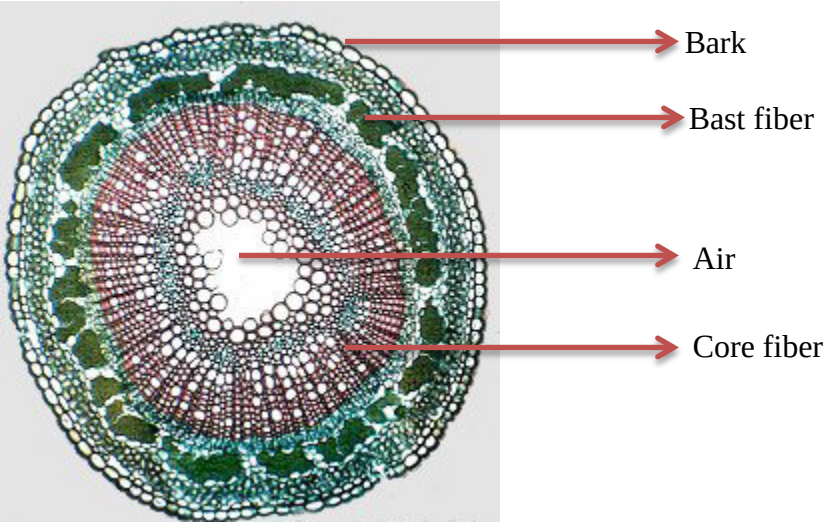

Figure 2.6: Cross section of the bast fiber depicting the various constituents of a bast fiber plant

Bast fibers are grouped by their region of growth. Temperate region fiber includes flax, hemp and nettle, while jute and kenaf are tropical region fibers [19].

Hemp: hemp plants are a member of the Cannabis family, Cannabaceae species. Cannabis sativa L. is also known as Indian hemp and is an herbaceous annual plant native to central Asia. The use of wild hemp dates back to 8000 B.C [20]. Currently, hemp is used for manufacturing a wide variety of products including food, textiles, paper, rope, fuel, oil, animal feedstock, medicine, and recreational products.

Hemp is among the fastest growing plants, one hectare of land produce close to 25 tons of dry fiber per year [21]. It can grow to 4m within 12 weeks [19]. It is considered to be an environmentally friendly crop due to low land and water demands and its ability to be cultivated without herbicide use [22].

Table 2.2: Mechanical properties of natural fibers in comparison to synthetic fibers [23-25]

Fiber	Density (g/cm3)	Elongation (%)	Tensile strength (MPa)	Young's modulus (GPa)
Jute	1.3-1.46	1.5-1.8	393-800	10-30
Flax	1.4-1.5	1.2-3.2	345-1500	27.6-80
Hemp	1.48	1.6	550-900	70
Ramie	1.5	2.0-3.8	220-938	44-128
E-glass	2.5	2.5-3.0	2000-3500	70.0
Aramid	1.4	3.3-3.7	3000-3150	63.0-67.0
Carbon	1.4	1.4-1.8	4000	230.0-240.0

Two types of fibers can be harvested from hemp plants: - bast, or long fibers and hurds, or short fibers. Bast fiber accounts for 20-30% of the stem. Fibers are separated from the stem by retting followed by decortification process. After decertification ultrasound, steam explosion, wet oxidation, or an enzyme treatment is used to generate long bundles of fiber for commercial use. The chemical composition and mechanical properties of hemp are tabulated in Table 2.1 and Table 2.2 respectively.

The mechanical, physical and chemical properties of the bast fiber have been well-reviewed [26]. Flax and hemp can be considered as same group with higher cellulose content and lower lignin content (Table 2.1). Further, they report that like flax, hemp has a long single fiber length, and relatively low moisture absorption capacity relative to other bast fibers.

In summary, hemp is an ideal bast fiber for reinforcement in composite, with its high tensile strength, high cellulose content, low lignin content, low density, and biodegradable properties.

2.3 Bio-based Polymers in Biocomposites

Definition: Biopolymers are those polymers that are manufactured from natural sources that may or may not be renewable.

For the purpose of this study, polymers derived from renewable resources such as polyhydroxyl alkanoate (PHA's), PLA, cellulose esters and starch plastics are biopolymers, and because biodegradable, they are considered to be green plastics. The life cycle of such biopolymers is presented in Figure 2.8. The advantages of such non-petroleum-based polymers are:

- Their raw materials are renewable agriculture resources [27]
- As plant-based materials, their production may contribute to reduced atmospheric carbon dioxide loads [28]
- These polymers are associated with energy savings [29]
- The materials are recyclable and compostable [30] and
- The use of agricultural resources helps the economics of the agricultural sector [31].

Poly lactic acid (PLA): PLA is a frequently used biopolymer because it is easily available and inexpensive relative to competing biopolymer materials. It is a thermoplastic resin with high rigidity and clarity. PLA results from the condensation polymerization reaction of lactic acid, which is derived from sugar or carbohydrate fermentation, but commercially it is manufactured by a ring-opening polymerization instead of polycondensation. [32]. PLA is used to make home textile and clothing, bottles, food packaging, and a variety of other durable goods [33].

2.4 Biocomposites with PLA as the Matrix

PLA has good mechanical properties: its tensile strength ranges from 50-70 MPa and it has an elastic modulus of 3000-4000 MPa [33]. It has a glass transition temperature in the range of 60-70 °C, and it is a brittle thermoplastic, fracturing through a crazing mechanism [34]. To reduce its brittle characteristics, PLA has been paired with various fibers such as kenaf [35-39], flax [40-44], jute [45-47], sisal [48], ramie [49-52], abaca [53], bamboo [54-56], pineapple leaf fiber [57], and hemp [58-64] to form more malleable biocomposites. Rice starch [65, 66], synthesized cellulose [53, 67], wood flour [68, 69], recycled newspaper [70], sugar beet pulp [71], and cordenka fibers [41, 72] have been tested as reinforcing materials as well.

Nishino *et al.* studied the mechanical properties of kenaf-PLA composites and reported that at a 70% volume fraction of fiber, the composites gave tensile strength of 62 MPa, which was comparable to that reported for other synthetic composites [36]. But Ochi *et al.* studied the influence of several factors on kenaf-PLA composites tensile strength and found that the fiber originating from the stem section closest to the ground had the highest tensile strength. Fabrication temperature also influenced tensile strength,

with 160°C being the maximum allowable temperature for fabrication. Higher temperatures resulted in composites with reduced tensile strength. Finally, biodegradation of plant fibers led to reduced tensile strength, with 91% strength loss observed after four weeks in a compositing soil at 80°C [37].

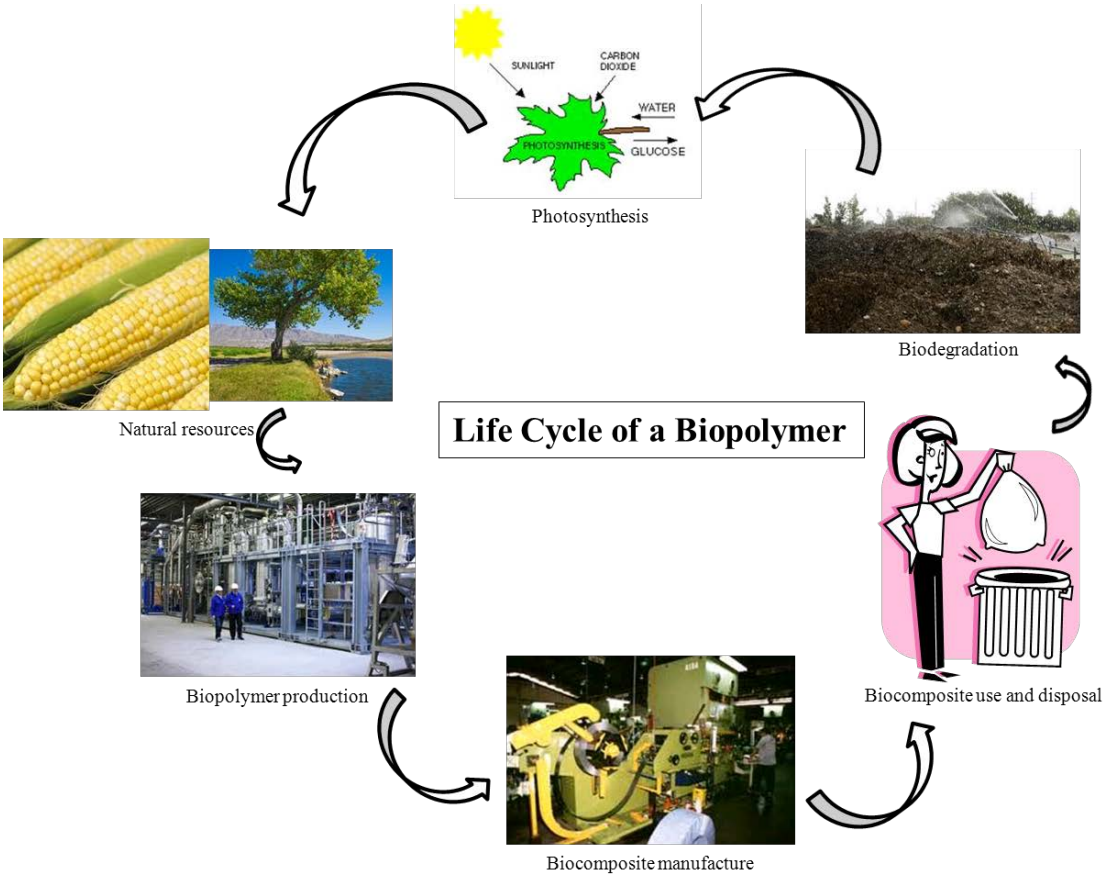

Figure 2.7: Life cycle of a bio-based polymer in a biocomposite

There are various research groups working to understand the properties of flax-PLA composites. Oksman *et al.* conducted experiments to understand whether flax-polypropylene (PP) composites could be replaced by flax-PLA for various industrial applications. They found flax-PLA composites to be 50% stronger than those made from flax-PP, but the interfacial adhesion of flax with PLA was poor and led to inferior

mechanical properties. Use of triacetin plasticizer offered no improved mechanical performance [40]. Bax *et al.* also studied the impact and tensile properties of flax-PLA composites and observed that at 30 wt.% fiber fraction they could obtain a Young's modulus of 6.31 GPa, but again, poor interfacial adhesion resulted in inferior tensile and impact properties [41].

When the biodegradability of flax-PLA composites was studied, woven and nonwoven flax fibers were employed as reinforcement with PLA and different amphiphilic additives affected biodegradability to vary degrees. The composites were buried in farmland soil, and biodegradation was measured as weight loss and observed as surface morphology changes. They found that mandelic acid addition accelerated biodegradation, with samples showing 20-25% weight loss in 50-60 d. Dicumyl peroxide treatment resulted in only 5-10% weight loss after 80-90 d [43].

The tensile strength and stiffness of PLA improves significantly with jute reinforcement [45]. A 40 wt. % composite of jute-PLA had double strength of a pure PLA sample, though the impact resistance between the specimens did not differ. The tensile strength increase was temperature dependent, and was contingent on the heating stage during composite formation not exceeding 210-220°C. Yu *et al.* found that jute-PLA composites showed optimum mechanical properties with 30% fiber volume fraction, and their thermogravimetric analysis showed that addition of fiber to the composite improved the degradation temperature [46]. Recently, Hongwei *et al.* reported that the optimum jute-PLA tensile and flexural properties were obtained at 15 wt. % fiber content and a processing temperature of 210°C and 220°C, respectively. They also found

improvement in jute-PLA mechanical properties when fibers were treated with alkali; the optimum alkali treatment was 12% sodium hydroxide (NaOH) solution for 8 h [47].

Li *et al.* used two coupling agents, MPS-g-PLA and PLA-co-PGMA, for the surface modification of sisal fiber and found that the tensile properties were improved but the impact strength decreased with both surface modifications [48].

Ramie-PLA fibers have been studied with respect to their fire retardancy and mechanical properties [52]. Three different techniques for preparing fire retardant composites were explored. They first blended PLA with ammonium polyphosphate (APP), which was then combined with ramie fibers. A second method exposed ramie fibers to flame-retardant treatment with APP, and they were then compounded with PLA. The third method combined both pre-treated APP-PLA and APP-ramie. The composites that pretreated each component for flame retardancy and then combined them had the best mechanical properties. Yu *et al.* pretreated ramie and PLA with alkali and silane and found marked improvement in the mechanical properties relative to controls with untreated fibers. Alkali treatment was the most effective treatment among the two treatments. Thermal studies suggested that the surface treatment likely yielded better properties due to improved interfacial adhesion [49].

Recently, M.J.A. van den Oever *et al.* evaluated the effect of undried and dried natural fibers on PLA degradation during processing on the mechanical properties of ramie-PLA composites. At different levels of moisture in the fiber had no significant effect on the PLA degradation or on the stiffness, flexural strength and Charpy impact of the composites. PLA hydrolysis was severely affected by the fiber diameter. [51].

2.4.1 Hemp-PLA Biocomposites

Hu *et al.* were the first group to study the hemp-PLA composites and they focused on the mechanical properties of composites made with hemp subjected to alkali pretreatment. Composite with 40% fiber volume fraction had best mechanical properties (54.6 MPa tensile strength, 8.5 GPa elastic modulus and 112.7 MPa flexural strength), and the alkali pretreatment yielded better interfacial adhesion between fiber and the polymer matrix [58]. Thermal degradation of composites is much faster than pure PLA specimens, and use of poly (ethylene glycol) (PEG) as a plasticizer did not improve the composite's thermal properties or enhance its mechanical properties [59]. The addition of synthetic cellulose fiber (Lyocell) to hemp-PLA composites increased their impact strength by 160% and tensile strength by 25% relative to cellulose-free hemp-PLA composites without lyocell. The enhanced strength was attributed to the high fiber elongation before breakage made allowable by the lyocell fibers [60].

When Islam *et al.* exposed (i) untreated and (ii) alkali pretreated hemp-PLA composite specimens to UV radiation and water spray at 50°C for different time intervals to simulate aging. Both the treated and untreated hemp-PLA composites showed decreased tensile and flexural properties and increased impact properties with increased aging. Overall, the alkali treated fibers outperformed the untreated fiber composite specimens [62]. These authors also compared the effect of fiber length and alignment on pretreatment impacts in hmep-PLA composites and found that specimens with 30% alkali treated long aligned hemp fibers had superior mechanical properties relative to specimens manufactured short-random or short-aligned hemp fibers. The tensile strength of the hemp-PLA composites with treated long aligned fibers were as high as 82.9 MPa, they

had an elastic modulus of 10.9 GPa, a flexural strength of 142.5 MPa, a flexural modulus of 6.6 GPa and an impact strength of 9 kJ/m^2 [61]. Alklai and silane pretreatment were compared on short random fibers and long aligned fibers of hemp that was incorporated into hemp-PLA composites. A specimen manufactured with a 35% hemp to PLA ratio using aligned long fibers pretreated with alkali yielded the best mechanical properties, with a tensile strength of 85.4 MPa, an elastic modulus of 12.6 GPa and an impact strength of 7.4 kJ/m^2 [63].

To conclude, the studies examining hemp-PLA composite performance focus on the effect of surface modifications on the bulk mechanical properties. However they do not elucidate any of the mechanisms by which material property changes occur. Such mechanisms might include a change in bond characteristics or bond energy. To advance the biocomposite science, there is a need to understand and elucidate such mechanisms so that they can be exploited, enhanced, molded, or mimicked in other systems.

2.5 Challenge: Fiber-matrix Adhesion

Most of the research related to natural fibers and polyolefins indicates that there is typically inferior adhesion between the fiber and hydrophobic matrices such as polyethylene (PE) [4]. Since the PLA molecule has slightly polar oxygen atoms that are capable of forming hydrogen bonds to the hydroxyl groups of the natural fibers, it could be assumed that PLA would have better interfacial adhesion with the natural fibers than PE (Figure 2.10). However, from the literature review [40, 41, 53, 67], it is evident that these hydrogen bonds have had little effect on improving fiber-matrix adhesion. Therefore, to obtain improved mechanical and thermal properties these natural fibers need to be subjected to surface modification.

(a) (b)

Figure 2.8: Chemical structure of D (a) and L (b) lactic acid [2]

2.6 Surface Modification of Natural Fibers

Surface modification of natural fiber is employed to improve a weak boundary region, form a tough and flexible interfacial layer, develop a highly cross-linked interfacial region, improve wetting between the fiber and matrix, form covalent bonds, and change the acidity of a surface [24]. Some methods include chemical treatment (alkali, permanganate, acetylation) [1, 73-75], use of coupling agents (silanes, maleic anhydride) [6, 76-79], physical modification (corona, plasma, steam explosion) [5, 80, 81] and biological (enzymes) [82, 83] modification with the aid of enzymes.

2.6.1 Chemical Treatment of Natural Fibers

Alkali treatment: This is one of the oldest methods used, and it involves treating fibers with NaOH for a specified duration to partially removal lignin and hemicellulose and completely removes pectin, wax and other organics from the surface. More cellulose molecules are exposed, which improves adhesion between the fiber and matrix [84, 85]. Alkali treatment changes the fine structure of native cellulose I to cellulose II (Equation 2.1).

$$\text{Cell–OH} + \text{NaOH} \rightarrow \text{Cell–O–Na} + + \text{H2O} + [\text{surface impurities}] \qquad [2.1]$$

[2] http://www.lactospore.com/about/background-info/

Alkaline treatment increases surface roughness, which aids adhesion, and it also increases possible reaction sites by exposing interior cellulose [4]. The NaOH, concentration, the soaking and drying temperatures, and the timing are all important factors for fiber quality. Mishra *et al.* reported that 5% NaOH treated fibers had more tensile strength than 10% NaOH treated fibers [86], and explained that the loss of tensile strength with higher base concentration was due to fiber degradation. Concentration, time, and temperature are considered factors that must be determined on a case-by-case basis for each fiber type and source and each polymer matrix.

Isocyanate treatment: The functional group of isocyanate is –N=C=O, which readily reacts with the hydroxyl group present on cellulose and lignin in the fibers. This reaction leads to formation of strong covalent bonds that can interlock well with the matrix.

Permanganate treatment: Fibers are soaked in a permanganate solution, and the concentration must be carefully controlled. Potassium permanganate is typically used. Paul *et al.* found that a concentration higher than 1% of $KMnO_4$ resulted in degradation of sisal fibers [87]. The treatment leads to the formation of a cellulose radical through the formation of a MnO_3^- ion (Equation 2.2).

$$\text{Cell} - \text{OH} + \text{KMnO4} \longrightarrow \text{Cell} - \text{H} - \text{O} - \underset{\underset{\text{O}}{\|}}{\overset{\overset{\text{O}}{\|}}{\text{Mn}}} - \text{OK}^* \qquad [2.2]$$

Acetylation treatment: Acetylation employs acetic anhydride and acetic acid and results in plasticization of fiber cellulose. The practice is also known as esterification.

Usually it is not done independently, but is preceded by pretreatment with NaOH. Acetylation reduces the moisture absorption capacity of fibers (Equation 2.3) [88].

$$\text{Fiber-OH} + CH_3\text{- C(=O)-O-C(=O)-}CH_3 \rightarrow \text{Fiber} - OCOCH_3 + CH_3COOH \quad [2.3]$$

Hill *et al.* reported that acetylation of coir fibers at 120°C resulted in structural damage and weaker mechanical properties, but acetylation at 100°C yielded improved fiber performance [89]. Rong *et al.* showed that the composites treated with 50% acetic acid showed better tensile strength and adhesion than untreated controls [90]. Sreekala *et al.* observed that flexural properties of oil palm fibers improved after acetylation [91].

Benzoylation treatment: This treatment reduces the hydrophilic nature of fibers. Benzoyl chloride is typically reacted to introduce a benzoyl group (C6H5C=O) on-to the fiber. Like acetylation, prior to treatment with benzyl chloride, a pretreatment with NaOH is common (Equation 2.4 and 2.5)

$$\text{Cell–OH} + NaOH \rightarrow \text{Cell–O–}Na^+ + H_2O + [\text{surface impurities}] \quad [2.4]$$

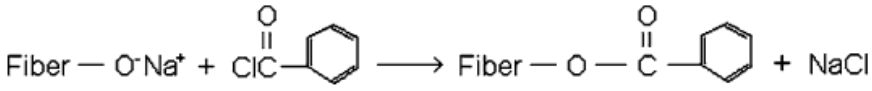

[2.5]

Nair *et al.* showed that the thermal properties of sisal fiber improved on benzoylation [92].

Peroxide treatment: The functional group of peroxide can be represented as ROOR. Most commonly used peroxides for this treatment are benzoyl peroxide and dicumyl peroxide. The main advantage of peroxide treatment is the quick decomposition of a peroxide yielding free radical that can react with the hydrogen group of the matrix and fiber. Like some of the other treatment methods, fibers are pretreated with alkali before treating with peroxides. The reactions that take place during peroxide treatment

are represented in the Equations 2.6, 2.7, 2.8, and 2.9 [4]. The matrix considered in these equations is polyethylene (PE).

$$RO - RO \rightarrow 2RO^{\cdot} \quad [2.6]$$

$$RO^{\cdot} + PE - H \rightarrow ROH + PE \quad [2.7]$$

$$RO^{\cdot} + Cellulose\text{-}H \rightarrow ROH + Cellulose \quad [2.8]$$

$$PE + Cellulose \rightarrow PE - Cellulose \quad [2.9]$$

where, PE is the polyethylene matrix

Peroxide treatment of oil palm fibers was optimized and improved the mechanical properties of composites relative to those of control composite specimens reinforced with non-pretreated fibers [93].

Graft copolymerization: Graft copolymers are a type of branched copolymers wherein the side chains are structurally distinct from the main chain. This technique initiates the free radicals on cellulose molecule that can react with the hydrogen bond on the matrix. Acrylic acid, acrylonitrile and vinyl monomers are used for graft copolymerization of natural fibers. Equation 10 depicts the reaction of acrylonitrile (AN) with the fiber [1].

$$Fiber - OH + CH_2 = CHCN \rightarrow Fiber - OCH_2CH_2CN \quad [2.10]$$

Mishra *et al.* observed that AN-grafted sisal fibers became more hydrophobic than the untreated fibers. This is an important observation, since reduced fiber moisture affinity improves the mechanical properties of composites. Grafted fibers showed a 25% increase in Young's modulus relative to untreated control fibers [94].

Silane Treatment: The chemical formula of silane is SiH_4. Silane pretreatment is a common modification of fibers destined for composite materials [95] [96]. In the

presence of moisture, hydrolysable alkoxy group form silanols, which react with the hydroxyl group of cellulose and form covalent bonds. The reactions are described in equations 2.11 and 2.12 [95].

$$CH_2CHSi\ (OC_2H_5)_3 \rightarrow CH_2CHSi\ (OH)_3 + 3C_2H_5OH \quad [2.11]$$

$$CH_2CHSi\ (OH)_3 + H_2O + \text{fiber-OH} \rightarrow CH_2CHSi\ (OH)_2\ \text{O-Fiber} \quad [2.12]$$

Agarwal *et al.* observed that the thermal stability of the henequen and oil palm fibers improved after silane treatment [95].

Maleated Coupling Agent: Maleic anhydride is a frequently used coupling agent used to modify the fiber surfaces destined for pairing with a polypropylene matrix. Equation 2.13 shows the reaction of cellulose fiber with hot maleic anhydride polypropylene (MAPP) copolymers.

Cantero et al. reported that composites made with flax fibers with 10 wt.% MAPP treated fiber had the highest flexural and tensile strength compared to untreated fiber, but no noticeable change in modulus values resulted from fiber pretreatment [97]. MAPP treated jute fibers in polypropylene composite specimens out-performed untreated composite specimens when tested for flexural strength, and the dynamic strength of MAPP modified composites increased by about 40% relative to controls [98]. Keener *et al.* observed peak performance in agro-fiber PP composites modified by MAPP. The MAPP modified composites performed better than other polyolefin coupling agents studied, and the results indicated that the modified fibers doubled the tensile strength and tripled the impact properties compared to composite specimens with untreated fibers [99].

A final chemical surface treatment option for fibers employs stearic acid ($CH_3(CH_2)_{16}$ COOH) in ethyl alcohol, sodium chlorite ($NaClO_2$) and triazine ($C_3H_3N_3$) [4].

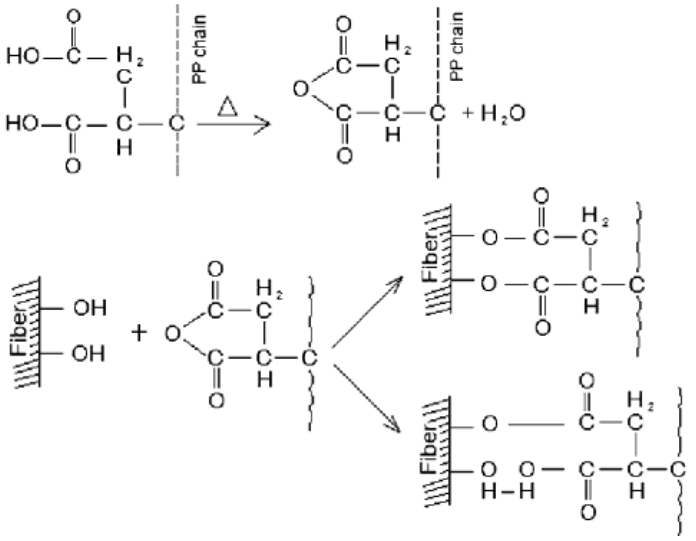

[2.13]

2.6.2 Physical Treatment of Natural Fibers

Natural fibers can be physically modified by stretching, calendaring, using thermo-treatment, or by applying electric discharge and production of hybrid yarn. Structural and surface properties of the fiber are changed by this treatment, which result in improved mechanical bonding to polymers. The two main reasons for physical treatment are separation of the fiber bundles into individual filaments and modification of fibers for composite preparation, respectively [5]. If separation of the fiber bundles is desired, methods like steam explosion and thermo-mechanical processing are adopted. If modification of the fiber surface is required, methods like plasma (thermal) treatment, dielectric barrier techniques (DBT) or corona (non-thermal) treatment are adopted.

Corona treatment modifies the surface oxidation activation of fibers which improves the interface between the hydrophilic fiber and the hydrophobic matrix. A

variety of surface modifications can be obtained in plasma treatment, depending on the type and nature of the gas used [100].

Corona discharge treatment (CDT) is an efficient and eco-friendly treatment that enhances the fiber/matrix interaction in composites. Moreover, it can be applied as a continuous processing, which is the common route in the textile or paper industry. In a recent study, that used CDT to improve the mechanical properties of hemp-polypropylene composites, specimen Young's modulus of the composite increased by 30%. The results were obtained by dynamic mechanical analysis and supported by scanning electron microscopic analysis [101].

Plasma modification of fiber surfaces has various modes of action, which occur at varying degree to effect improved adhesion [5]. It cleans the fiber surface; it etches the surface and roughens it to promote better adhesion. It leads to cross linking at the fiber surface, which can strengthen the surface layer. Finally, it can introduce free radicals that modify the surface chemical structure

Morales *et al.* studied plasma treatment for polystyrene films and natural fibers and observed that interface strength increased by as much as 70% in specimens that included pretreated fibers relative to untreated controls. But at longer exposure times, specimen strength decreases which could be attributed to fiber degradation as particles continually impacted the fiber. The author's concluded that the plasma pretreatment improved interfacial strength by increasing adhesion between fiber and matrix [102].

2.6.3 Biological Treatment of Natural Fibers

Currently bio-based composites are manufactured with chemically modified fiber for better interfacial adhesion. Such fiber treatment means there are opportunities for

chemical waste generation, and a search continues for more environmentally benign pretreatment methods. The idea of using biological methods, such as enzymes for fiber surface modification is not new, since the textile industry is already using cellulase and hemicellulase to modify the surface properties of cellulosic fibers [103].

Gulati *et al.* were the first research group to look into the effect of biological treatments on the fiber matrix adhesion of composites. They studied the effect of fungal treatment (*O. ulmi*) on surface characteristics, tensile strength and moisture absorption of hemp fibers with unsaturated polyester resin, Stypol 040-8086. They found that treated fibers had improved acid-base characteristics, better resistance to moisture, and better mechanical properties [82].

In summary, chemical surface modifications are the most frequently used methods, to modify fibers before their incorporation into composite materials, and a variety of pretreatment regimes are available. In this study, three different chemical methods were selected for study and additional review: alkali, silane and acetic anhydride treatment. Alkali treatment was chosen since it is one of the oldest and proven methods not only in the composite industry but also in textiles. Silane was chosen as a representative effective coupling method. Acetic anhydride treatment was chosen because this treatment is expected to improve material properties, but it has mainly been applied in wood fiber studies and only to a limited extent in composites.

2.7 Research Focus

Previous studies related to hemp-PLA composites have focused on their mechanical properties, and there has been a brief study on their thermal properties. Fiber pretreatment for these composites has included conventional alkali and silane. However,

these studies lack systematic investigation on fiber-matrix interface on material properties of biocomposites, such as mechanical strength, thermal stability and biodegradability. Therefore to fill in the knowledge gap, the research in this study aims to understand the effect of fiber-matrix interaction at microscopic level on the bulk material properties of biocomposites. To accomplish this research goal, the following three questions will be systematically investigated in this study.

1. How surface functionalization of hemp fiber would affect the mechanical and thermo-mechanical properties of a hemp-PLA composite?
2. How surface functionalization of hemp fiber would affect the thermal stability of a hemp-PLA composite?
3. How surface functionalization of hemp fiber would affect the biodegradability of a hemp- PLA composite at the end of life cycle?

CHAPTER 3 : RESEARCH METHODOLGY

Goddard *et.al* defined research methodology as a way to systematically solve a given research problem. In differentiating between research method and methodology they mention that "*research methodology is not just research methods; methodology considers the logic behind the methods that are used in the content of research study and explain why a particular method or technique was used, so that research results are capable of being evaluated by the researcher himself or by others*"[70].

This chapter elucidates the research methodology adopted in this study to answer the research questions. The flow chart in Figure 3.1 depicts the research methodology adopted.

3.1 Hemp Fiber Surface Treatment

Fibers are a vital component of a fiber-matrix composites system. Synthetic fibers have been extensively used since the past eight to nine decades, but they are not environmentally benign and are manufactured from non-renewable resources. In current times, increased environmental awareness in composite industry has led to the usage of natural fibers. These fibers, along with being obtained from renewable resource provide advantages such as light weight, low cost, relatively high strength and high stiffness [104]. Though natural fibers have varied advantages they have the disadvantage of being hydrophilic which reduces their chance of being used with hydrophobic polymer matrix.

The opposite characteristics of natural fiber and polymer matrix are the main reason for inferior adhesion. Therefore, to obtain a natural fiber composite (NFC) with superior properties, it is essential to modify the fiber surface so as to improve the interfacial adhesion between fiber and matrix. This is normally done by subjecting the fiber to different types of surface modifications such as, physical, chemical, or biological modifications.

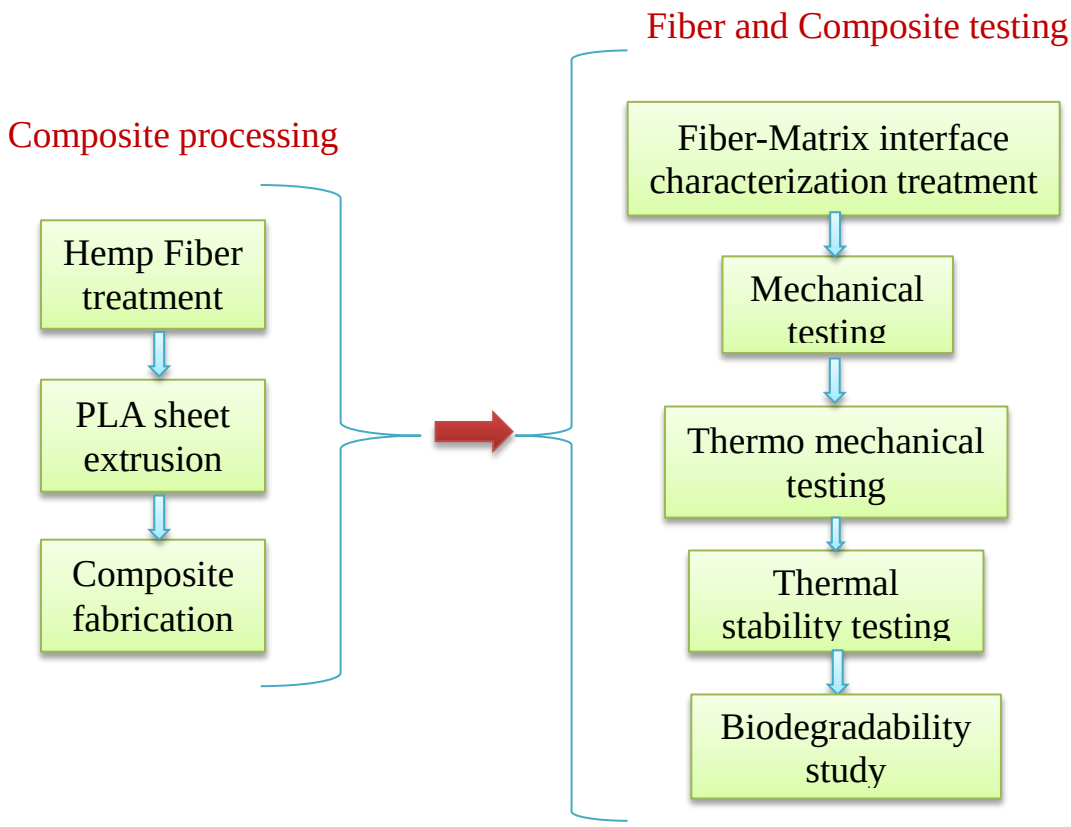

Figure 3.1: Flow chart detailing the research methodology adopted in the study

In this study three different surface modification of hemp are investigated. They are: alkalization, silane treatment and acetylation. Alkalization was chosen because it is one of the oldest and most commonly used fiber surface treatment methods. In this

method, sodium hydroxide (NaOH) is used to modify the surface of the fiber. This modification results in partial removal of lignin and hemicellulose and complete removal of pectin, wax and other organics present on the surface of the fiber. Alkalization is expected to expose more cellulose molecules thereby increasing the number of reaction sites for a better interfacial adhesion [105]. Silane treatment was chosen since this treatment is expected to modify the fibers by removing impurities along with forming covalent bonds (Si-O-Si) with matrix and resulting in enhanced interfacial adhesion [106]. Acetylation is a process of treating fibers with acetic anhydride in presence of an acid catalyst. It is a well know esterification (C-O) process resulting in plasticization of the cellulosic fibers. This method was previously used in wood industry to improve the properties of wood related to moisture absorption, and environmental degradation. Acetic anhydride is also expected to increase hydroxyl group concentration and improve the interfacial adhesion [88].

3.2 Materials and Methods

Industrial hemp fibers with a length of 25 mm were obtained from Hempline Inc. (Ontario, Canada). The average density of the fiber was 1.24 g/cm^3. The moisture content of the raw industrial hemp fiber ranged from 6% to 7%. Poly-(lactic acid) (PLA) pellets having a density of 1.24 g/cm^3 melt flow rate of 6 g/10min, and a melting temperature of 210°C were obtained from Nature Works LLC. (Nebraska, U.S.A). NaOH pellets, glacial acetic acid and acetic anhydride were obtained from Fisher Scientific (New Jersey, USA), and the silane solution (triethoxyvinylsilane) was obtained from Sigma Aldrich Inc. (Missouri, USA).

Untreated fiber: Hemp obtained from the manufacturer was cleaned, washed in distilled water and dried at 80 °C for 10 h before treatment or testing as untreated fiber.

NaOH modification: Hemp fibers were treated using 5 wt. % of NaOH solution. Fibers were immersed in the NaOH solution for 16 h at 50 °C then washed with distilled water till the pH became neutral (Figure 3.2). Hemp fibers were then dried in the oven at 80 °C for 10 h and stored in desiccators prior to composite preparation.

Silane modification: Hemp fibers were treated using 5 wt. % of silane solution. Silane solution was prepared by adding a 50v/50v ethanol/water mixture to the silane. 50v/50v acetic acid was added to adjust the pH of 5 wt. % silane solution to be in the range of 4–5. Fibers were then washed till their pH value ranged from 6.0 to 7.0 (Figure 3.3). Hemp fibers were then dried in an oven at 80 °C for 10 h and stored in desiccators prior to composite preparation.

Acetic anhydride modification: Hemp fibers were immersed in glacial acetic acid solution for 1 h at room temperature. Then the fibers were soaked in 2.5 wt. % acetic anhydride solution for a period of 2 h then washed with distilled water till the pH became neutral (Figure 3.4). Hemp fibers were then dried in the oven at 80 °C for 10 h and stored in desiccators prior to composite preparation.

The ratio of fiber to treatment solution mixture during all treatments was maintained at 1:10 (fiber: solution). The dried fibers were stored in a Ziploc bag inside a desiccator until testing.

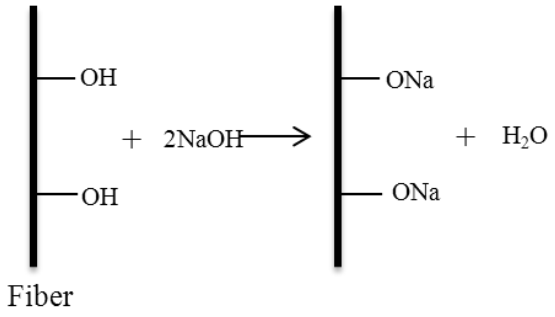

Figure 3.2: Reaction mechanism of NaOH with cellulose in hemp fiber

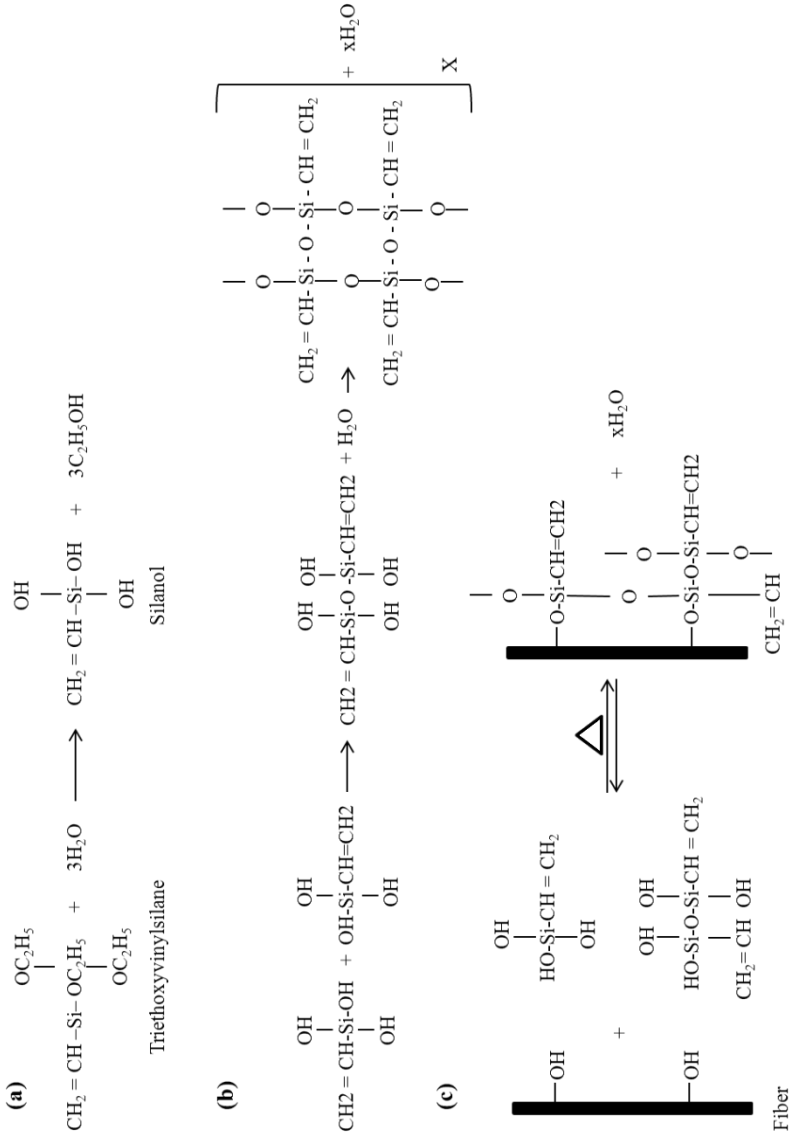

Figure 3.3: Reaction mechanism of silane with cellulose in hemp fiber

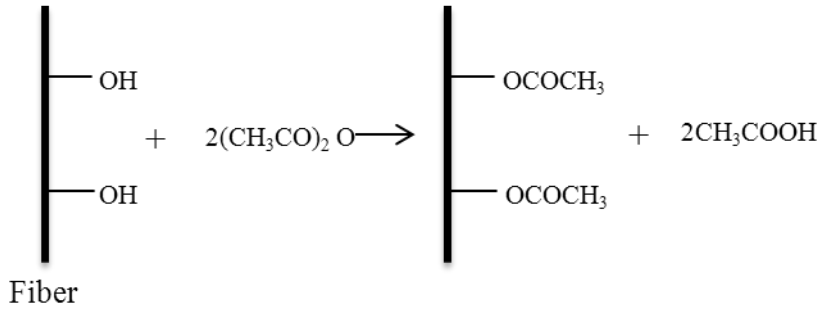

Figure 3.4: Reaction mechanism of acetic anhydride with cellulose in hemp fiber

3.3 Composite Preparation

A two-step manufacturing process was used in order to improve the surface adhesion of the natural fiber and the matrix. First, PLA was processed separately into thin films using a C.W. Brabender 19.05mm single-screw extruder. The extruder was operated at a temperature of 175°C with an extruder rotation speed of 8 rpm. A compression molding technique was used to manufacture composites with different polymeric films using a custom mold. Each composite was manufactured by sandwiching a layer of fiber in between two layers of PLA films. The weights of hemp fiber and PLA layers were controlled to achieve target fiber volume fraction values of a 20%, 30%, and, 40%. The fiber volume fraction V_f was determined by using the following equations:

$$V_f = (W_f/\rho_f)/ (W_m/\rho_m) + (W_f/\rho_f) \quad [3.1]$$

$$V_m = 1- V_f \quad [3.2]$$

Where V_f denotes the volume fraction of hemp fiber, $W_{f\ is}$ the weight of hemp fiber sandwiched in the composite, and ρ_f is the density of hemp fiber. $V_{m,}$ $W_{m,}$ and ρ_m represent the volume fraction, weight, and the density of PLA matrix, respectively. Composites were prepared with both, untreated and chemically treated fibers for all above mentioned fiber volume fractions (Table 3.1). Pure PLA panel was prepared by melting the pellets in the mold at 175 °C to obtain a panel of uniform thickness.

3.4 Characterization and Testing

The surface modified and unmodified hemp fibers were subjected to different characterizations, such as Fourier transform Infrared Spectroscopy (FTIR), Scanning electron microscope (SEM) and thermal stability (using thermo-gravimetric analyzer, (TGA)). The tensile strength of the treated and untreated single fiber was also measured. Composite were tested for mechanical, thermo-mechanical, thermal stability and biodegradability.

Table 3.1: Details of the composites manufactured in the study

Composites	Fiber volume fraction (%)	Polymer (PLA) volume fraction (%)
Untreated hemp-PLA	20	80
Untreated hemp-PLA	30	70
Untreated hemp-PLA	40	60
NaOH treated hemp-PLA	20	80
NaOH treated hemp-PLA	30	70
NaOH treated hemp-PLA	40	60
Silane treated hemp-PLA	20	80
Silane treated hemp-PLA	30	70
Silane treated hemp-PLA	40	60
Acetic anhydride treated hemp-PLA	20	80
Acetic anhydride treated hemp-PLA	30	70
Acetic anhydride treated hemp-PLA	40	60

3.4.1 Fourier Transform Infrared Spectroscopy (FTIR)

Solid, liquid or gas can be analyzed with the aid of FTIR. In the FTIR, the data is collected and converted from an interference pattern to a spectrum. The wavelength of light absorbed is a characteristic of a specific bond. By interpreting the infrared absorption spectrum, the chemical bonds in a molecule can be determined.

In this study, Infrared spectra were obtained using a Perkin Elmer FTIR spectrometer model Spectra 100 (Figure 3.5). IR spectra were obtained in the range of

4000-650 cm^{-1} at a scanning speed of 2mm/s, with a resolution of 16 cm^{-1}. The number of scans was set to sixteen. 10-20 mg of fiber was placed directly on the scanner to obtain the spectra.

Figure 3.5: Perkin Elmer FTIR spectrometer

3.4.2 Scanning Electron Microscopy (SEM)

SEM is a microscope that uses electrons instead of light to form an image. The SEM has many advantages over traditional microscopes such as; large depth of field, which allows more of a specimen to be in focus at one time, higher resolution, so closely spaced specimens can be magnified at much higher levels, and use of electromagnets rather than lenses, aids researcher to have more control with the degree of magnification. The working of SEM is well described by Purdue University radiological and Environmental Management webpage as “A beam of electrons is produced at the top of the microscope by an electron gun. The electron beam follows a vertical path through the microscope, which is held within a vacuum. The beam travels through electromagnetic

fields and lenses, which focus the beam down toward the sample. Once the beam hits the sample, electrons are ejected from the sample"[3] (Figure 3.6).

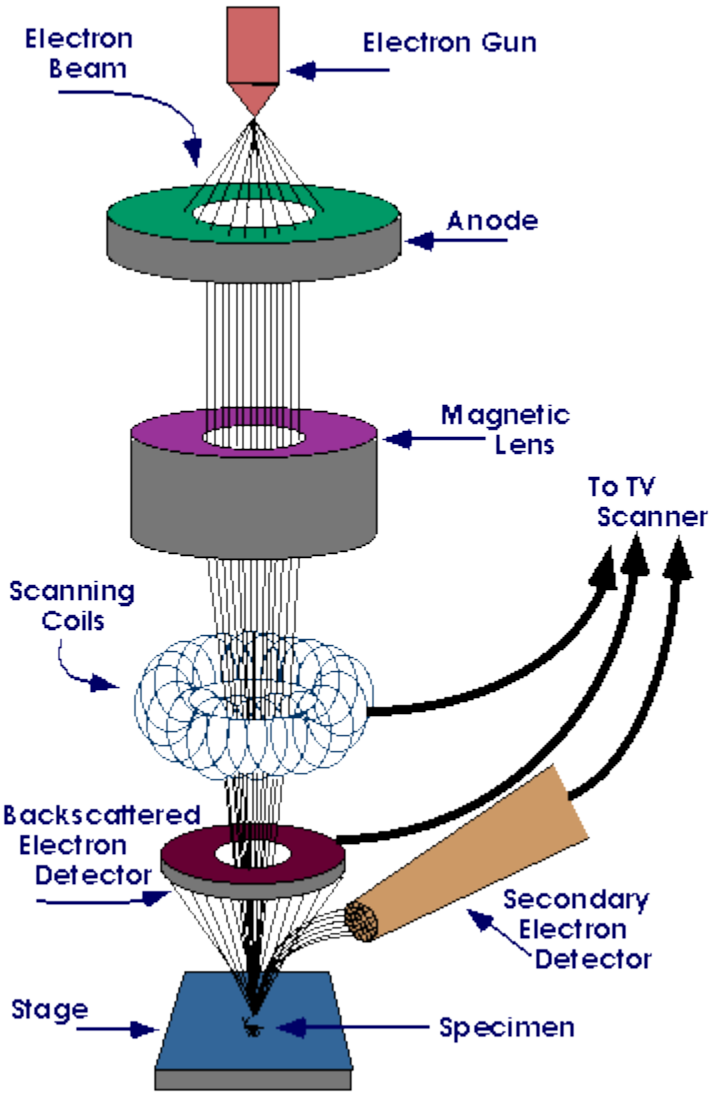

Figure 3.6: Working principal of a scanning electron microscope

SEM pictures were obtained using a JEOL JSM-6480 SEM (Figure 3.7). To improve the conductivity of the treated and untreated hemp fiber, hemp fiber was coated with gold using Denton Desk IV Sputter. The thickness of gold coating was maintained

[3] http://www.purdue.edu/rem/rs/sem.htm

in the range of 0.5 – 0.55 nanometer. The gold coated fibers were then observed under SEM and pictures were taken at 200, 100, 50, 20, 10 and 5 μm magnifications.

The alignment of the SEM were set as follows, the accelerating voltage was maintained at 8kV, spot size of 30, objective aperture on the electron optical column was set at 2, the chosen signal was second electron image (SEI), and the working distance (WD) was maintained between 7-10 mm. The pictures were taken at a slow scanning speed (Scan 4) to obtain higher quality image.

Figure 3.7: JEOL JSM-6480 SEM

3.4.3 Thermogravimetric Analysis (TGA)

Thermogravimetric analysis (TGA) is a technique where in the weight loss of a substance is measured as a function of time or temperature as the substance is subjected to controlled temperature in an atmosphere. In a TGA thermal curve, the abscissa can be displayed as time or temperature and the ordinate (Y-axis) can be displayed as weight (mg) or weight percent (%).

Thermal decomposition of untreated, treated hemp fiber, hemp-PLA composites and pure PLA was analyzed with TA Instrument model Q600 (Figure 3.8) with a heating rate of 10°C/minute, from 25 to 550 °C in a nitrogen atmosphere. The amount of sample

used was in the range of 10 to 12 mg. For every sample five replicates were tested. The testing was conducted as per ASTM E 1131[107].

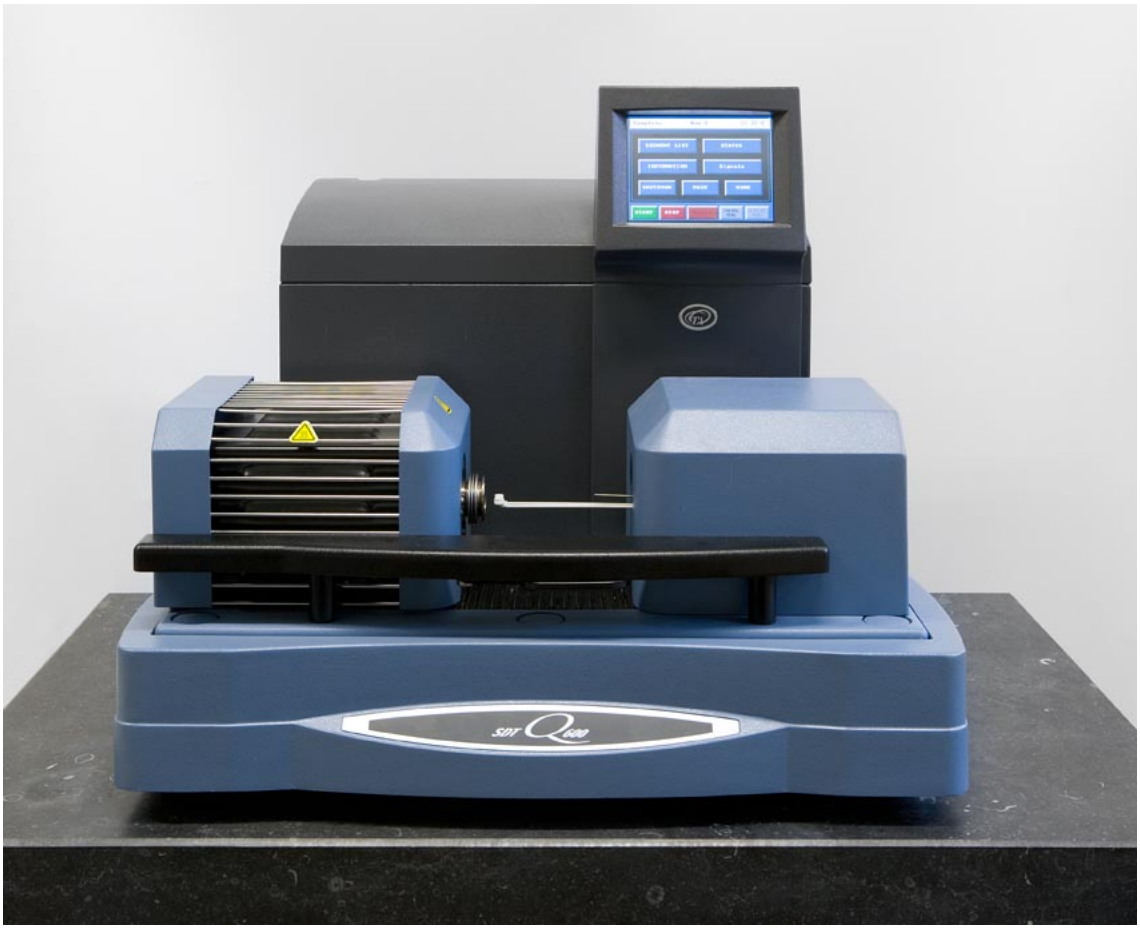

Figure 3.8: TGA from TA Instrument model Q600

3.4.4 Mechanical Properties of the Fiber Pre and Post Treatment

Sample preparation: Samples were prepared by carefully removing single fibers from the fiber bundles. Due to the inherent fragile nature of the fibers, a single fiber was attached to a piece of cardboard with glue to avoid direct contact with the grips of the testing machine using the tabbing technique (Figure 3.9a). The single fiber was mounted on the cardboard sample holder, which had dimensions of 50×20 mm with a 12.7 mm

diameter hole in the center. The resin was then cured for 4-6 hrs. The gage length of the fiber was 25.4 mm as per ASTM C 1557-03 [108].

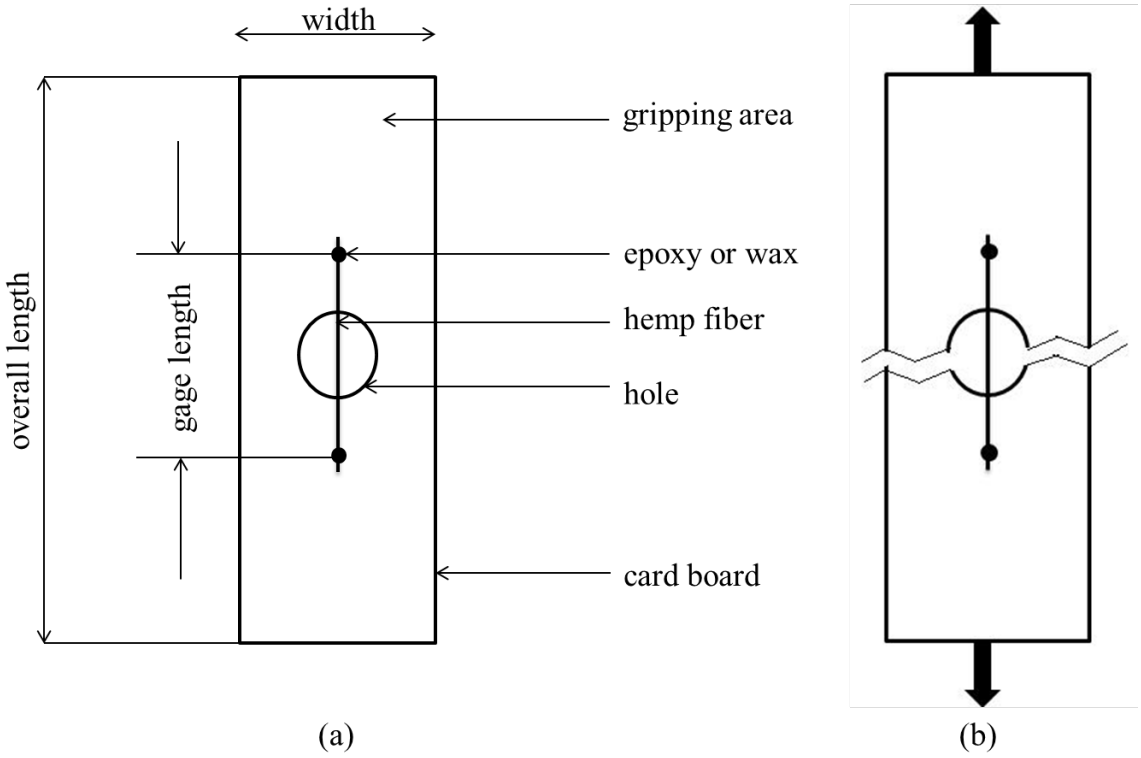

Figure 3.9: Illustration of the preparation of single fiber for tensile test. (a) single fiber was mounted on a cardboard holder with epoxy resin; (b) the sides of the card board were cut off after the sample holder was mounted on the HK-10 test machine.

The fibers were inspected under Microscope (Model Micromaster II from Fisher Scientific) to ensure that only a single fiber was present on each card. Diameters of fibers were then measured under the same microscope by means of a calibrated slide. The average diameter of each selected fiber was determined by taking eight diameter measurements at different locations along the fiber length, and then taking an average of those measurements.

Single fiber test: Tensile properties of single fiber were tested on the Tinius Olsen (Figure 3.10), with the following settings:

Gauge length: 25.4 mm.

Cross-head speed: 0.50 mm/min (10% of initial specimen length/min)

Load cell: 5.0 N

All tests were conducted under standard environmental conditions (25±2 °C and 50 ± 2% relative humidity).

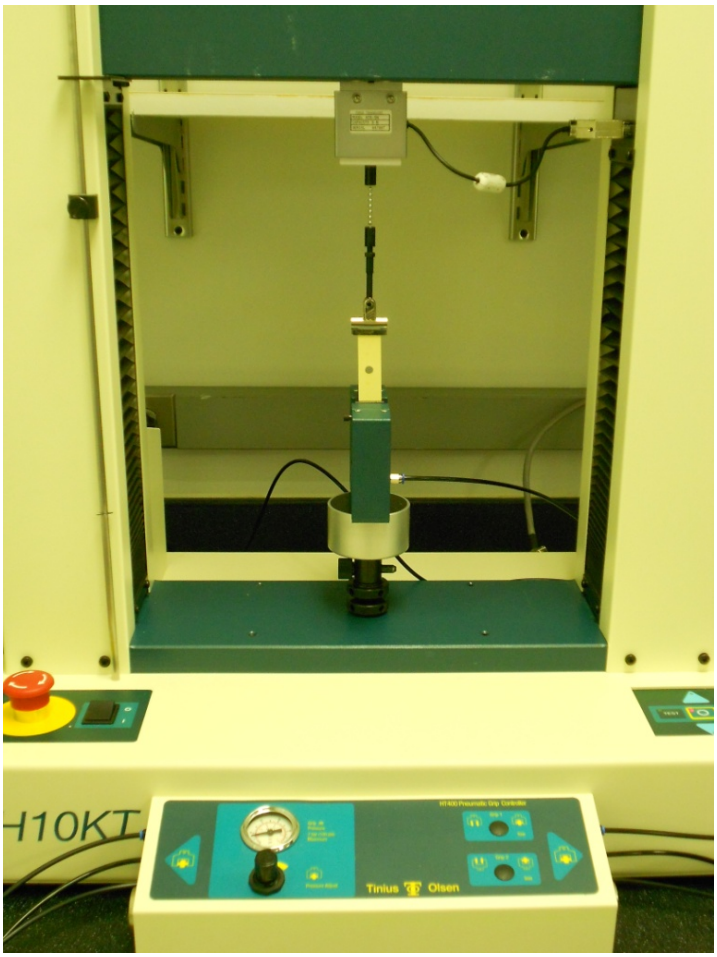

Figure 3.10: Tinius Olsen H10KT tensile tester

After the sample was mounted on the grips of the tester, the sides of the cardboard were cut off (Figure 3.9b). Then the force-extension curve was measured. If a sample slipped in the grips, broke at the edge or in the grips, the sample was discarded. Thirty

specimens where tested for both untreated and treated hemp. The specimens were picked in a completely random order.

3.4.5 Tensile Testing

Tensile testing of composites was performed according to ASTM D3039 [109] with seven specimens per sample in an Instron 5582 constant rate of extension (CRT) universal testing machine. The speed of the crosshead was 1.3 mm/min, air temperature of 23°C, and 65% relative humidity (Figure 3.11). Each test was performed until tensile failure occurred. Tensile stress–strain behaviors of hemp-PLA composites were analyzed including the reported maximum tensile strength, Young's modulus at 1% strain and strain at maximum tensile strength.

3.4.6 Flexural Testing

Flexural testing of composites was performed according to ASTM D790 [110] with seven specimens per sample in an Instron 5582 constant rate of extension (CRT) universal testing machine. The speed of the crosshead was 1.3 mm/min, air temperature of 23°C, and 65% relative humidity (Figure 3.12). Each test was performed until flexural failure occurred. The flexural stress-strain behavior along with maximum flexural strength, strain at maximum strength, and the flexural modulus at 2% strain were documented.

Figure 3.11: Instron loaded with a composite specimen for testing in tensile mode

Figure 3.12: Instron loaded with a composite specimen for testing in flexural mode

3.4.7 Modeling of Tensile Strength of Single Fibers

The two frequently used models for predicting the tensile strength of a composite system are rule of mixtures and Kelly-Tyson equation. Rule of mixture is based on the assumptions that; fibers are uniformly distributed throughout the matrix, there is a perfect bonding between fibers and matrix, matrix are free of voids, applied loads are either parallel or normal to the fiber direction, and fiber and matric behave as linearly elastic materials. This method approximately estimates the composite material properties such as density, coefficient of thermal expansion, modulus of elasticity, shear modulus, Poisson's ratio and tensile strength. [111]. In discontinuous fiber reinforced composites, length and diameter of the fiber along with fiber-matrix adhesion influence significantly the macroscopic properties of the composites. It is observed that below the critical fiber length, there will not be an effective reinforcement. Factoring the critical length parameter, Kelly Tyson extended the "rule-of-mixture" for strength prediction of composites reinforced with fibers aligned in loading direction. Kelly- Tyson model assumes that the matrix is rigid plastic and interfacial shear stress, τ, is everywhere equal to the matrix yield stress in shear, τ_y which results in the equation

$$\sigma_f = \frac{4}{d}\tau_y\, x \qquad [3.3]$$

The strength equation is given by

$$\sigma_{uc} = \eta_o\, \eta_L\, V_f\, \sigma_f + V_m \sigma_m \qquad [3.4]$$

where σ_f, is the fiber tensile strength, σ_{um}, is the matrix strength at the fiber failure strain, which is assumed to be equal to $E_m * \sigma_f/E_f$ and V_f is the fiber volume fraction, σ_{uc} is the ultimate composite strength, η_L is the fiber length efficiency factor and η_o is the fiber orientation factor, which is 3/8 for random-in-plane fiber composites.

$$\eta_L = \frac{1}{V_f}\left[\sum \frac{L_i V_i}{2L_c} + \sum V_j\left(1 - \frac{L_c}{2*L_c}\right)\right] \quad [3.5]$$

where L_c, is the critical fiber length according to Kelly-Tyson

$$L_c = \frac{\sigma_f * d}{2 * \tau} \quad [3.6]$$

where, V_i is the fiber volume fraction of fibers having length L_i shorter than L_c, V_j is the fiber volume fraction of fibers having length L_i longer than L_c, d is the diameter of the fiber and τ is the fiber-matric interfacial shear strength.

The advantage of this model over rule of mixtures is that, it takes into consideration to relate average fiber length and critical length. One of the disadvantages of the Kelly-Tyson model is the higher estimation of strength than actually measured. To obtain data in agreement to experimental data Thomason *et. al.* determined a value of η_o = 0.2 by fitting η_o to strength data. Therefore, Kelly-Tyson model for strength prediction of composites can be written as

$$\sigma_{uc} = 0.2 * \eta_L V_f \sigma_f + V_m \sigma_m \quad [3.7]$$

or

$$\sigma_{uc} = 0.2 * \eta_L V_f \sigma_f + (1 - V_f)\sigma_{um} \quad [3.8]$$

3.4.8 Dynamic Mechanical Analysis

Dynamic mechanical analysis (DMA) is a technique where in oscillatory force is applied at a set frequency for a sample and the mechanical properties such as stiffness and damping are measured as a function of temperature or time or both. The stiffness is reported as modulus and the damping in reported as tan delta. Since the force is applied as sinusoidal, in the in-phase component is expressed as storage modulus (E') and the out-phase component is expressed as loss modulus (E"). Storage modulus measures the

elastic behavior of the material and the viscous portion is measured as loss modulus. Loss modulus represents the energy dissipated as heat. The ratio of loss to storage modulus is tan delta or damping (δ) (Figure 3.13). It is a measure of how well a material can absorb energy. To summarize, DMA studies tie together material behavior in relation to the molecular structure, processing conditions and product properties (Figure 3.15). In this study correlation between crystallinity, temperature performance and temperature are related.

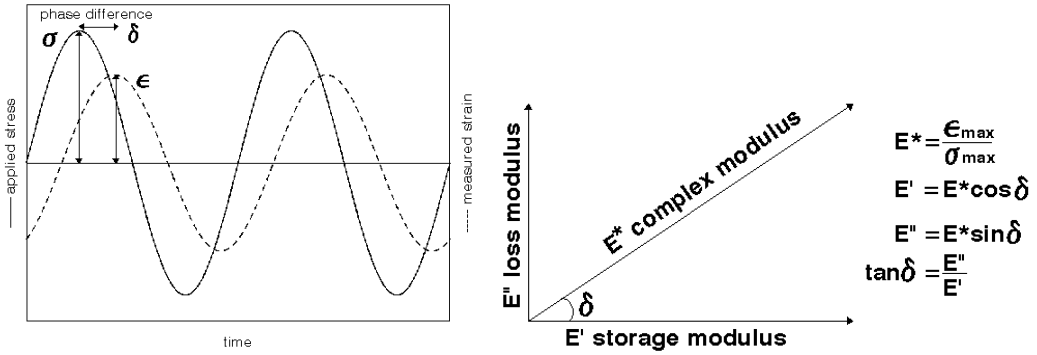

Figure 3.13: The relationship of the applied sinusoidal stress to strain with the resultant phase lag and deformation[4].

DMA analysis was done for all the composites listed in Table 3.1 along with pure PLA. The TA Instruments Q800 series DMA was used for the studies (Figure 3.14). Testing was conducted in a 3-point bending mode. The testing conditions were controlled in the temperature range of -25 to 100°C, with a heating rate of 3°C per minute, fixed frequency of 1Hz, preload of 0.1N, amplitude of 15μm, and force track of 125%. The average dimension of the sample was 20mm×13mm×2mm, as per the specifications provided by TA Instruments for the testing mode used. Storage modulus, loss modulus,

[4] http://www.anasys.co.uk/library/dma1.htm

tan delta and T_g was reported from this testing. Five specimens were analyzed for each sample.

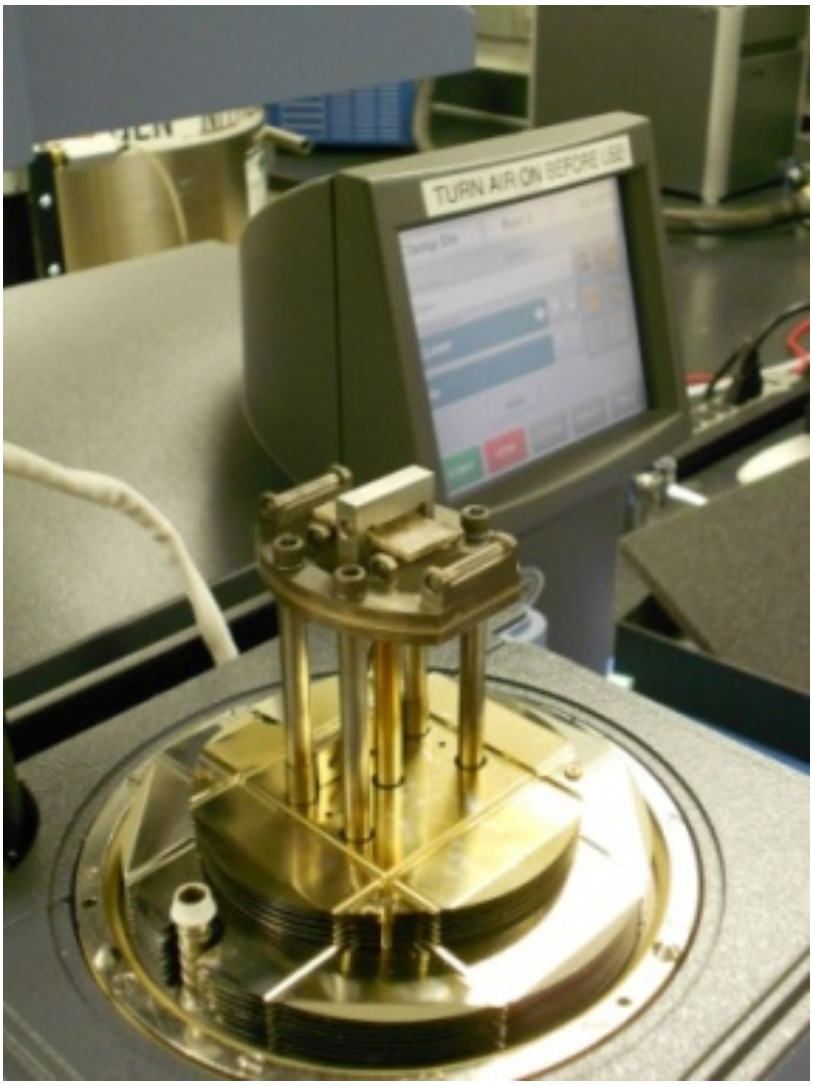

Figure 3.14: TA Instruments Q800 DMA

CHAPTER 4 : EFFECT OF SURFACE FUNCTIONALIZATION ON CHEMICAL AND MECHANICAL PROPERTIES OF HEMP FIBERS

4.1 Introduction

In this chapter, the hemp fiber characterization and tensile property testing results of untreated and treated hemp have been presented. After the hemp fibers were surface treated, both the untreated and treated hemp fibers were subjected to different characterizations, such as Fourier transform Infrared Spectroscopy (FTIR), Scanning electron microscope (SEM) and testing such as thermal stability (using thermo-gravimetric analyzer, (TGA)). The tensile strength of the untreated and treated single fiber was also measured.

4.2 Results and Discussion

4.2.1 Fourier Transform Infrared Spectroscopy

The FTIR spectra of untreated, NaOH treated, silane treated, and acetic anhydride treated hemp fiber are as shown in Figure 4.1. From this figure it could be observed that in comparison to untreated fiber, all the three treatments removed pectin and wax, at the peak around 1750 cm^{-1}. All the chemical modifications are effective in removing good amount of lignin and hemicellulose, which is indicated by the increase in intensity at 1250 cm^{-1} and around 1600–1650 cm^{-1}. The increase in intensity for NaOH treated fibers

at 1000 cm^{-1} and 3300–3500 cm^{-1} is due to the increase in -OH groups on the fiber, which provides active site for interaction between the fiber and thermoplastic matrix. Mwaikambo *et. al.* also found similar peaks when hemp was treated with NaOH [74]. The presence of peak at 1110 cm^{-1} in silane treated hemp is due to the formation of Si-O-Si bonds, which indicate the occurrence of chemical reaction between hydrolyzed silane and hemp fiber, and the existence of polysiloxane network. Sgriccia *et. al.* also found similar peaks when hemp fiber was treated with 3-glycidoxypropyltrimethoxysilanes [112]. In case of acetic anhydride treatment, peak around 1735 cm^{-1} is due to the esterification of hydroxyl group.

Table 4.1: FTIR peaks and corresponding bonds of the peak for untreated and treated hemp fiber

Wave length cm^{-1}	Associated Chemical group	Untreated hemp	NaOH treated hemp	Silane treated hemp	Acetic anhydride treated hemp
1000	-OH intensity	Low	High	High	High
1110	Si-O-Si	Not observed	Not observed	Observed	Not observed
1250	Lignin	Predominant	Reduced	Reduced	Reduced
1600-1650	Hemicellulose	Predominant	Reduced	Reduced	Reduced
1735	Esterification of –OH due to acetyl group	--	--	--	Observed peak
1750	Pectin-Wax	Present	Removed	Removed	Removed
2850	Methylene group	Present	Removed	Removed	Removed
3200-3600	-OH stretching	Low	High	High	High

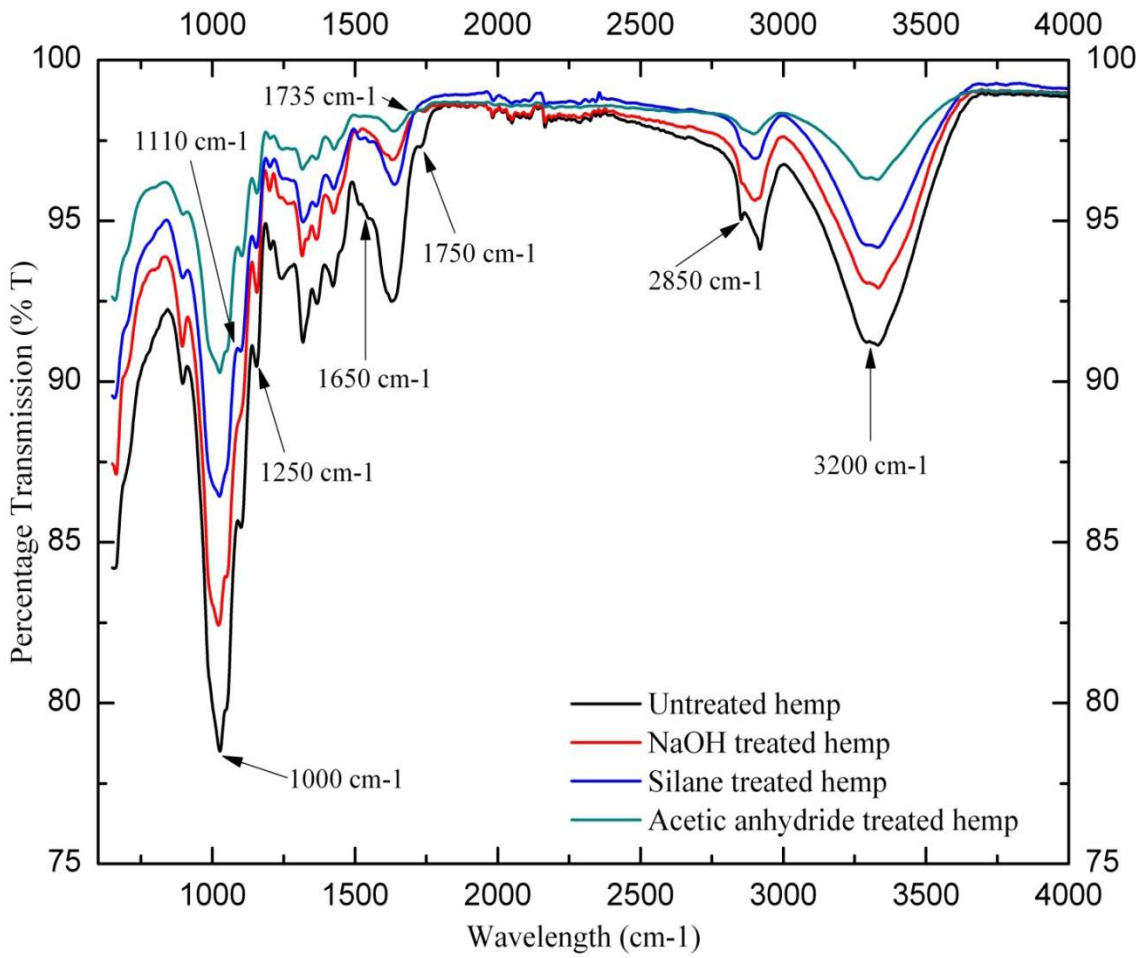

Figure 4.1: FTIR spectra of untreated, NaOH, silane and acetic anhydride treated hemp fibers.

In summary, alkali, silane and acetic anhydride treatments removed the pectin, wax, and partially removed the hemicelluloses and lignin from hemp fiber resulting in increased percentage of cellulose structure. With silane treatment formation of Si-O-Si bond was observed and for acetic anhydride a peak was observed for the esterification of hydroxyl group (C-O), suggesting the plasticization of the cellulose in hemp fiber.

4.2.2 Scanning Electron Microscopy

SEM images depict the surface morphological change of untreated, and all the three types of treated hemp fibers (Figure 4.2). Untreated fibers exhibit smooth surface

due to the presence of wax/pectin and other surface impurities. On the other hand, the rough surface of treated hemp fibers indicated the removal of these surface impurities. As a consequence of the surface treatment, the surface area has been increased to provide more reaction site for fiber–matrix interface. In addition, the increased surface roughness of hemp fiber would likely result in more mechanical interlocking between hemp fibers with PLA matrix. The enhanced interlocking will result in better mechanical and thermal properties for the composite. SEM results are in good agreement with FTIR results.

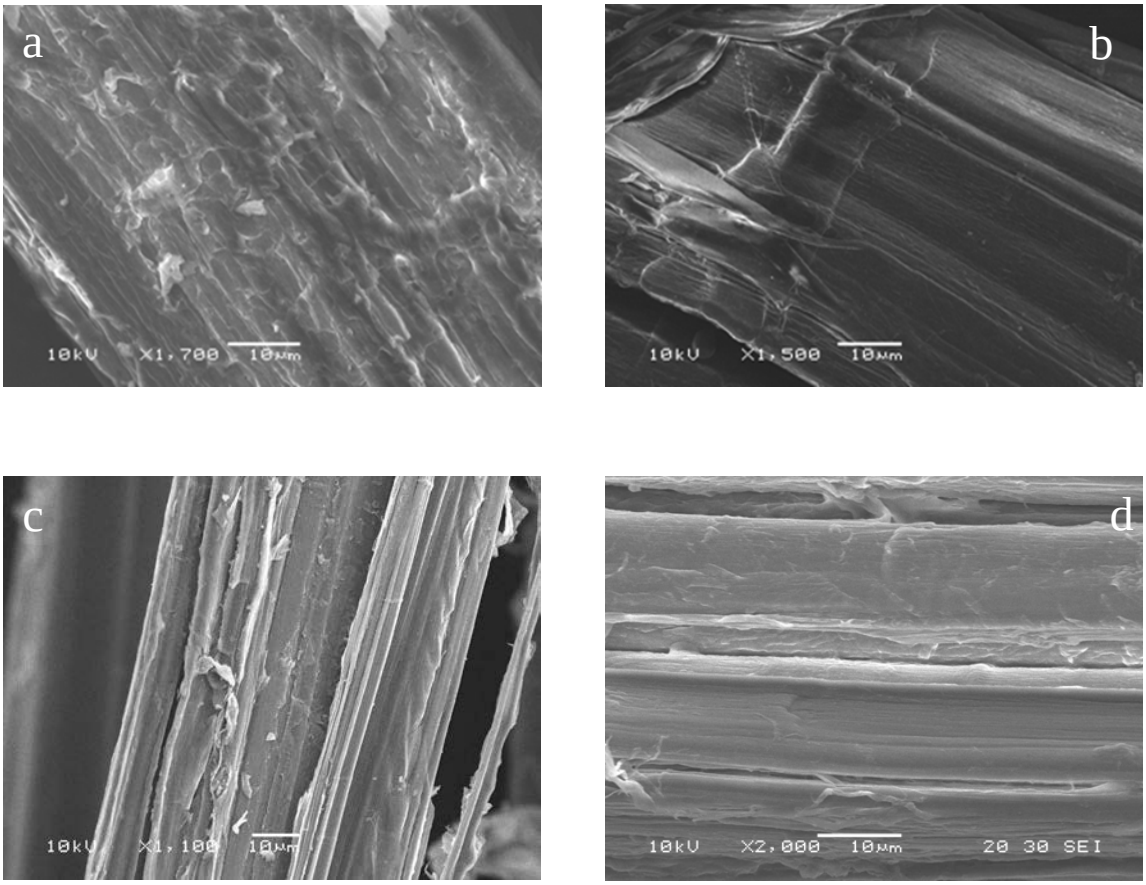

Figure 4.2: Scanning electron microscopic pictures of (a) untreated hemp with impurities, (b) NaOH treated hemp enhanced roughness, (c) silane treated hemp - coating, (d) acetic anhydride treated hemp –coating

4.2.3 Thermogravimetric Analysis

TGA was used to identify the thermal degradation process of the untreated and treated fiber. TGA curves of untreated and treated fibers are represented in Figure 4.3. The curves were obtained at 10°C/min in the range 25 to 550°C. In the case of hemp fiber, thermal degradation takes place in two stages for both untreated and treated fiber. The initial 6-8% of weight loss can be attributed to the inherent moisture in the fiber. But after 250°C, the fiber decomposes rapidly and the complete fiber is degraded by 350-360°C. This second stage degradation involves the degradation of hemicellulose, lignin and cellulose. These tempertures are in the similar range as analysed by the U.S. Department of Agriculture for wood, hemicellulose, cellulose and lignin. In their extensive literature review study of thermal degradration of various wood and wood components, they found that hemicellulose is the least thermally stable compound which degrades around 300°C. Lignin degradation begins around 300°C and completes around 450°C. Cellulsose degradation started at 275°C and was found to completely degrade at around 550°C [113].

The thermal stability of treated fiber is higher than the untreated fiber due to the removal of organic impurties such as pectin and wax present on the surface of the hemp fiber. For NaOH treated fibers, the fibers showed higher thermal stability because, the treatment removes most of the impuities and exposes more cellulose molecules. In case of silane and acetic anhydride treatment, the treatment results in surface coating rather than surface etching as in case of NaOH treatment. This results in reduced thermal stability compared to NaOH, but improved thermal stability in comparison to untreated fibers [84]. The thermal stability of the treated fibers is better than the thermal stability of

the untreated fibers in the order of; NaOH treated > acetic anhydride treated > silane treated > untreated. The degradation of pure PLA is a one step process. The degradation process does not start till 300°C, but after 300°C it proceeds very rapidly and the polymer completely degrades by 400°C. The degardation temperatures at variny percentage weight loss is given in Table 4.2.

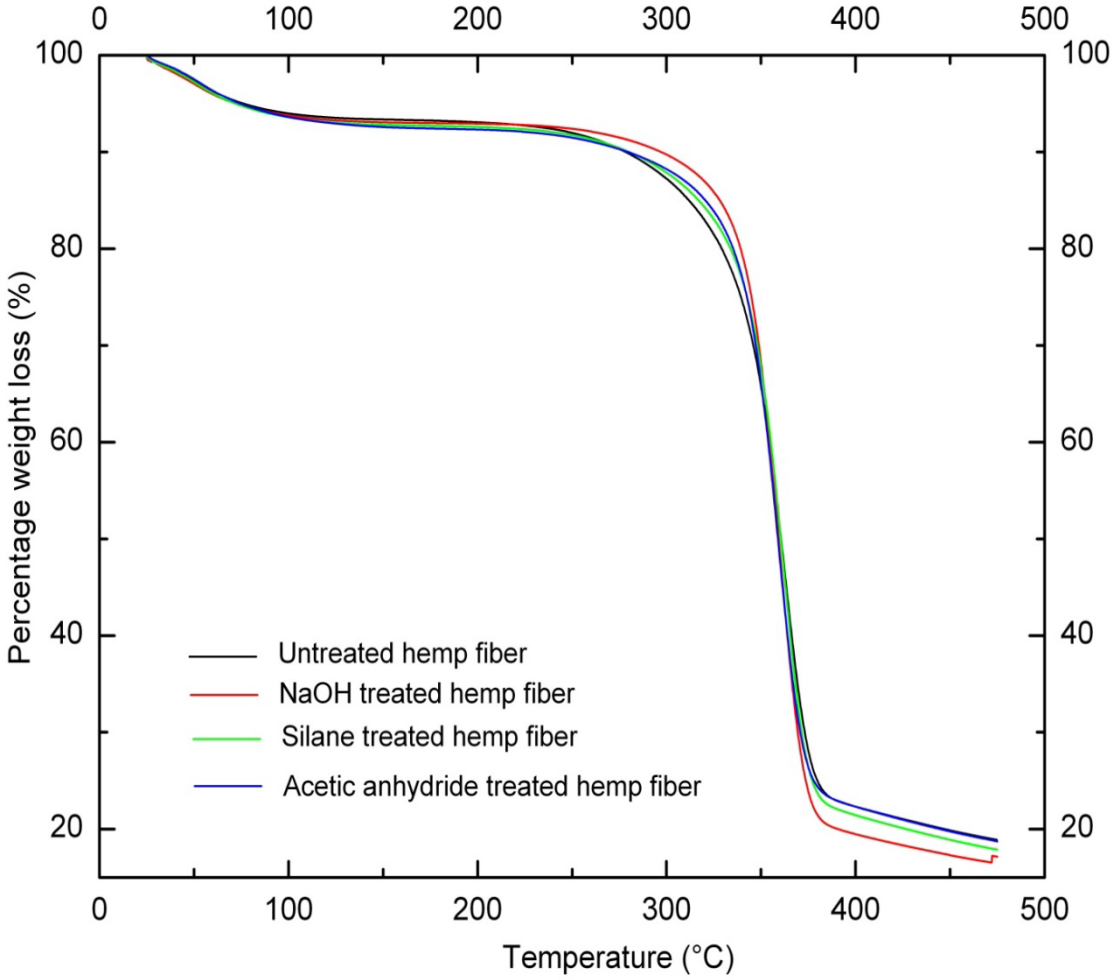

Figure 4.3: TGA curves of pure PLA, untreated and treated hemp fibers

Table 4.2: Degradation temperature (in °C) for untreated and treated hemp fibers

Percentage weight loss	Thermal degradation temperature (°C)			
%	Untreated	NaOH treated	Silane treated	Acetic anhydride treated
10	278.58 (1.36)	297.10 (2.10)	275.50 (5.25)	273.00 (3.53)
15	312.08 (0.66)	328.20 (0.89)	315.38 (1.39)	320.00 (5.01)
25	339.58 (0.12)	345.00 (0.59)	342.19 (0.12)	342.45 (1.07)
50	360.92 (0.51)	359.30 (0.57)	360.31 (0.43)	358.90 (0.38)

4.2.4 Tensile Properties of Single Hemp Fibers

The tensile testing of the single fibers for both untreated and treated hemp fiber was conducted as per ASTM C1557-03 [108]. The average values with standard deviation of the tensile strength of these single fibers are presented in Table 4.3. The results indicated that there was no significant difference in the tensile strength of the fiber after alkali modification; however, there was marginal increase in tensile strength for silane and acetic anhydride modified fiber. The increase in tensile strength with these two surface modifications can be explained as a result of the type of surface modification mechanism. Silane and acetic anhydride results in a coating mechanism, whereas alkali results in etching mechanism. The coating mechanism marginally increases the diameter of the fiber resulting in increased tensile strength.

The stress strain curves for all the fiber specimens tested is given in APPENDIX E.

Table 4.3: Tensile strength of single fiber tested

Fiber type	Tensile strength, MPa	Standard deviation
Untreated hemp fiber	247.51	92.37
NaOH treated hemp fiber	243.73	97.62
Silane treated hemp fiber	275.89	100.87
Acetic anhydride treated hemp fiber	280.89	76.57

4.3 Conclusion

From the surface characterization and testing of untreated and treated hemp fibers, it could be concluded that,

Alkali treatment removes the organic impurities and exposes higher amount of cellulose in the fiber, thus increasing the reaction sites on the fiber. The thermal stability of the alkali treated fiber is higher than the untreated and silane and acetic anhydride treated hemp fiber, since the fiber has been enriched with cellulose with the removal of organic impurities and partial removal of hemicellulose and lignin. Although, the maximum tensile strength of the alkali treated single fiber (243 MPa) is marginally lesser than the untreated fiber (248 MPa), but this is not a significant different.

Silane treatment also aids in removal of organic impurities from the fiber surface as seen by the FTIR spectra of these fibers. In addition to that the silane treatment leads to the formation of Si-O-Si bonds on the surface of the fiber. The thermal stability of the silane treated fiber is higher than the untreated fiber, but lower than the alkali treated fiber since silane treatment does not involve result in an etching mechanism similar to alkali. The effectiveness of the treatment is seen only after the composite formation when a network if formed at the fiber-matrix interface. Silane treatment results in coupling reactions and alkali results in mechanical interlocking. The maximum tensile strength of silane treated fiber (276 MPa) is higher than the untreated fiber (248 MPa). However, this difference is not significant owing to the larger standard deviation in the tensile testing.

Acetic anhydride treatment removes organic impurities from the fiber surface. The esterification of the –OH molecules of cellulose were confirmed by the FTIR spectra. The thermal stability of the acetic anhydride treated fiber is higher than the untreated

fiber, but lower than the alkali treated fiber since this treatment does not involve result in an etching mechanism similar to alkali. The maximum tensile strength of acetic anhydride treated fiber (281 MPa) is higher than the untreated fiber (248 MPa). The acetic anhydride treatments result in the plasticization of cellulose molecules due to esterification which result in addition of bulkier molecule (CH_3CO) on to the cellulose. As mentioned with silane this difference is not significant.

CHAPTER 5 : EFFECT OF SURFACE FUNCTIONALIZATION ON THERMAL STABILITY OF HEMP-PLA COMPOSITES

5.1 Introduction

In the past, several researchers have conducted studies to understand the kinetics of thermal degradation of different natural fibers through examining the activation energy of fiber with chemical additives after surface functionalization. The different modeling methods for calculating activation energy are summarized in Table 1. Kissinger method is based on differential scanning calorimetry analysis (DSC) in which, analysis of decomposition or formation processes is related to the peaks obtained due to calorimetry analysis at various heating rates. Friedman and F-W-O introduced the isoconversional method for determination of activation energy. Friedman used the differential isoconversional method and F-W-O has used the integral isoconversional methods. In both the methods, activation energy is obtained from the isoconversional lines. The modified Coats-Redfern method is also a multiple heating rate application which uses Coats-Redfern equation.

Research related to the effect of fiber chemical treatment on the thermal degradation properties of hemp-PLA composites have not been studied in depth. There are very few studies which have correlated the effect of surface treatment of natural fiber, with activation energy of thermal degradation. However, Yao *et al*. have studied the thermal decomposition processes of ten types of natural fibers commonly used in the polymer composite industry, and calculated the activation energy using various

degradation models including the Kissinger, Friedman, Flynn–Wall–Ozawa, and modifiedCoats–Redfern [114]. Alvarez *et al.* studied the kinetic parameters of commercial blends of starch and cellulose derivatives with sisal fibers using a variety of conventional thermogravimetric methods [115]. They observed that activation energy of these biocomposites did not vary much with the conversion rate suggesting that the thermal degradation mechanism was similar for all.

Only a few studies have been conducted on the hemp-PLA composites with respect to their fabrication, mechanical, and thermo-mechanical properties [58, 60, 116]. In particular, there are no studies currently reporting the kinetics of thermal degradation of hemp-PLA based biocomposites in correlation to activation energy. Therefore, the main objective of this study was to understand the effect of chemical modification on thermal degradation of hemp-PLA biocomposites by using activation energy approach. Among all the available models F-W-O model was chosen since the kinetics parameters for this model can be calculated by conducting experiments at varying heating rates using the thermogravimetric analysis (TGA). This method makes no assumption about the reaction order and is applicable at all points of the TGA curve and activation energy calculated is independent of the conversion rate. Further, the study investigates the effect of fiber loading on thermal degradation in the biocomposite using TGA.

5.2 Theoretical Approach

Thermogravimetric analysis has been used for rapidly assessing the thermal decomposition of the polymeric composites. In the past decade, an increasing number of kinetic studies have been done using TGA for determining rate constants, activation energies, reaction orders and Arrhenius pre-exponential constants [114, 115, 117].

Kinetics studies generally apply one basic rate equation:

$$\frac{d\alpha}{dt} = k.f(\alpha) \quad [5.1]$$

where dα/dt is the rate of conversion at a constant temperature, k is the rate constant. f (α) is the reaction model, and α is the conversion rate which is determined using equation (2)

$$\alpha = \frac{W_o - W_t}{W_o - W_f} \quad [5.2]$$

W_t, W_o and W_f are the time t, initial and final weights of the sample. In the case of polymer degradation, it is assumed that the rate of conversion is proportional to the concentration of material that has to react. Extending the assumption to composites results in equation (3)

$$f(\alpha) = (1 - \alpha)^n \quad [5.3]$$

where, n is the apparent order of reaction. One of the ways to conduct a kinetic study in a TGA is to use a heating rate

$$\beta = dT/dt \quad [5.4]$$

where, β is the heating rate and dT/dt is the change in temperature with respect to time.

The rate constant k is generally given by the Arrhenius equation:

$$k = A.\exp\{-E_a/RT\} \quad [5.5]$$

where, E_a is the activation energy, A is the pre-exponential factor, T is the temperature, and R is the gas constant. By combining equations 1 through 5, equation 6 is obtained as follows

$$d\alpha/(1 - \alpha)^n = \frac{A}{\beta}.exp\left\{\frac{-E_a}{RT}\right\}.dT \quad [5.6]$$

Equation 6 is the most fundamental equation used for studying kinetic parameters using TGA.

Ea, Activation energy is the minimum energy required to start a chemical reaction and the units are normally given in kilojoules per mole. If the bond dissociation energy for reactants is high then activation energy required for the reaction will also be high. Ea can be calculated using various models as depicted in Table 5.1. Flynn-Wall-Osawa is an integral method which gives –Ea/R from the slope of the line obtained by plotting log β against 1/T at any conversion rate. The parameters for activation energy calculation can be calculated from the TGA curves at varying heating rates.

5.3 Results and Discussion

TGA was used to identify the thermal degradation process of pure PLA and hemp-PLA composites. The study was conducted in two parts. In the first part, the thermal stability of the fiber with respect to the effect of chemical treatment and thermal stability of the composites with respect to chemical treatment and fiber loading was studied. For this study, TGA and DTG curves were obtained for untreated and treated fiber, pure PLA and composites with different fiber loadings (20, 30, and 40%) at 10°C/min in nitrogen atmosphere. In the second part of the study, the activation energy of thermal degradation for the composites with 30% fiber volume fraction (both with untreated and treated hemp-PLA composites) were studied. The heating rate for the second part of the study ranged from 5 to 30°C/min in nitrogen atmosphere.

5.3.1 Effect of Fiber Loading

The effect of fiber loading on thermal stability of hemp-PLA composites was studied with both untreated and treated hemp-PLA composites. The fiber volume fractions studied are 20%, 30%, and 40%. For untreated (Figure 5.1) and NaOH (Figure 5.2) treated composites the degradation rate increased with increase in the fiber content.

But in case of silane (Figure 5.3) and acetic anhydride (Figure 5.4) treated composites, the thermal stability increased with an increase in fiber content up to 30% and started to decrease at 40% fiber content. This can be explained by the chemical bond energy at the interface of fiber and matrix. The NaOH treated fiber forms hydrogen bonding (-OH groups) with the matrix, which has a bond energy of 435 KJ/mole. In case of silane and acetic anhydride the bonds formed are Si-O and C=O (ester), with bond energies 460 and 749 KJ/mole [118] respectively. Compared to the NaOH treated hemp-PLA composite, the bond energy of silane treated composite is 5.40% higher and acetic anhydride treated composite is 41.92% higher. The higher bond energy indicates the better fiber matrix adhesion which results in enhanced thermal stability of the silane and acetic anhydride treated hemp composites. But at higher fiber loading of 40%, the amount of matrix available for the fiber is reduced, resulting in insufficent bonding and there by, decreased thermal stability. The comparison of thermal degradation of untreated and treated hemp-PLA composites at 25% weight loss with varying fiber loading is plotted in Figure 5.5. From these results, it could be concluded that 30% fiber volume fraction gives the best thermal stability for both silane and acetic anhydride treated hemp-PLA composites and acetic anhydride treated hemp-PLA composites performs much better than silane treated hemp-PLA composites. This enhanced thermal stability in silane and acetic anhydride treated hemp fiber composites is due to the increased bond energies which results in enhanced thermal stability upto 30% fiber volume fraction. But at 40% volume fraction, the interface adhesion at the interface of the fiber and polymer will be reduced due to decreased amount of polymer for the given amount of fiber.

Table 5.1: Different models available for activation energy calculation [119-122]

Method	Expressions	Plots
Kissinger	$\ln\left\{\frac{\beta}{T_P^2}\right\} = ln\{AR/E_a\} + \{1/T_P\}\left\{\frac{-E_a}{R}\right\}$	$ln\{\beta/T_P^2\}$ against $1/T_P$
Friedman	$ln\frac{d\alpha}{dt} = ln[A\, f(\alpha)] - \frac{E_a}{RT}$	$ln\frac{d\alpha}{dt}$ against 1/T
Horowitz-Metzer	$ln\left[ln\left\{\frac{1}{1-\propto}\right\}\right] = \frac{E_a\ \theta}{R\ T_s^2}$	$ln\left[ln\left\{\frac{1}{1-\propto}\right\}\right]$ against θ
Flynn and Wall	$\frac{-dlog\beta}{d\langle 1/T\rangle} = 0.457\ \frac{E_a}{R}$	-dlogβ against 1/T
Flynn-Wall-Ozawa	$logF(\alpha) = log\left\{\frac{AE_a}{R}\right\} - log\beta - 2.315 - 0.4567\frac{E_a}{RT}$	Logβ against 1/T for a fixed degree of conversation

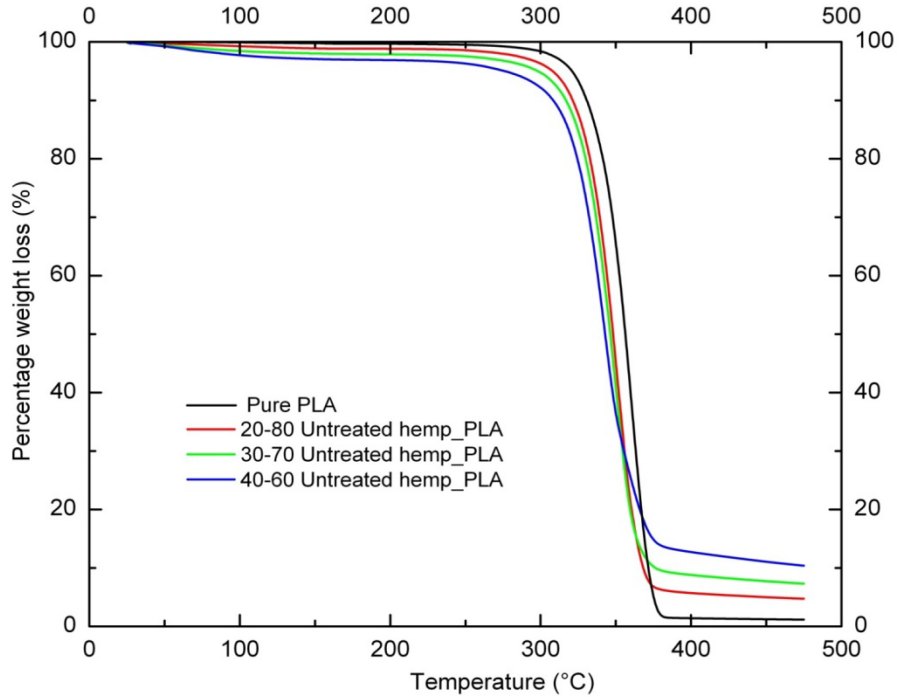

Figure 5.1: TGA curves of untreated hemp-PLA composites at various fiber volume fractions

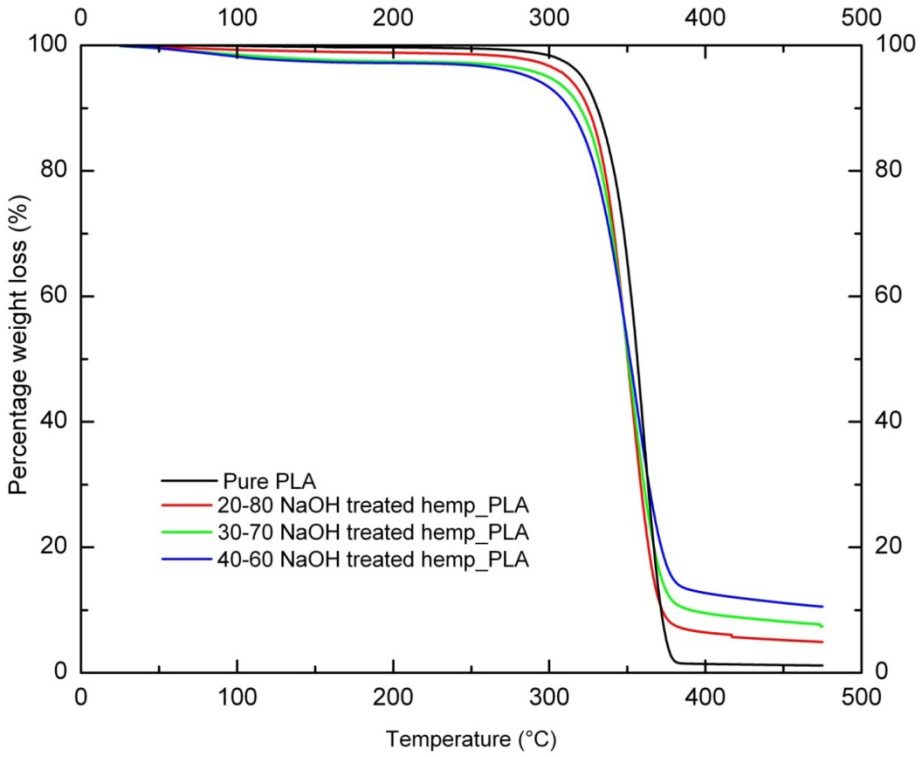

Figure 5.2: TGA curves of NaOH treated hemp-PLA composites at various fiber volume fractions

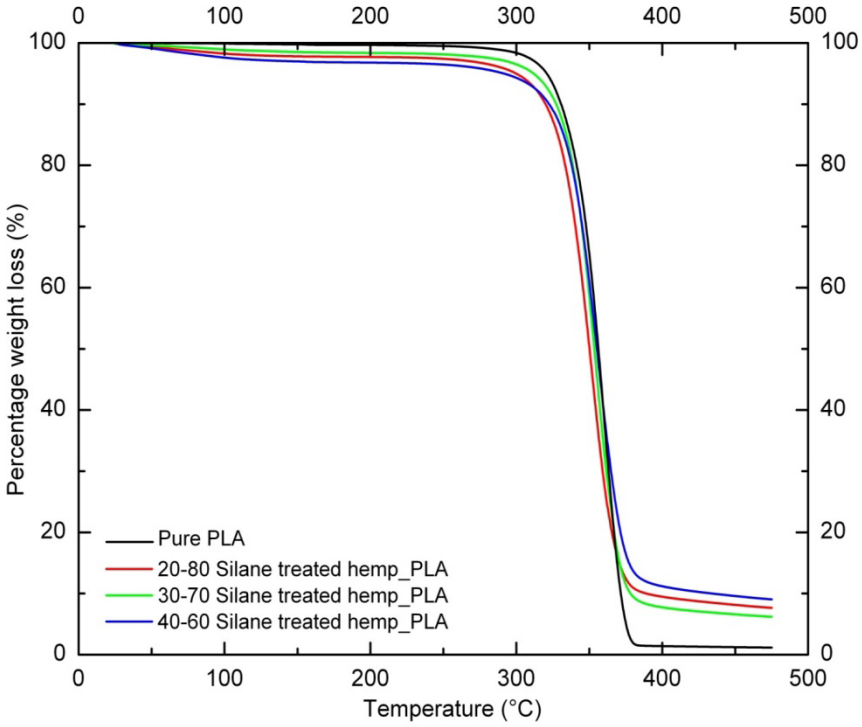

Figure 5.3: TGA curves of Silane treated hemp-PLA composites at various fiber volume fractions

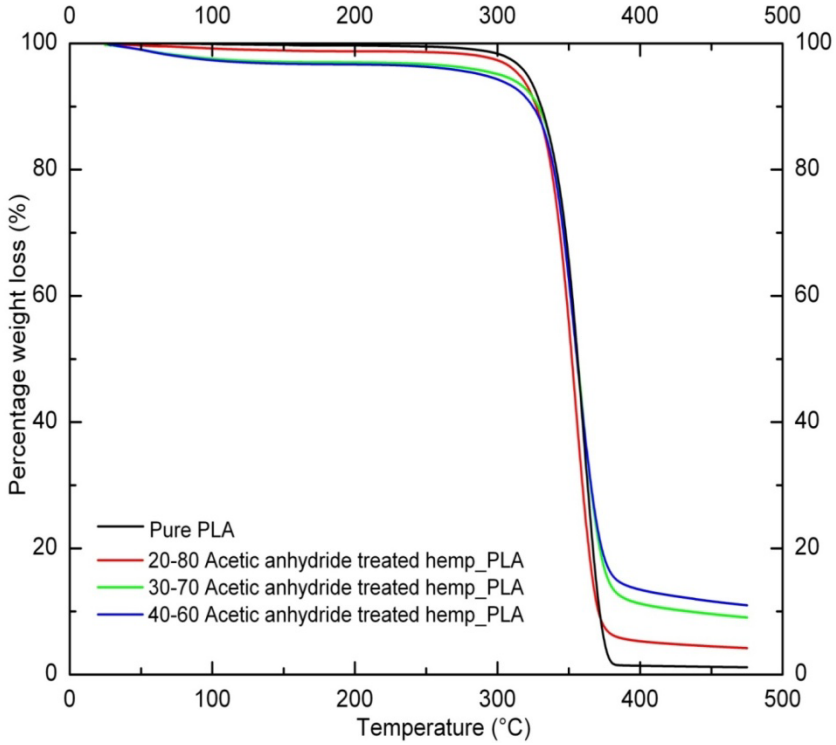

Figure 5.4: TGA curves of Acetic anhydride treated hemp-PLA composites at various fiber volume fractions

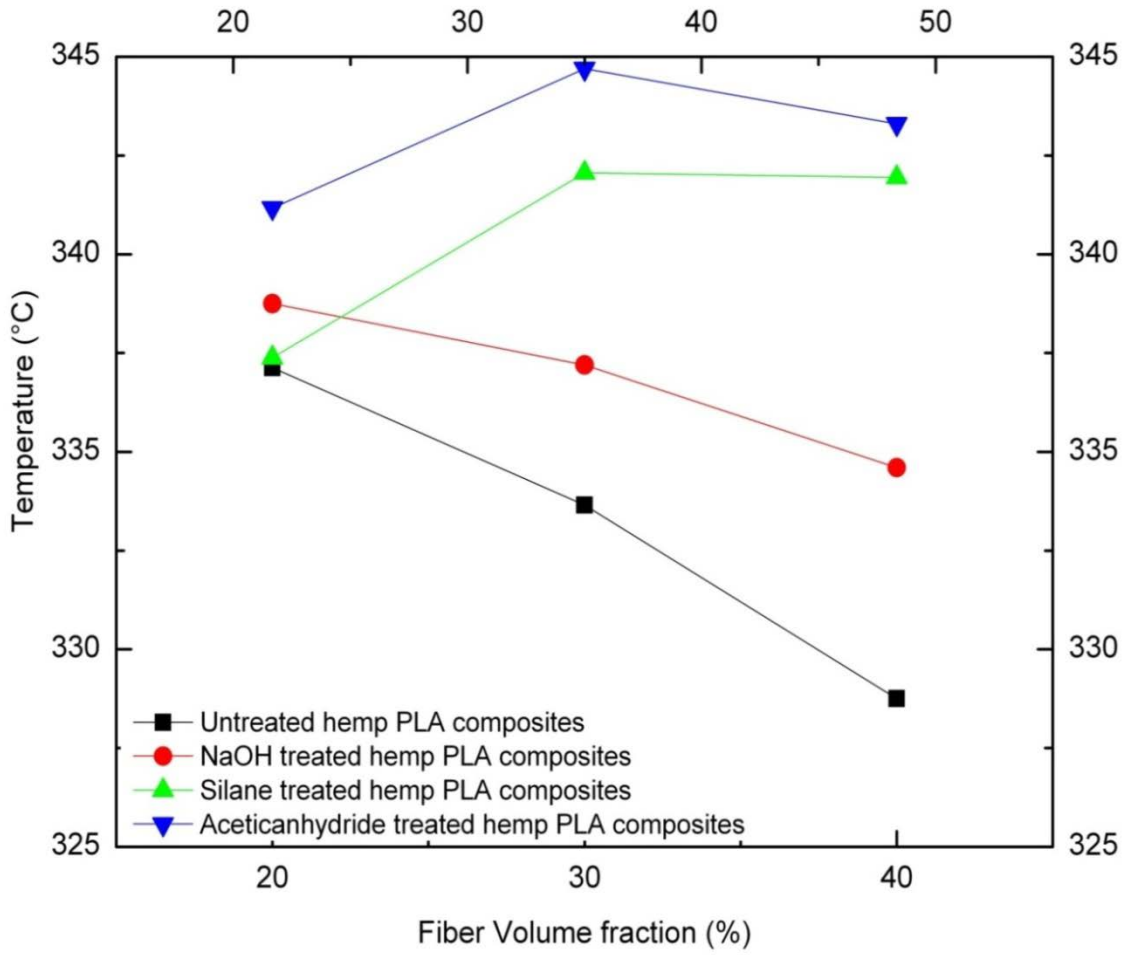

Figure 5.5: Degradation temperature at 25% weight loss for untreated and treated hemp-PLA composites at various fiber fractions

5.3.2 Activation Energy of Thermal Degradation

Previous studies suggest that to avoid compensation effects in determinig kinetic constants, different heating rates have to be used to determine kinetic parameters [115]. Therefore, in this study we have used heating rates of 5, 10, 20, 25, and 30°C to study the thermal degradation kinetics of 30% fiber volume fraction of hemp-PLA composites. The TGA and DTG curves for untreated (Figure 5.6) , NaOH (Figure 5.7), silane (Figure 5.8), and acteic anhydride (Figure 5.9) treated hemp-PLA composite at different heating rates are presented. The trend was similar trend with all hemp-PLA composites. It can be

observed that with increase in heating rate the maximum degradation increased. Similar to what was reported by Alvarez *et. al.*[115].

The average activation energy of thermal degradation was calculated from the conversion range of 0.1 to 0.7 through iso-conversional F-W-O method for both untreated and treated hemp-PLA composites. Figure 5.10 depicts the linear plot for acetic anhydride treated hemp-PLA composites at various conversion rates. The same trend was observed in case of other treated and untreated hemp-PLA composites. From these plots it can be observed that the reaction mechanism of thermal degradation for both treated and untreated hemp-PLA composite is similar. Activation energies at varying conversion rate were calculated from the slope of these curves. Table 5.2, gives the summary of the activation energy values with the R^2 values for these lines.

The plots of activation energy as a function of conversion rate for $\alpha = 0.1\text{-}0.7$ for all the four composites is given in Figure 5.11. Activation energy changed drastically from low conversion (10%) to high conversion rate (40%) and was quite stable at higher conversion, which indicate that the degradation mechanism at low conversion was different than at higher conversion. This could be explained by the thermal degradation temperatures of the TGA curves. The thermal degradation tempearture range for 10% conversion is around ~ 310°C and for 40% conversion is around ~350°C. This is the part of the TGA curve where in the slope is maximum, suggesting that this is the region where in higher thermal degradation takes place. As discussed previously, maximum degaradtion of hemicellulose, cellulose and lignin take place in this temperature range [113]. Therefore, activation energy changes drasically below 40% conversion since the mechanism involving the decomposition of these ligno-cellulosic matter is different and

once most of these materials are degraded, that is, the decomposition mechanism after 40% is different resulting in quite stable activation energy values A similar trend was observed by other groups who studied activation energy for fibers [114, 115, 123]. Both untreated and treated hemp fiber composites showed similar trend. Although the composites showed similar trend, the activation energy values with acetic anhydride treated hemp-PLA composite was 10-13% higher than untreated hemp-PLA composites. The value of activation energy can be ranked as acetic anhydride treated hemp-PLA composite (157-163 KJ/mole) > silane treated hemp-PLA composite (148-153 KJ/mole) > NaOH treated hemp-PLA composite (138-150 KJ/mole) > untreated hemp-PLA composite (136-141 KJ/mole). The higher activation energy of the acetic anhydride treated hemp-PLA composite can be explained as the result of higher bond energy that results from the acteic anhydride treatement which consecutively results in higher thermal stability of these composites in comparison to other composites.

Table 5.2: Activation energy at various conversion rates

	Untreated hemp-PLA		NaOH treated hemp-PLA		Silane treated hemp-PLA		Acetic anhydride treated hemp-PLA	
Conversion rate (α), %	Activation Energy, Ea, KJ/mol	R^2	Activation Energy, Ea, KJ/mol	R^2	Activation Energy, Ea, KJ/mol	R^2	Activation Energy, Ea, KJ/mol	R^2
10	136.64	0.9989	138.68	0.9954	148.28	0.9423	157.853	0.9985
20	137.20	0.9983	144.35	0.9981	152.08	0.9893	163.391	0.9984
30	138.70	0.9985	146.23	0.9984	153.06	0.9955	163.398	0.9988
40	140.22	0.9985	147.79	0.9986	153.33	0.9976	162.091	0.9986
50	140.66	0.9979	148.59	0.9987	152.75	0.9989	161.226	0.9988
60	140.95	0.998	148.64	0.9989	151.14	0.9983	161.246	0.9988
70	140.63	0.9975	150.45	0.9993	151.27	0.9966	159.705	0.9991

5.4 Conclusions

In this study, the effect of chemical surface modification on the thermal degradation characteristics of the hemp-PLA composites was studied by using activation energy approach. Further, we also investigated the effect of fiber loading on thermal degradation behavior. From the results it can be concluded that NaOH treated hemp fibers have the highest thermal stability compared to the other two treatments and untreated hemp fiber. NaOH treatment of hemp can be suggested as an etching mechanism resulting in removal of organic impurities and exposing higher amount of cellulose. On the other hand, the treatment with silane and acetic anhydride is more of a surface coating mechanism (coupling), where in the reaction will be complete once the fibers are embedded in the matrix. When the treated fibers are used for manufacturing composites with PLA, acetic anhydride and silane treated hemp composites result in the higher thermal stability because the coupling reactions are complete once the fibers are brought in contact with the matrix. These coupling reaction result in strong covalent bonds, such as the Si-O-Si. In case of untreated and NaOH treated fibers, thermal stability decreased with increased fiber loading. NaOH treated fibers result in only hydrogen bonding with the matrix and these bonds are not as strong as the covalent bonds created by the silane or acteic anhydride. In the case of silane and acetic anhydride treated fibers, thermal stability increased with increase in fiber loading upto 30% and started to decrease at 40% fiber loading. This could be attributed to the higher bond energies with these treatments. This was further justified by the activation energy calculation, where in it was observed that acetic anhydride treated hemp composite has highest activation energy in the range of 158-163 KJ/mole. This indicates that higher

energy is required to break these bonds, which could be attributed to enhanced fiber-matrix adhesion after treatments.

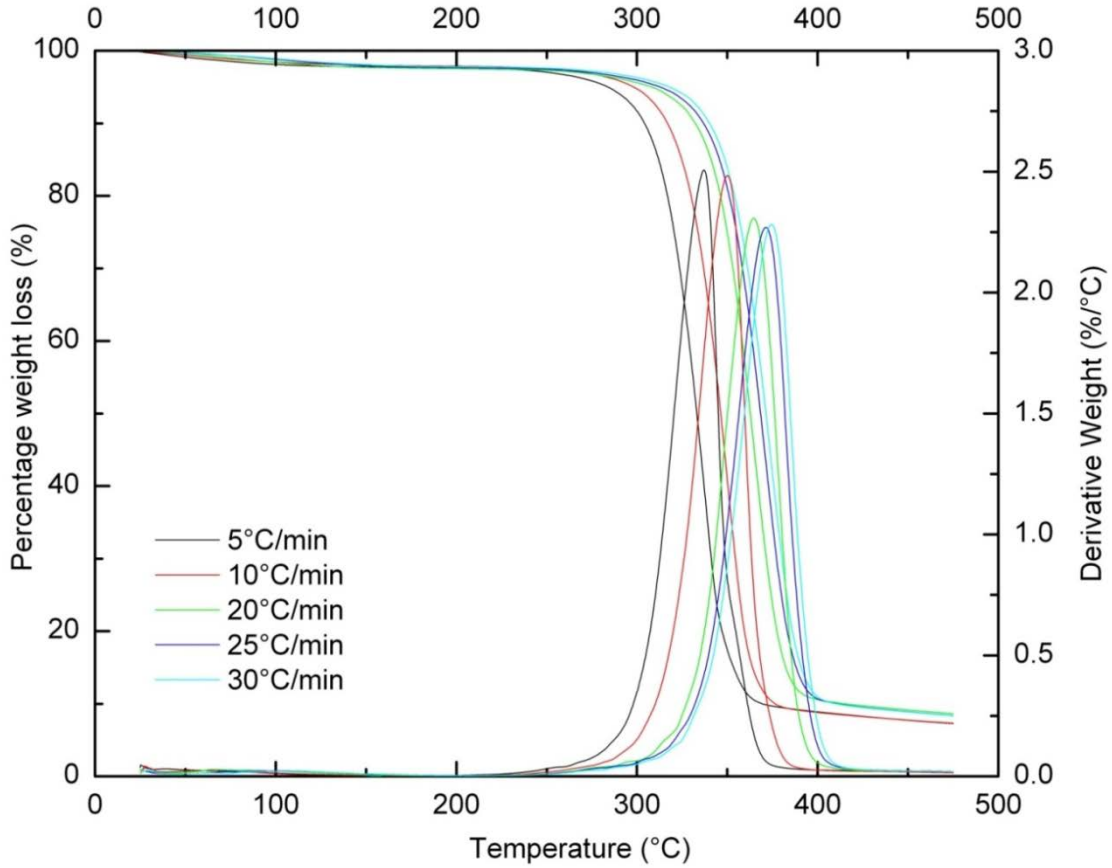

Figure 5.6: TGA and DTG curves for 30-70 untreated hemp-PLA composites at various heating rates

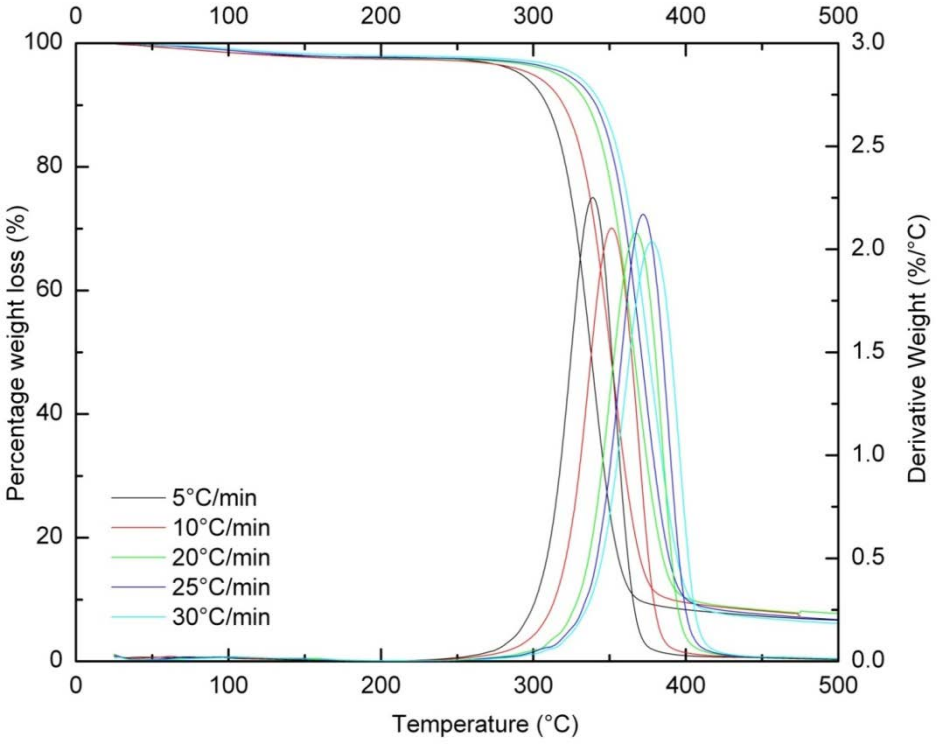

Figure 5.7: TGA and DTG curves for 30-70 NaOH treated hemp-PLA composites at various heating rates

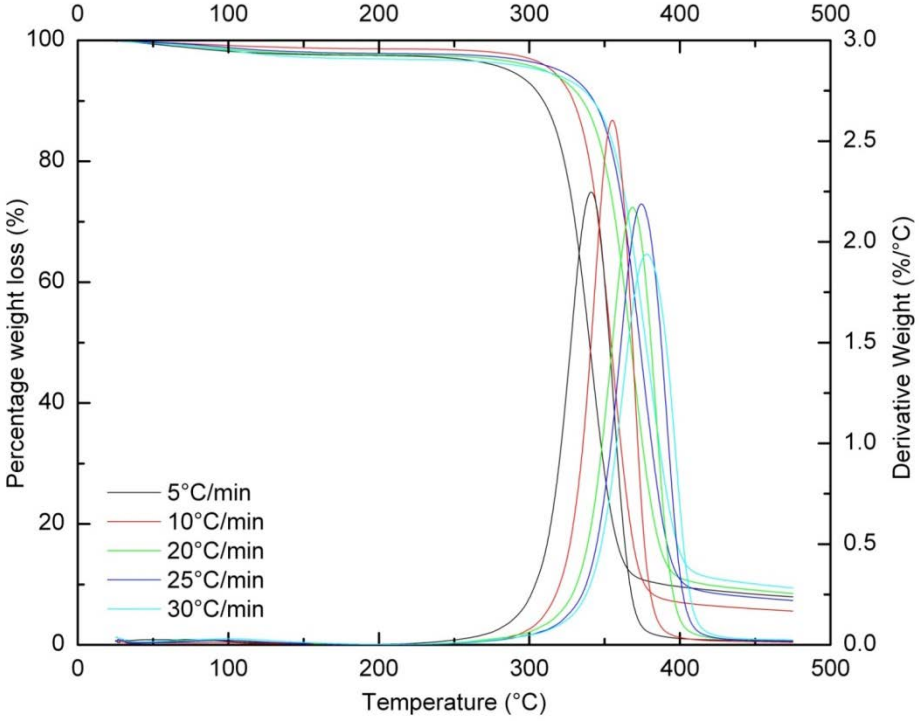

Figure 5.8: TGA and DTG curves for 30-70 silane treated hemp-PLA composites at various heating rates

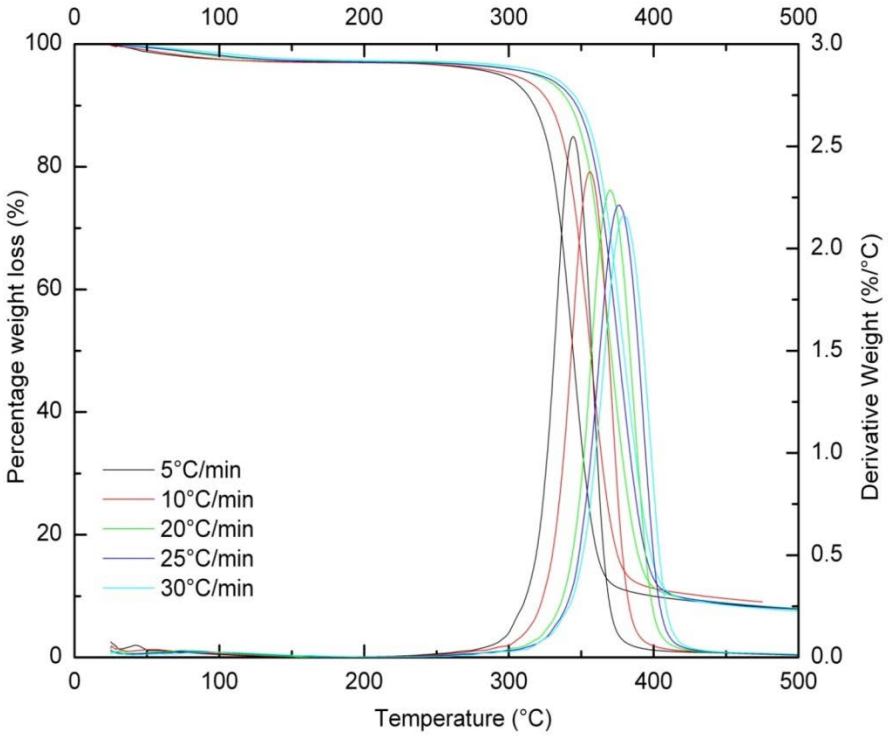

Figure 5.9: TGA and DTG curves for 30-70 acetic anhydride treated hemp-PLA composites at various heating rates

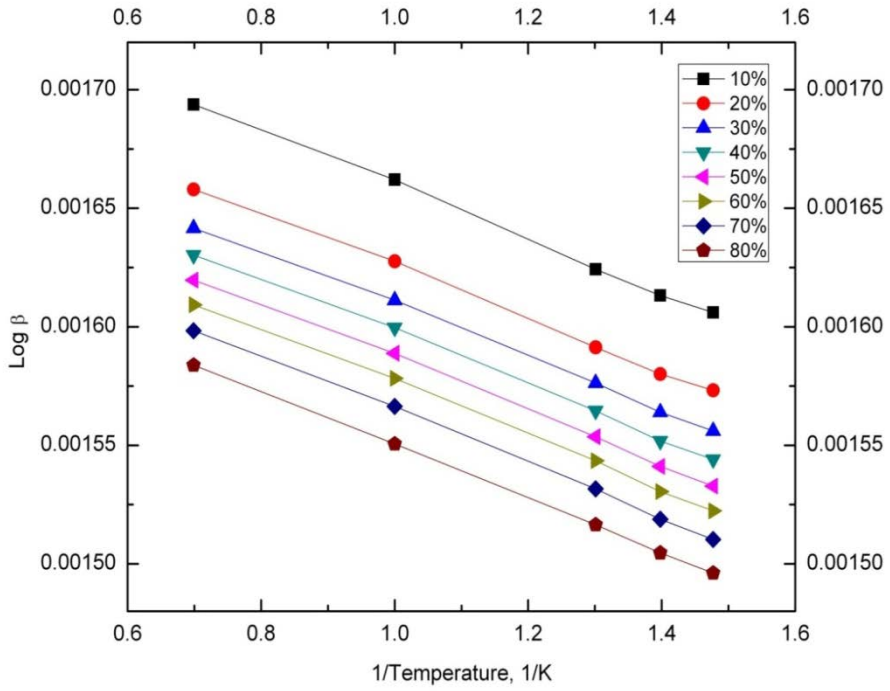

Figure 5.10: Plot for calculation activation energies at various conversion rates (30-70 acetic anhydride treated hemp-PLA)

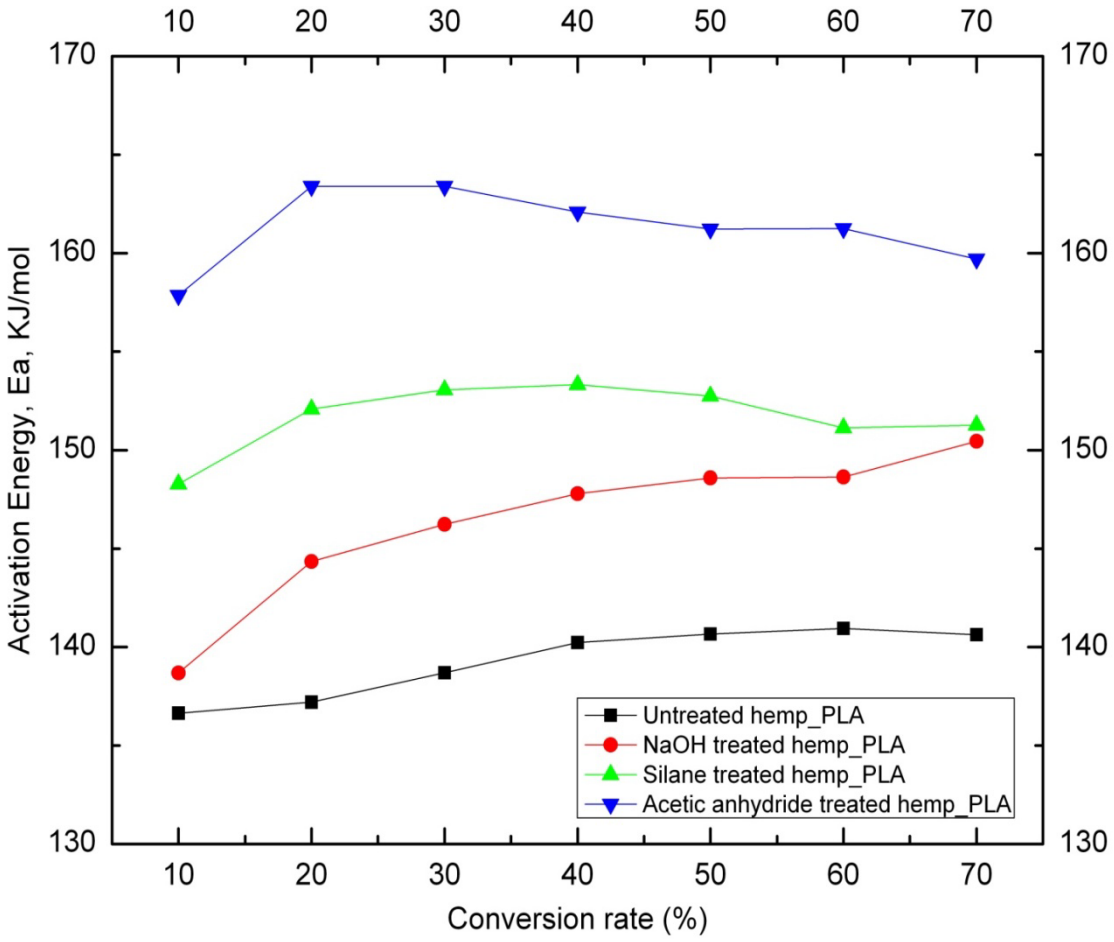

Figure 5.11: Activation energy at various conversion rates for all hemp-PLA composites at 30-70 ratio

CHAPTER 6 : EFFECT OF SURFACE FUNCTIONALIZATION ON MECHANICAL AND THERMO MECHANICAL PROPERTIES OF HEMP-PLA COMPOSITES

6.1 Introduction

The term biocomposites refers to a new class of engineered materials comprised mainly of natural fiber and a plastic component, which is derived from natural sources. Currently, PLA has been a frequent choice of matrix for biocomposites. Initially, these composites were considered only for non-structural, non-load bearing applications, and these materials were not subjected to harsh environmental conditions. However, with extensive research on fiber-matrix interphase adhesions, these materials are being considered as an alternative to traditional building materials. The main obstacle in utilizing these materials as structural members is the general lack of understanding about the effect of surface modifications on the bulk mechanical and thermo-mechanical properties of these composites.

Both natural fiber and matrix exhibit time and temperature dependent behavior, mainly due to their viscoelastic nature. Previous work by Huda et al. has shown that storage and loss modulus of the PLA based composites increased with the addition of fibers. Yet in another work Huda et al. found that alkali pretreated silane treated fiber significantly improved mechanical properties. Due to the temperature-dependent performance of PLA, further investigation of the biocomposite material should be conducted in order to quantify changes in the mechanical performance due to change in temperature. In this study, along with static mechanical testing, an attempt has been made

to understand the effect of operating temperature (-25 °C to 100 °C) on the mechanical performance of hemp-PLA composite formulations.

Static (tensile and flexural) and dynamic mechanical analysis were employed to monitor changes in mechanical performance due to temperature. The testing method and specifications adapted for mechanical and thermo-mechanical testing can be found in Chapter 3. This chapter reports the results and discussion for those experiments and concludes with the summary of the findings.

6.2 Tensile Testing – Results and Discussion

Tensile strength of pure PLA and hemp-PLA composites (both with untreated and treated hemp fiber) were carried out in general accordance with ASTM 3039 standards [109]. The test was conducted on a rectangular-shaped specimen with dimensions of 152.4 mm length, 25.4 mm width, and 2.5 mm thickness.

The representative stress-strain curves for hemp-PLA composites for varying fiber volume fractions are plotted for untreated (Figure 6.1), NaOH (Figure 6.2), silane (Figure 6.3), and acetic anhydride (Figure 6.4) treated hemp-PLA composites. A comparison of tensile strength and Young's modulus at 1% strain, between untreated and treated hemp-PLA composites at various fiber volume fractions, is given in Figure 6.5 and Figure 6.6, respectively.

Effect of fiber loading: Composites were manufactured with three levels of fiber loading: 20%, 30% and 40%. In the case of untreated, silane, and acetic anhydride treated hemp-PLA composites, the tensile strength increases with an increase in fiber loading up to 30%. At 40% fiber loading, the tensile strength decreases for all three composites. In the case of alkali treated hemp-PLA composite, the tensile strength is

maximum at 20% and decreases drastically with an increase in fiber loading at higher fiber volume fractions. This trend in alkali treated hemp-PLA composites could be explained due to the difference in the type of bond formation after treatment. In the case of NaOH, the fiber-matrix has a hydrogen bond. However, in case of silane, the bonds formed are covalent bond and in case of acetic anhydride the composite has C=O bonds due to the esterification reaction during surface treatment. The covalent bond of Si-O-Si network and C=O are much stronger bonds than the -OH, which results in poor interface adhesion in the case of alkali treated hemp-PLA composites. The summaries of tensile testing data are tabulated in Table 6.1 and Table 6.2.

Table 6.1: Tensile strength for composites at various fiber volume fractions

Tensile Strength, MPa						
	20/80		30/70		40/60	
		Std.dev		Std.dev		Std.dev
Untreated hemp-PLA	21.43	2.44	28.09	2.40	18.80	3.57
NaOH-treated hemp-PLA	33.29	1.36	29.16	2.90	21.29	1.81
Silane treated hemp-PLA	16.38	1.59	29.66	1.09	27.38	1.60
Acetic Anhydride treated hemp-PLA	34.52	3.53	35.55	1.26	30.38	3.46

*Std.dev – Standard deviation obtained by testing 7 specimens per sample

Effect of surface treatment: Comparing all the three different treatments, it could be concluded that acetic anhydride treatment enhance the tensile properties significantly compared to NaOH and silane treatment. Compared to untreated hemp-PLA composites, acetic anhydride treated hemp-PLA composites result in 61.1, 26.6 and 61.6 % higher tensile strength at 20, 30 and 40% fiber volume fraction, respectively. In case of silane treated hemp-PLA composites, there is no significant improvement at 20% fiber loading but at 30 and 40% fiber loading, the tensile strength is 5.6 and 45.6% greater than untreated hemp-PLA composites, respectively. Comparing alkali treated hemp-PLA

composite to untreated hemp-PLA composites, fiber tensile strength at 20, 30, and 40% fiber volume fraction is 55.34%, 3.8% and 13.24% higher, respectively. With NaOH treatment the tensile strength decreases marginally (from 20% to 30% fiber volume fraction). The Young's modulus showed similar trend as that of tensile strength.

Table 6.2: Tensile modulus at 1% strain for composites at various fiber volume fractions

Young's Modulus at 1%, GPa						
	20/80		30/70		40/60	
		Std.dev		Std.dev		Std.dev
Untreated hemp-PLA	1.37	0.15	1.76	0.18	1.23	0.19
NaOH-treated hemp-PLA	1.47	0.14	1.48	0.16	1.20	0.16
Silane treated hemp-PLA	1.08	0.06	1.77	0.13	1.39	0.23
Acetic Anhydride treated hemp-PLA	1.71	0.35	1.78	0.09	1.58	0.18

*Std.dev – Standard deviation obtained by testing 7 specimens per sample

Pure PLA panels resulted in 25.4 MPa tensile strength and 1.92 GPa Young's modulus. Incorporation fiber in composites resulted in enhanced tensile properties for all the composites.

From these results, it was concluded that 30% fiber volume fraction is optimum for hemp-PLA composites. Although, all the three surface modifications resulted in higher tensile strength compared to untreated fibers, acetic anhydride treated hemp-PLA composite resulted in highest tensile strength. The fracture pictures and stress strain curves of each specimen tested is presented in Appendix A and B respectively.

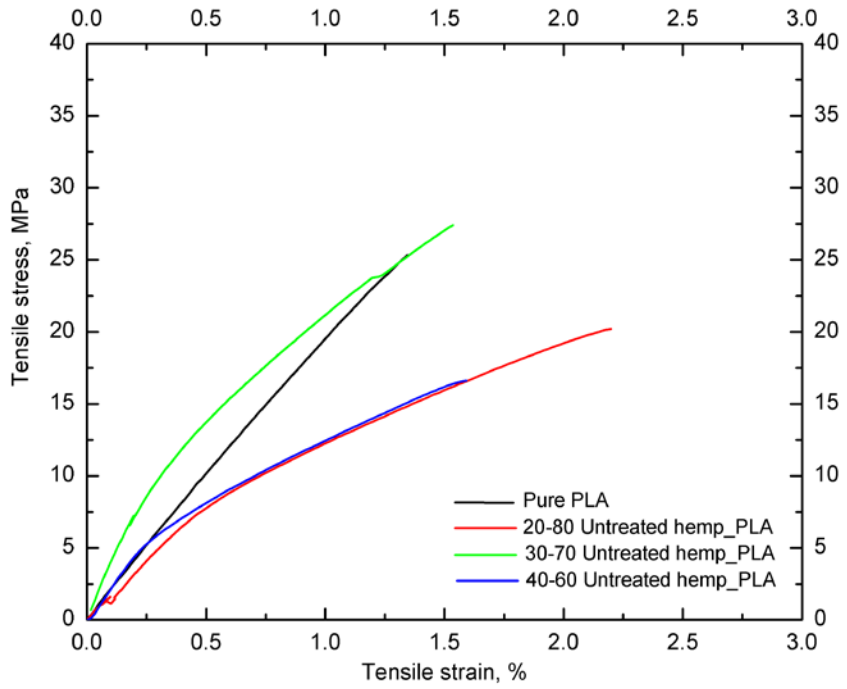

Figure 6.1: Representative stress-strain curve of untreated hemp-PLA composites at varying fiber volume fraction

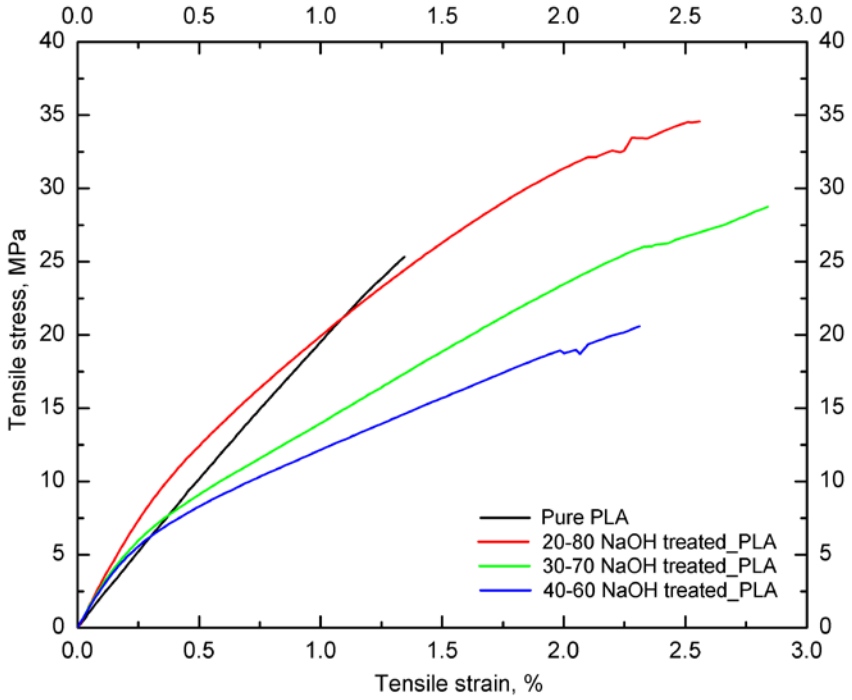

Figure 6.2: Representative stress-strain curve of NaOH treated hemp-PLA composites at various fiber fractions

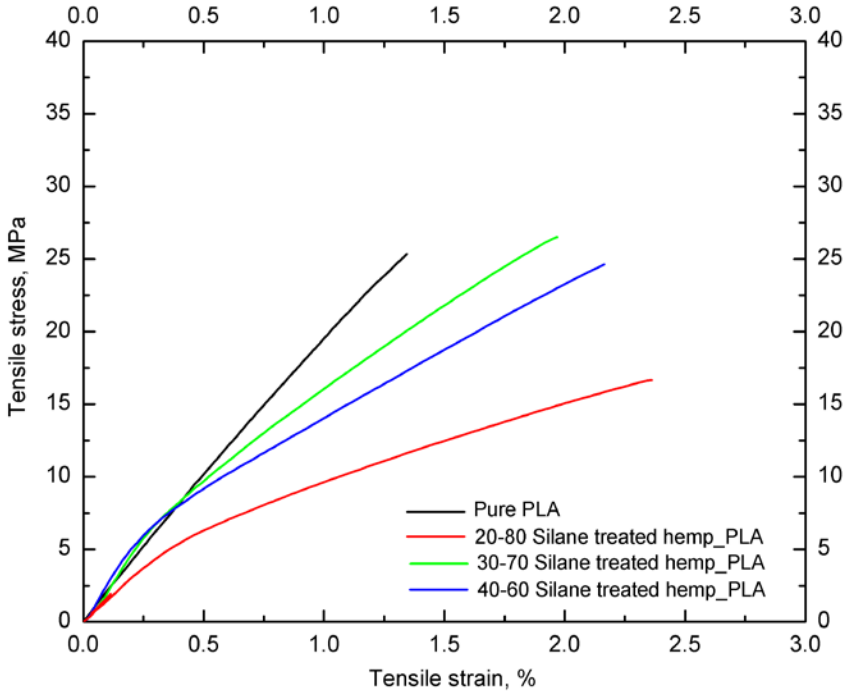

Figure 6.3: Representative stress-strain curve for Silane treated hemp-PLA composites at various fiber fractions

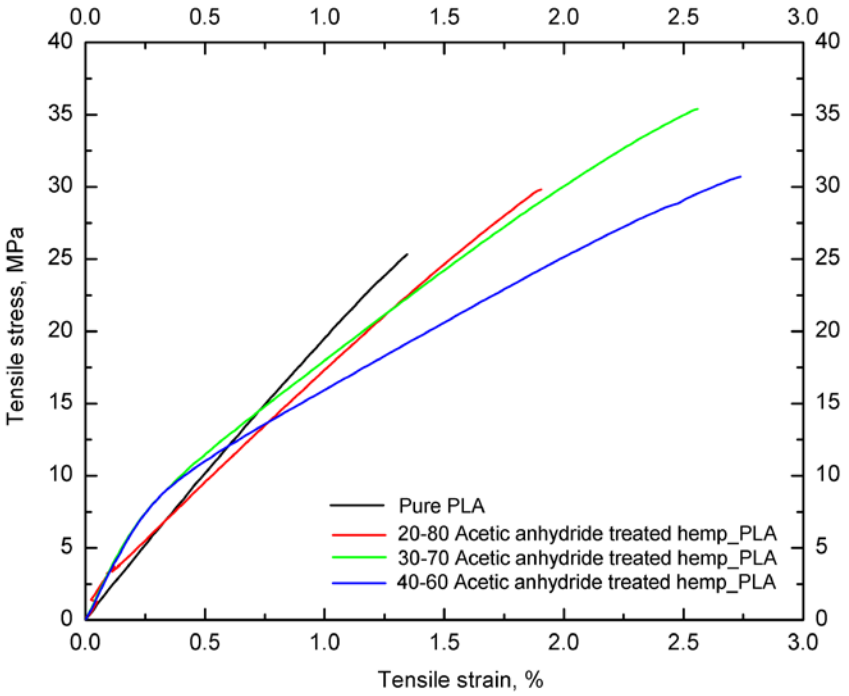

Figure 6.4: Representative stress-strain curves for acetic anhydride treated hemp-PLA composites at various fiber fractions

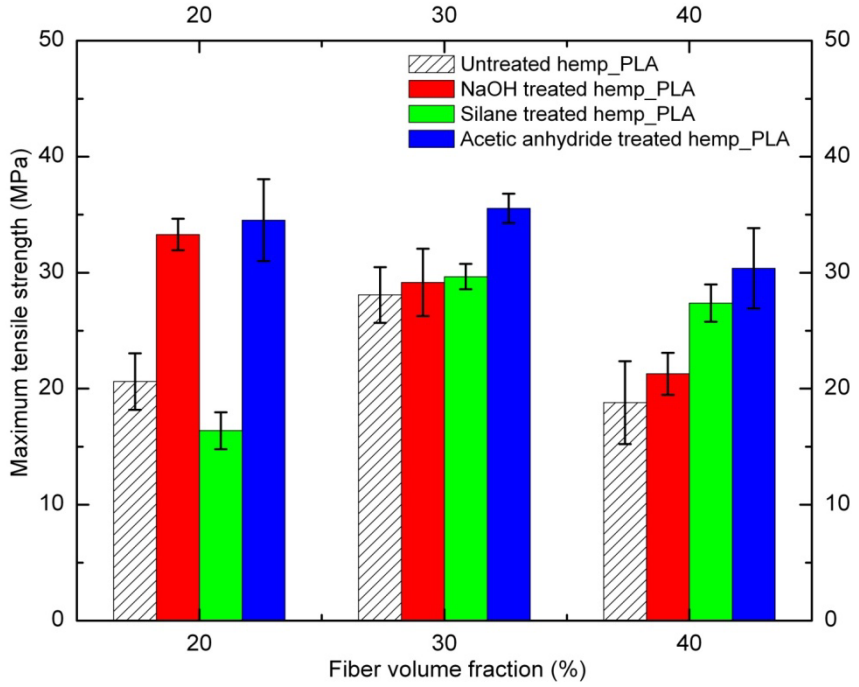

Figure 6.5: Tensile strength versus fiber volume fractions for both untreated and treated hemp-PLA composites

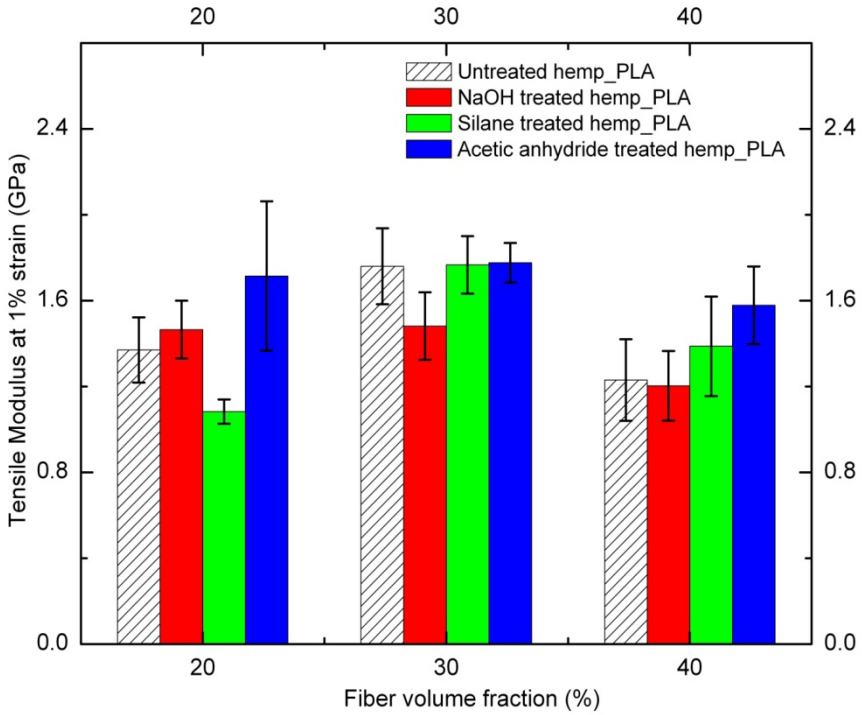

Figure 6.6: Tensile modulus at 1% strain at different fiber fractions for both untreated and treated hemp-PLA composites

6.3 Flexural Testing – Results and Discussion

Flexural strength of pure PLA, and hemp-PLA composites (both with untreated and treated hemp fiber) were recorded in accordance with ASTM 790 [110] standards. The test was conducted on a rectangular shaped specimen with dimensions of 152.4 mm length, 25.4 mm width, and 6 mm thickness.

The maximum flexural strength and flexural modulus at 2% strain of the hemp-PLA composites for both untreated and treated composites at various fiber volume fractions are given in Figure 6.7 and Figure 6.8, respectively.

Effect of fiber loading: Composites were manufactured with three levels of fiber loading: 20%, 30% and 40%. The flexural strength decreased with increased fiber content for NaOH and silane treated hemp-PLA composites. For untreated and acetic anhydride treated hemp-PLA composites, flexural strength increased with fiber content up to 30% and decreased at 40%, suggesting that the amount of PLA available for effective wetting is lesser at 40%. In addition, the above finding is consistent with the tensile strength results of hemp-PLA fiber composites, with the exception of silane treated hemp-PLA composites. Although in literature the observed trends are different. Sawpan et al.[124] Serizawa et al.[39] and Huda et al.[38] found that flexural strength decreased with increase in fiber content but the flexural modulus increased with an increase in fiber content, for both untreated and treated composites.

The hemp-PLA composites having higher flexural strength but lower flexural modulus characteristics can be explained as follows; PLA is brittle polymer (measured flexural strength of 37.73 MPa and flexural modulus at 2% strain being 0.28 GPa), and the addition of hemp fiber decreases the brittleness of the PLA. The lowering of flexural

modulus indicates that the composites have higher flexibility compared to that of pure PLA after the addition of fibers. This characteristic of the hemp-PLA composites is advantageous because higher flexibility results in lesser chance of fracture under stress.

Effect of treatment: Acetic anhydride treated hemp-PLA composites yielded 121.24 MPa flexural strength at 30% fiber volume fractions which is 23% higher than the untreated hemp-PLA composite at the same fiber fraction. The higher flexural strength in case of acetic anhydride treated hemp-PLA is due to the presence of C=O bond in the composites due to the esterification reaction during surface treatment. The C=O bond has higher bond energy compared to the Si-O and -OH bond; therefore, acetic anhydride treated hemp-PLA composite result in better mechanical properties. NaOH treated hemp-PLA composite had flexural strength of 103.11 MPa strength which is 10% higher than the untreated hemp-PLA composites. The lower strength of NaOH in comparison to acetic anhydride treatment can be suggested due the hydrogen bonds after NaOH treatment. The reduction in flexural strength of silane can be said to be an anomaly. Table 6.3 and 6.4 summarizes the results of flexural testing.

The fracture pictures and stress strain curves of each specimen tested is presented in Appendix C and D respectively

Table 6.3: Flexural strength for composites at various fiber volume fractions

Maximum Flexural Strength, MPa						
Fiber-matrix ratio	**20/80**		**30/70**		**40/60**	
Type of Composite	**MPa**	**Std. devi**	**MPa**	**Std. devi**	**MPa**	**Std. devi**
Untreated hemp-PLA	87.87	4.20	93.11	6.49	29.14	3.36
NaOH treated hemp-PLA	104.94	3.07	103.11	5.18	86.67	11.05
Silane treated hemp-PLA	95.69	3.56	88.57	5.19	44.08	3.85
Acetic Anhydride treated hemp-PLA	77.41	3.31	121.24	6.38	91.71	2.68

Table 6.4: Flexural modulus at 2% strain for composites at various fiber volume fractions

Flexural Modulus at 2% strain, GPa						
Fiber-matrix ratio	**20/80**		**30/70**		**40/60**	
Type of Composite	**GPa**	**Std. devi**	**GPa**	**Std. devi**	**GPa**	**Std. devi**
Untreated hemp-PLA	0.29	0.02	0.23	0.01	0.29	0.03
NaOH treated hemp-PLA	0.16	0.01	0.14	0.00	0.13	0.01
Silane treated hemp-PLA	0.18	0.01	0.14	0.01	0.17	0.01
Acetic Anhydride treated hemp-PLA	0.14	0.02	0.13	0.01	0.13	0.01

*Std.dev – Standard deviation obtained by testing 7 specimens per sample

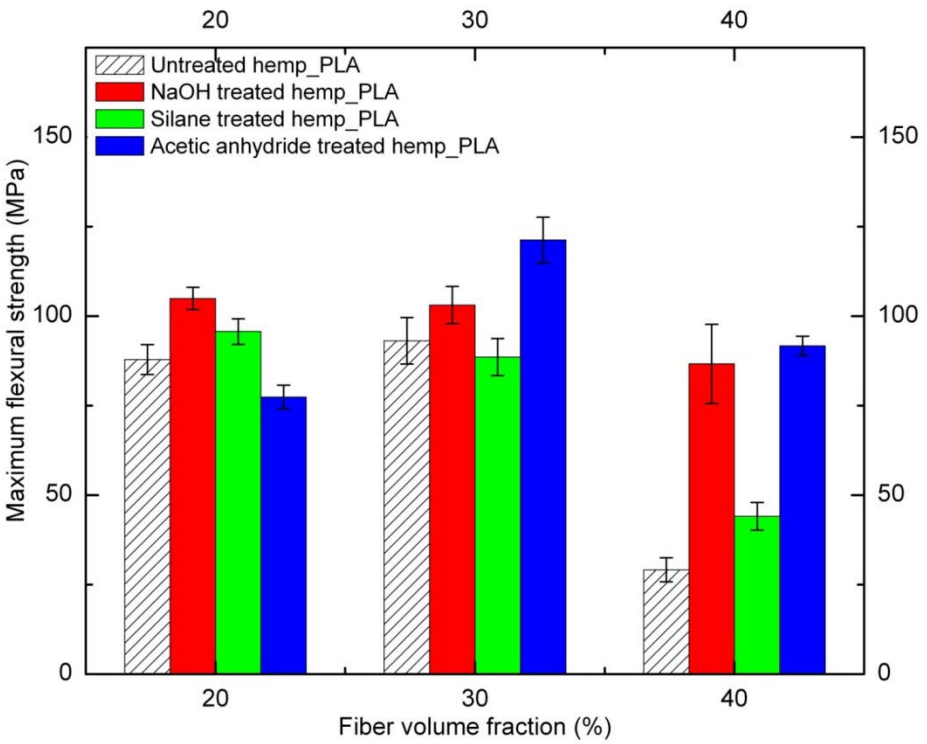

Figure 6.7: Flexural strength at various fiber volume fractions for both untreated and treated hemp-PLA composites

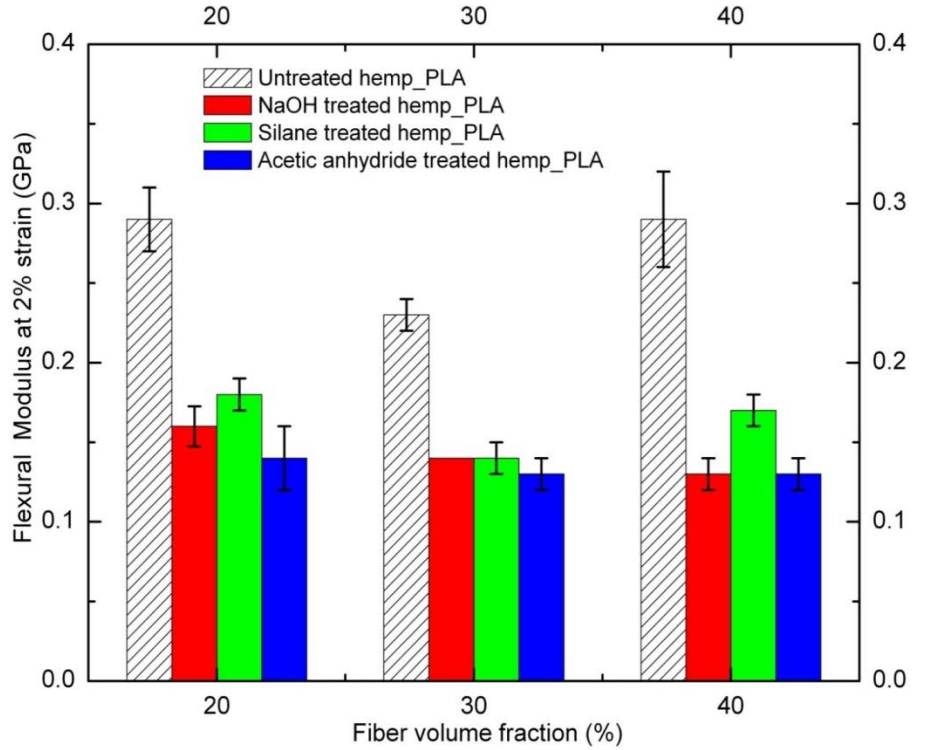

Figure 6.8: Flexural modulus at 2% strain at different fiber fractions for both untreated and treated hemp-PLA composites

6.4 Kelly-Tyson Model – Results and Discussions

The Kelly-Tyson model was adopted to calculate the tensile strength of the composites. The tensile strength of the single fiber required for model calculation was obtained from single fiber testing as explained in Chapter 3 and the results of which are presented in Chapter 4. The parameters used for the model calculations are presented in Table 6.5. The experimental versus the calculated model tensile strength values are presented in Table 6.6 and Table 6.7, respectively.

The experimental tensile strength results in comparison to the values obtained through The Kelly-Tyson model is presented in Figure 6.9. From this figure it can be concluded that the model equation yields tensile strength as directly proportional to the fiber volume fraction. This can be attributed as the drawback of the model since; it does not take into consideration the fiber-matrix interaction and the formation of different types of bonds with varying treatment. Further, the model results suggest that alkali treatment is better than silane and acetic anhydride, and is superior to untreated fiber. This is due to the interfacial shear strength obtained from literature data. There are only two studies [61, 64] which have investigated the interfacial shear strength of hemp-PLA composite and just one [64] which has used all the three treatments; alkali, silane and acetic anhydride. The literature data suggest that alkali treated hemp show the highest interfacial shear strength (Table 6.5). Due to the interfacial shear strength values the model results reflect that alkali treated hemp-PLA composites performs better than the other two treatments.

Table 6.5: Parameters for model calculation obtained from single fiber testing

	Units	Untreated hemp fiber	NaOH treated hemp fiber	Silane treated hemp fiber	Acetic Anhydride treated hemp fiber	Comments
Avg. Diameter of single fiber	Micron	36.44	54.00	52.83	56.38	Avg. from single fiber test
No. of single fibers tested		35	30	30	30	
σ f, fiber tensile strength	MPa	247.51	243.73	275.89	280.89	Avg. from the single fiber test
τ, fiber-matrix interfacial shear strength	MPa	5.55	11.41	8.22	6.29	From literature
Lc, critical fiber length	Mm	0.8125	0.5767	0.8866	1.2589	Calculated
L, fiber length	Mm	25.4	25.4	25.4	25.4	Gage length fixed at 25mm, as per ASTM
L>Lc or L<Lc		Super critical	Super critical	Super critical	Super critical	
σum, PLA tensile strength	MPa	25.04				From pure PLA tensile testing
ηL		0.98	0.99	0.98	0.98	

Table 6.6: Tensile strength in MPa (experimental data)

Maximum tensile strength, MPa, (experimental)			
	20/80	30/70	40/60
Untreated hemp-PLA	21.43	28.09	18.80
NaOH-treated hemp-PLA	33.29	29.16	21.29
Silane treated hemp-PLA	16.38	29.66	27.38
Acetic Anhydride treated hemp-PLA	34.52	35.55	30.38

Table 6.7: Tensile strength in MPa (model data)

Maximum tensile strength, MPa, (model)				
	20/80	30/70	40/60	50/50
Untreated hemp-PLA	29.77	32.14	34.51	36.88
NaOH-treated hemp-PLA	29.82	32.21	34.60	36.99
Silane treated hemp-PLA	29.76	32.12	34.48	36.84
Acetic Anhydride treated hemp-PLA	29.69	32.01	34.33	36.66

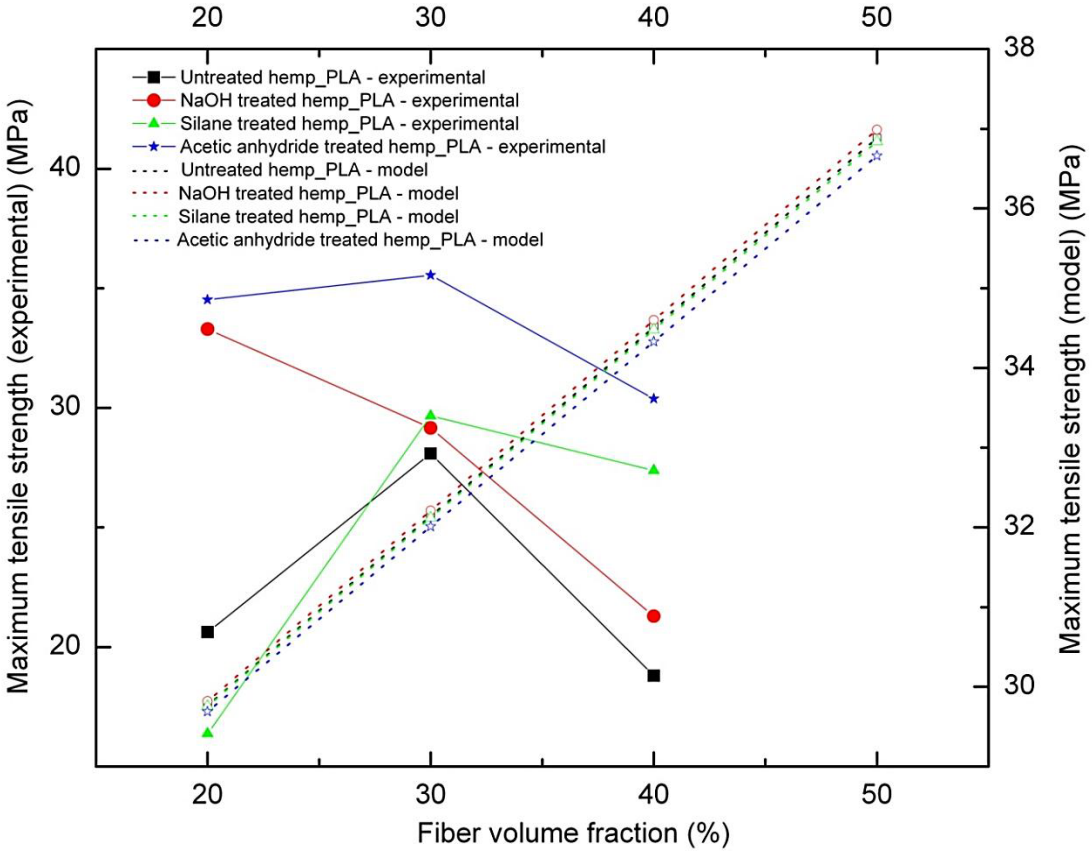

Figure 6.9: Kelly-Tyson model and experimental tensile strength comparison for hemp-PLA composites at various fiber fractions

6.5 Thermo Mechanical Analysis – Results and Discussions

Thermo mechanical analysis of pure PLA and hemp-PLA composites (untreated and with all three treatments) was conducted with TA instruments Q800 DMA. The storage modulus, loss modulus and tan delta were recorded for all composites at 20, 30, and 40 % fiber volume fraction.

6.5.1 Storage Modulus

The value of storage modulus indicates the material's ability to store the energy of external forces without permanent strain deformation. Therefore, higher storage modulus is associated with a higher elastic property of materials. The storage modulus with respect to temperature for hemp-PLA composites for varying fiber volume fraction are plotted for untreated (Figure 6.10), NaOH (Figure 6.11), silane (Figure 6.12) and acetic anhydride (Figure 6.13) treated hemp-PLA composites. These results can be analyzed from two perspectives: effect of fiber loading and effect of fiber surface treatment.

Effect of fiber loading: For untreated hemp-PLA composites (Figure 6.10) it could be observed that as the fiber content increased from 20% to 30% of volume fraction, the storage modulus of composite increased. This indicated an increase of material stiffness with an increase of fiber loading. However, the stiffness of composites dropped drastically at 40% fiber loading, as observed in the storage modulus curve. This can be explained as a result of insufficient amount of matrix for the amount of fiber to form strong interface, resulting in inadequate transfer of stress between the matrix and fiber. The same trend was also noticed for all the three surface modified hemp-PLA composites. Therefore, it is suggested that 30% fiber loading is optimum amount of fiber for design of hemp-PLA composite. The storage modulus values at 25°C for hemp-PLA

composites at various fiber fractions are presented in Figure 6.14 and tabulated in Table 6.8

Effect of surface treatment: The results indicated that chemical treatments significantly affect the storage modulus of a composite. Storage modulus increased for the treated fibers in comparison to that of untreated fibers. It was observed that NaOH treatment not only aids surface roughness on hemp but also removes significant amounts of hemicellulose and lignin from the fiber matrix exposing more cellulose. The exposure of higher amount of cellulose molecules results in increased number of free hydroxyl (-OH) groups for intermolecular and intramolecular bonding at the fiber–matrix interface. The compact packing of the molecular chains results in higher stiffness compared to the untreated hemp-PLA composite. Silane treatment also improves the stiffness of composites due to the formation of both covalent bonding and coupling mechanism. The silane molecule forms covalent bond with the -OH group of the fiber and the organofunctional. The bond energy for esterification is higher compared to the other two treatments resulting in highest modulus for acetic anhydride treated composites at 30% fiber volume fraction.

Table 6.8: Storage modulus at various fiber volume fractions

Storage Modulus at 25°C, MPa				
	20/80	30/70	40/60	
Untreated hemp-PLA	2183.60	2120.00	2108.67	
NaOH treated hemp-PLA	1515.50	2562.00	1952.50	
Silane treated hemp-PLA	2164.40	2593.80	2317.00	
A Anhydride treated hemp-PLA	1747.00	2630.60	2173.00	
Pure PLA				1807.00

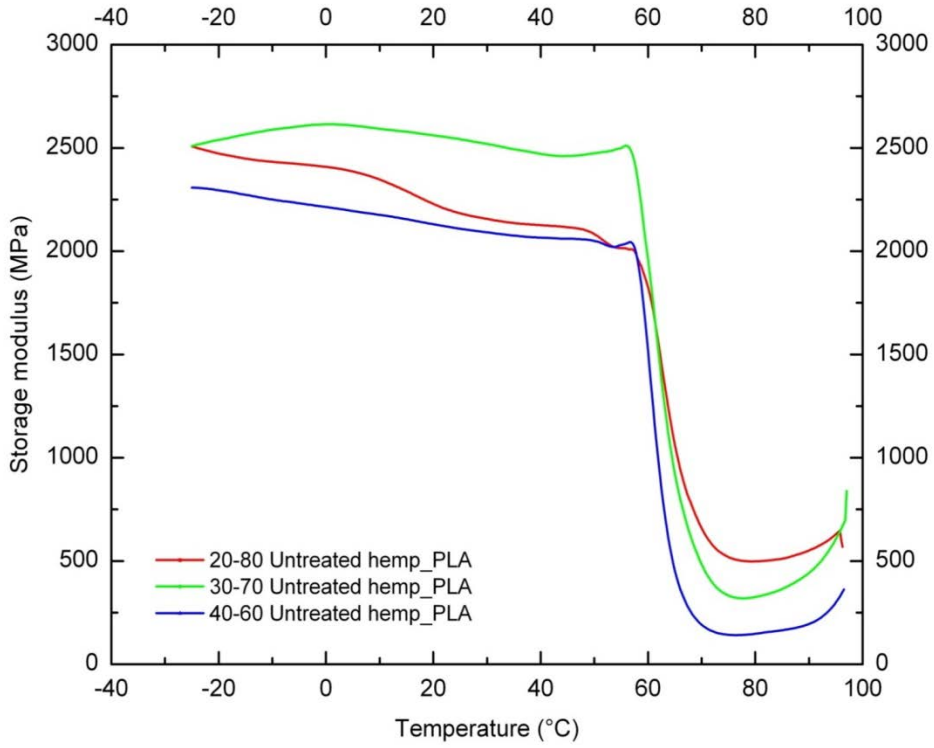

Figure 6.10: Storage modulus of untreated hemp-PLA composites at various fiber volume fractions

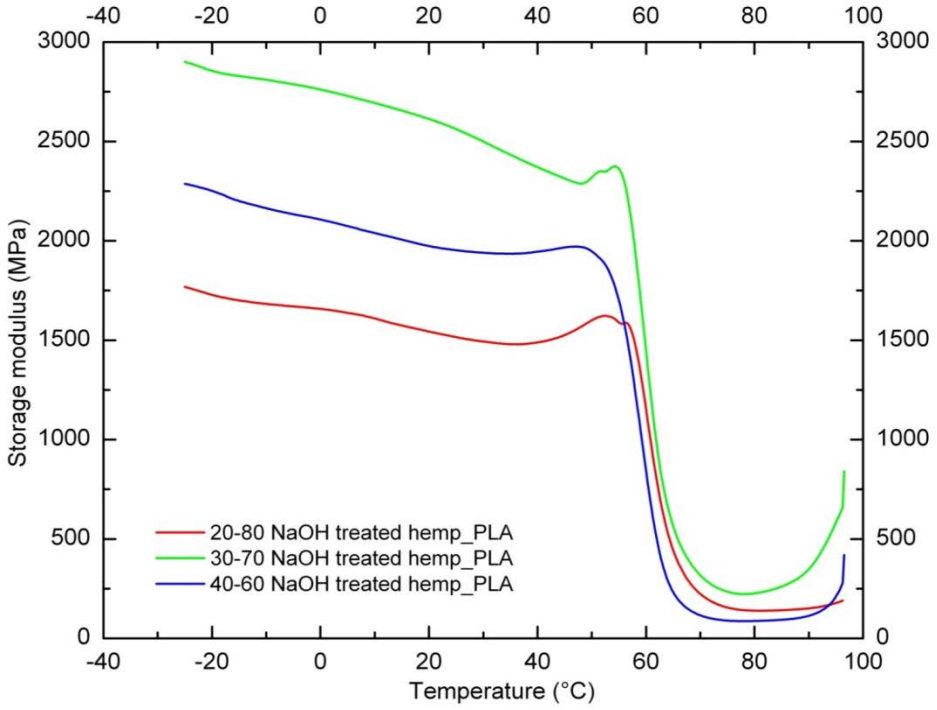

Figure 6.11: Storage modulus of NaOH treated hemp-PLA composites at various fiber volume fractions

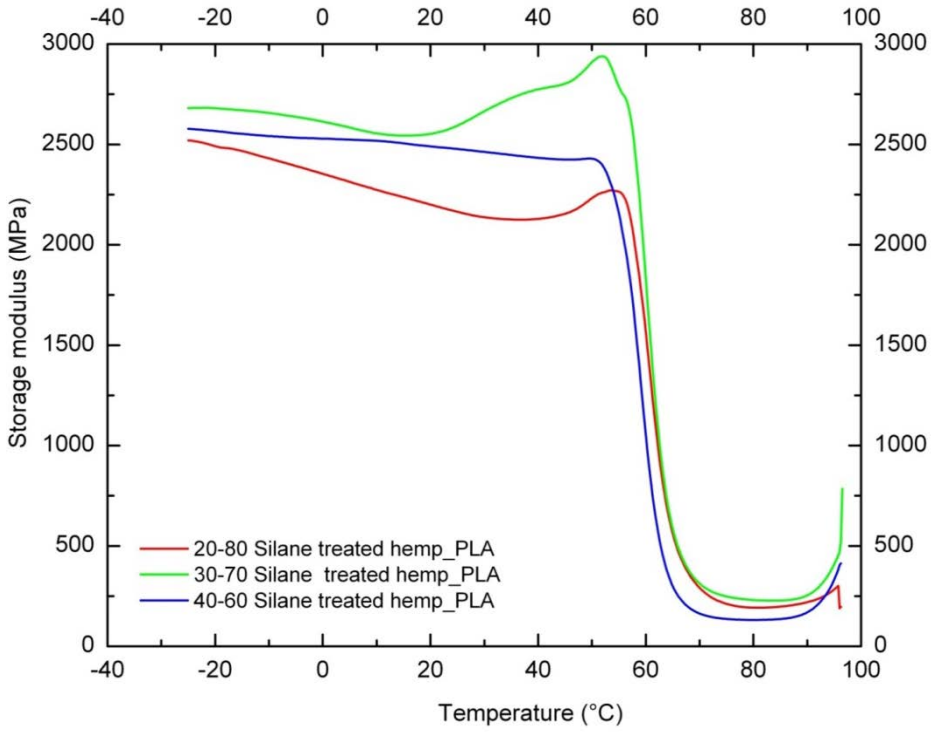

Figure 6.12: Storage modulus of silane treated hemp-PLA composites at various fiber volume fractions

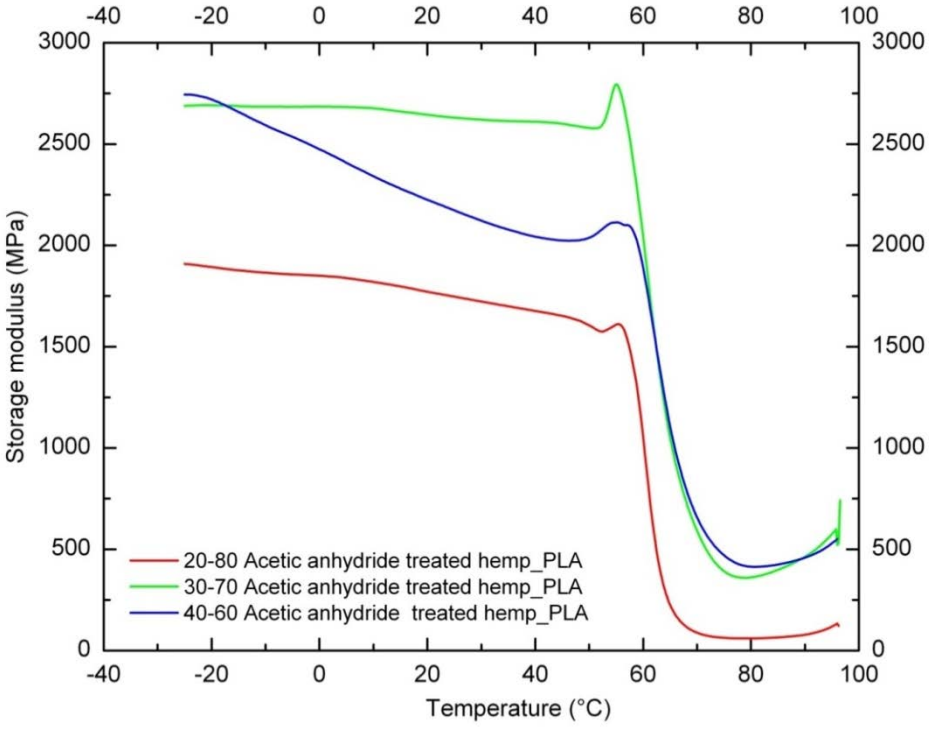

Figure 6.13: Storage modulus of acetic anhydride treated hemp-PLA composites at various fiber volume fractions

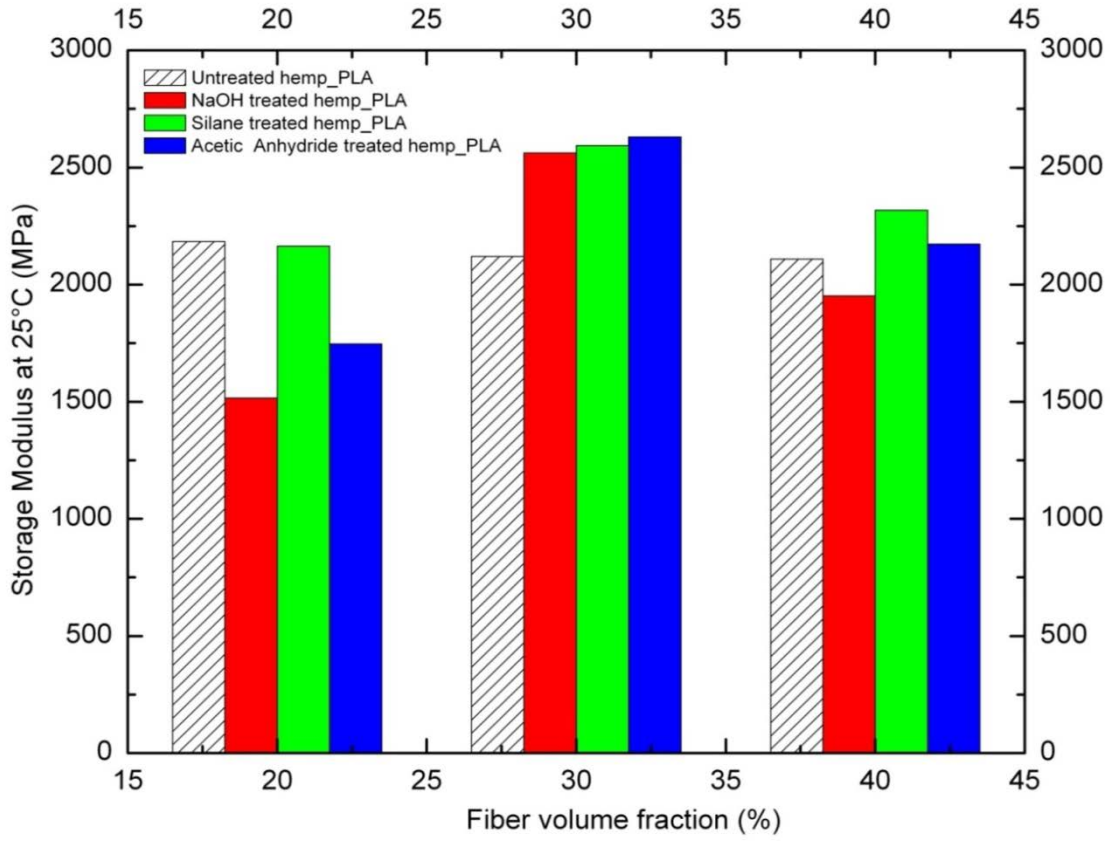

Figure 6.14: Storage modulus at 25C for hemp-PLA composites at various fiber volume fractions

6.5.2 Loss Modulus

Loss modulus is a good indicator of the viscous behavior of the material, and is sensitive to the molecular motions. Figure 6.16 shows the variation of the loss modulus of the PLA and its composites with temperature. The glass transition temperature (T_g) is interpreted as the peak of either the loss modulus or tan delta curve during the dynamic mechanical test. But the T_g from loss modulus is considered to be better indicator. As seen in the Figure 6.16 and Table 6.9, due to the fiber present in the PLA matrix, the T_g of all the hemp-PLA composites shifted to lower temperatures suggesting that the PLA in the composites has decreased in crystallinity due to the introduction of the fiber. It can also be seen that loss modulus peak values increases with increase in fiber content up to

30% and the highest value was obtained in case of acetic anhydride treated hemp-PLA composites.

Table 6.9: Loss modulus value at the peak of the curve and corresponding T_g temperature

Loss modulus at the peak & T_g temperature						
	20_80		30_70		40_60	
	MPa	°C	MPa	°C	MPa	°C
Untreated hemp-PLA	461.78	61.50	509.10	60.50	599.27	60.00
NaOH treated hemp-PLA	346.33	59.75	582.47	60.25	434.33	58.75
Silane treated hemp-PLA	541.24	60.25	695.44	59.75	599.52	58.75
Acetic Anhydride treated hemp-PLA	633.87	60.00	722.10	59.25	447.13	61.50

6.5.3 Tan Delta

The damping coefficient of a material is expressed as tan delta (Tan δ), which indicates the energy dissipation of that material under cyclic load. The Tan δ (Tan δ = loss modulus E" /storage modulus E') is used to predict how well a material would perform at absorbing and dissipating energy. Tan delta is a better indicator to be considered than loss modulus since it is independent of geometry. In a composite system, the Tan δ decreases with the increase in fiber loading, this is mainly due to the existence of effective interracial bonding between fiber–matrix. Figure presents Tan δ value for pure PLA, untreated, and the three treated composites with 30% fiber volume fraction, measured in the temperature range of -40 °C to 100 °C. The tan delta peak increased in magnitude for both untreated and treated composites in comparison to pure PLA (Table 6.10). This could be explained as the disruption of the crystalline phase of PLA by the presence of fibers. The thermo-mechanical results indicated that addition of fiber to PLA increased the stiffness up to 30% fiber loading and acetic anhydride treated hemp-PLA resulted in higher storage and loss modulus for the composites studied

Table 6.10: Tan delta value at the peak of the curve and corresponding Tg temperature

Tan delta at the peak & Tg temperature						
	20_80		30_70		40_60	
	MPa	°C	MPa	°C	MPa	°C
Untreated hemp-PLA	0.3351	65.25	0.3730	65.25	0.6194	64.75
NaOH treated hemp-PLA	0.4329	64.50	0.4754	63.50	0.6732	63.75
Silane treated hemp-PLA	0.6220	64.50	0.5637	63.75	0.6699	63.25
Acetic Anhydride treated hemp-PLA	0.7590	64.25	0.3524	65.00	0.3052	66.25

6.6 Conclusion

This study confirmed that composites with enhanced mechanical and thermo-mechanical properties could be successfully developed using hemp fibers as a reinforcing agent in PLA matrix. The results of the study indicated that surface treatment improves the compatibility between hemp fiber and PLA. Both, the mechanical and thermo-mechanical properties of hemp-PLA composites were significantly higher than those of the PLA matrix itself. This is due to the improved interfacial interaction, resulting in higher stiffness. Surface modified hemp in hemp-PLA composites possessed superior mechanical properties when compared to untreated hemp-PLA composites. The acetic anhydride treated fiber reinforced composites gave higher tensile and flexural properties compared to the other hemp-PLA composites. DMA results showed that the surface modified fiber reinforced composites have higher storage modulus resulting in significantly improved stiffness. The storage modulus of acetic anhydride treated composite was shown to be much higher (at 30% fiber volume fractions) than that of the other systems. Surface treated fiber reinforced composites had higher storage moduli than the untreated fiber reinforced composites, which suggested better adhesion between the treated fibers and the matrix. Loss modulus curves showed that T_g of the composite decreased in comparison to the pure PLA suggesting the disruption on PLA bonds and

resulting in higher amorous nature of the composite. Both mechanical and thermo-mechanical properties of the composites deteriorated at 40% fiber volume fraction suggestion that the optimum fiber volume fraction for hemp-PLA composites is 30%.

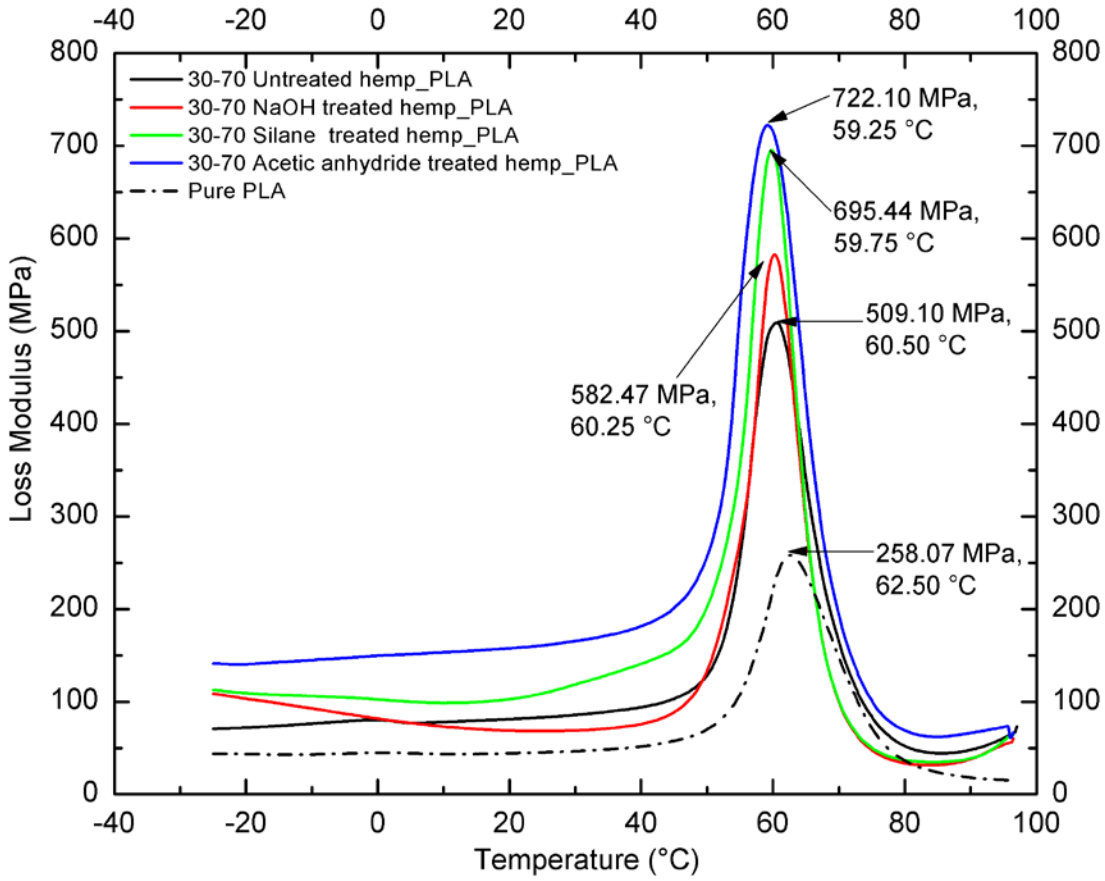

Figure 6.15: Loss modulus curves for 30-70 hemp-PLA composites along with pure PLA

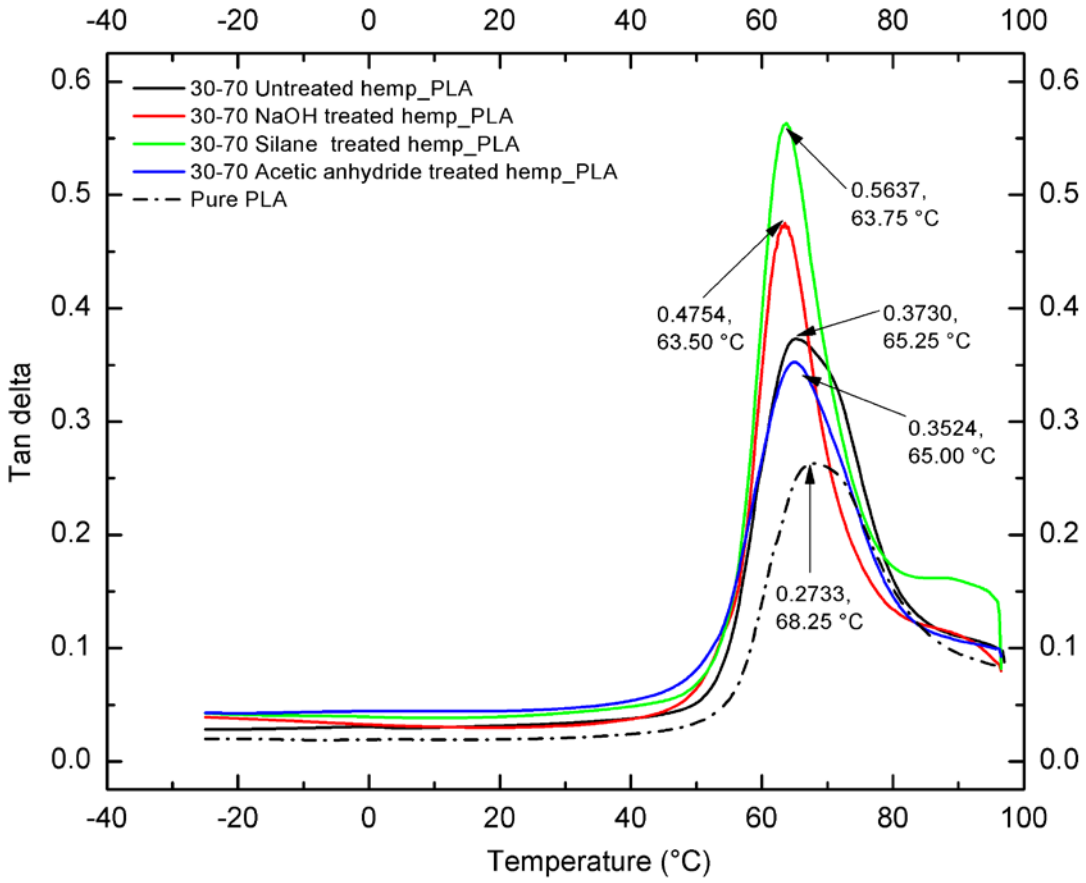

Figure 6.16: Tan delta curves for 30-70 hemp-PLA composites along with pure PLA

CHAPTER 7 : EFFECT OF SURFACE FUNCTIONALIZATION ON BIODEGRADABILITY OF HEMP-PLA COMPOSITES

7.1 Introduction

New sustainable engineering design and manufacturing directives are driving demand for more renewable and environmentally benign materials. Consistent with this new trend, the raw materials for composites are being evaluated. Extensive research is underway to evaluate the feasibility of using natural plant fiber as a replacement for synthetic fiber, such as e-glass, carbon, or aramid for various applications in the automotive, construction, and building industries [1, 2]. Researchers are also looking towards complete replacement of fossil fuel-based materials, such that the polymer matrix is also derived from natural sources. Therefore, environmental consequences of raw material extraction would be reduced which would offer other advantages such as biodegradability, good strength, and easy processability.

Biopolymers including poly (lactic acid) (PLA), poly (ε-caprolactone) (PCL), poly (butylene succinate) (PS) and poly (3-hrdroxybutrate-co-3-hydroxyvalerate) (PHBV) have created increased commercial interest. Among these biopolymers, PLA is particularly attractive in terms of cost [33]. It is a thermoplastic material produced by condensation polymerization of lactic acid, which is derived by fermenting sugars from such sources as corn, potato, and sugarcane. Normally, higher molecular weight PLA is produced from ring-opening polymerization. Along with being biodegradable, PLA is a

stiff and brittle polymer with low deformation at break. To improve upon these mechanical properties, PLA can be reinforced with various types of ligno-cellulosic fibers, including kenaf, hemp, jute, sisal, ramie, or abaca. These fibers are biodegradable and impart good mechanical properties at low specific mass. PLA-based biocomposites are being evaluated and used in building and construction applications, such as roof elements, stay-in-place bridge forms, ceiling tiles, furniture, windows, and doors [9].

The pursuit of completely biodegradable materials has led to intense and diverse research activities to develop biocomposites adapted for various applications. After concerns about the life cycle impacts of these new substitute products arose, another important line of investigation including the environmental impacts of crop production and product disposal. Franklin associates have conducted a comparative study on the effect of energy consumption, solid waste generation, and environmental emissions to air and water of PLA and other petroleum-based resins, such as polystyrene, polypropylene, and polyethylene terephthalate, for five different consumer products. In their studies they observed that there is no significant difference between PLA as a choice of raw material, in comparison to petroleum-based resins [125]. From such studies, it could be protracted that biodegradable products are still preferable in terms of raw materials.

The end life of biopolymers has been the subject of much research. Although there is an intuitive expectation that if natural raw materials are used, a product will be subject to natural biodegradation, the rate and degree to which this occurs vary widely. The propensity of microorganisms to transform or degrade a particular substrate depends on many factors, including their biochemical affinity for the material and the environmental conditions that exist. The various scenarios in which waste can be

disposed are incineration, compositing, landfill and anaerobic digestion. While the first two methods adopt thermal and aerobic degradation, respectively, the last two methods practice anaerobic degradation. Depending on the usage of the material during its life, the final fate is decided. For example, if PLA is used to make bottles or cups, the fate of this product would be compositing, but if PLA is used in composite system for building applications, the probable fate would be landfill (in USA). While comparing the various fates, studies have shown that anaerobic digestion to be the most environmentally friendly option due to less emissions and less energy consumption [126]. Biodegradation studies are critical, to understand the unique properties of a material, its utility, and applications. Further, these studies address the wider issue of life cycle comparisons between biocomposites and the conventional materials they are intended to replace.

7.2 Review of Biodegradation Studies

Biodegradation of PLA [127-132] and PLA bottles[133] have been studied extensively. But assessments of the biodegradability of composite materials in which PLA is one of the components are limited, and their results are difficult to interpret. In the strictest sense, biodegradation may not result in the complete breakdown of a composite material to rudimentary nutrients. The U. S. Environmental Protection Agency (USEPA) defines biodegradation as “a process by which microbial organisms transform or alter (through metabolic or enzymatic action) the structure of chemicals introduced into the environment”, thus allowing the transformations of intermediates to qualify as biodegradation under their definition. A range of methods have been used to demonstrate biodegradability of composites that contain PLA; ASTM and ISO standards have been applied in some, but not all cases.

Several studies employed soil burial, which may or may not provide anaerobic conditions, depending up on the depth of burial. Shogren *et. al.* buried specimens of injection molded tensile bars of corn starch, PLA, and poly (hydroxyester-ether) (PHEE) in soil 6 inch deep and measured biodegradation in terms of weight loss after one year. They found that PHEE addition to starch-PLA blend accelerated biodegradation[134]. When Naozumi *et. al.* did a similar study for 180 d, they found that there was no weight loss for 100% PLA specimens, but PLA specimens with 10% w/w abaca fibers that were either untreated or treated with acetic anhydride all showed 10% weight loss after 60 d [135]. Yussuf *et. al.* compared PLA-kenaf and PLA-rice husk composites to pure PLA specimens buried for of 90 d. Weight loss for kenaf composites was threefold that of pure PLA controls; for rice husk it was twofold that of controls. The higher degradation in composites was attributed to the enzymatic degradation of cellulosic chains in the fibers. The higher weight loss in composites was attributed to the low crystallinity of composites in relative to specimens of pure PLA [136].

Lee *et al.* studied the effects of lysine-based di-isocynate (LDI) as a coupling agent, on the properties of biocomposites from PLA and bamboo fiber. Subsequent biodegradability exposed the specimens to two different enzyme (Proteinase K and Lipase PS) cultures. Pure PLA degraded slower than the composites, but the presence of LDI in composites slowed their enzyme-mediated degradation. The improved interfacial adhesion afforded by LDI, evidently slowed the, degradation rates. When Proteinase K enzymatic degradation was coupled with soil burial, PLA-corn starch composites without LID degraded faster than the composites with LDI [54]. Thus, for this composite (PLA-

corn starch) and its disposal fate (soil burial) biodegradability may be controlled by using LDI to manipulate the degree of interfacial adhesion [137].

To study biodegradation of PLA biocomposites under aerobic condition, Wu *et al.* tested specimens of pure PLA and, maleic anhydride-grafted PLA (PLA-g-MA) with green coconut fiber (GCF) in a *Burkholderia cepacia* BCRC 14253 compost for 21 d. The PLA-g-MA based composites degraded more than pure PLA and the weight loss of PLA-g-MA composites also accelerated compared to pure PLA. The degree of biodegradation increased with increasing GCF content [138].

Iovino *et al.* were one of the early groups to study biodegradability of PLA-based composites using ISO 14855 protocol (aerobic biodegradation under controlled composting conditions). They manufactured a PLA-based composite using maleic anhydride as the coupling agent and then composted the composite and pure PLA specimens according to the protocol for 90 d. The starch completely biodegraded, and overall the composite matrix showed a higher degree of biodegradation than was observed in pure PLA due to the presence of starch [139]. Similarly, PLA composites with starch and wood flour tested under this protocol yielded similar results with the biodegradation rate increasing from 60% to 80% as the starch content increased from 10% to 40% after 80 d [140].

Ranjan *et al.* studied biodegradation of PLA-wheat straw and PLA-soy straw composites in accordance to ASTM D 5338 specifications. This method of testing involves the aerobic biodegradation under controlled compositing conditions, incorporating thermophilic temperatures. They observed that the biodegradation was

same in both the composites, and the rate of biodegradation of composites was higher than neat PLA [141].

This review on biodegradability studies suggest that if PLA-based composite materials were to be composted aerobically, the degree to which the composites would degrade would depend on the type and percentage of fibrous material present; the PLA itself appears to be relatively resistant to microbial activity. In the soil burial studies, both the oxygen and microorganism concentrations were low; therefore, it is not surprising that less degradation was observed. It is also less likely that PLA composite materials would be subject to soil burial, since this is not among the common waste management practice options used today. It is more likely that any burial option serving as an alternative to composting would be landfilling, which is different from soil burial. Landfills are highly engineered systems, where soil is used as intermediate cover, but it is not the primary medium surrounding the buried waste. The population of microorganisms in landfill cells is typically denser and more diverse than that of soil.

Thus, there is a need to evaluate biodegradation of PLA-based composites under conditions that simulate landfill conditions, which is one of the most common waste management options employed in the U.S. For materials that may be used in the construction and building industries, landfilling is a likely end-of-life fate, and appropriate inquire into the anaerobic biodegradability of these materials is warranted. Further, anaerobic processes are less energy intensive and, if properly managed, can yield useful byproducts, such as methane gas for energy harvest. Briefly, microbial anaerobic biodegradation is accomplished through the simultaneous action of four major groups of microorganisms. One group performs hydrolysis, a process in which large proteins,

polysaccharides, and fats are converted into smaller water soluble molecules that other microbes can process. For example, the activity of a second and third group can use these smaller molecules as food, producing acetic acid and gases like H_2 and CO_2 in the process. Finally, these by-products are converted to CO_2 and CH_4 by yet another group of microbes called methanogens.

The purpose of this study was to assess the biodegradation of various hemp-PLA composite specimens under anaerobic conditions simulating those in a landfill. The ASTM Standard protocol for ASTM D 5511-02 was used with few modifications to compare the biodegradability of the specimens relative to positive and negative control. Scanning electron microscope (SEM) was used to supplement the assessment of composite biodegradation.

7.3 Materials and Methods

ASTM method D 5511-02: “Standard test method for determining anaerobic biodegradation of plastic materials under high-solids anaerobic digestion conditions” was used with few modifications. Briefly, this protocol calls for a 15-30 d thermophilic (~ 52°C) incubation of specimens with a 20% solids content, where the inoculum has been pre-fermented for 7 d prior to addition of any test specimens. Biodegradation is calculated as the mass sum of gaseous carbon generated as CO_2-C and CH_4-C. To better simulate landfill conditions, specimens in this study were incubated at 35°C for 50 days. Studies on landfill temperatures have observed that temperature in landfills increase at a rate of approximately 2 to 4°C/a and, elevated temperatures in excess of 30°C were observed after 5.5 years and under 42 m of waste height only[142].

Inoculum: Inoculum was obtained from anaerobic digesters at The Mallard Creek Water Reclamation Facility in Charlotte, NC. The plant receives conventional municipal wastewater, and the digesters are operated at mesophilic temperatures. The inoculum was approximately 20% total solids (w/v). It was incubated for 7 d at 33±1°C, as prescribed by the ASTM procedure, a step that allows easily biodegradable particles to be consumed so that background readings during testing are lower.

Test specimens and controls: Four different types of composites were tested: untreated hemp-PLA; NaOH treated hemp-PLA; silane treated hemp-PLA; and acetic anhydride treated hemp-PLA. In each case, hemp fiber made up 30% by volume of the material. The method by which each composite was prepared is described in Chapter 3. A pure PLA specimen was made by extruding PLA pellets (2003D grade – 35% crystalline) into thin sheets and then compressing them to obtain a panel of 2mm thickness. A hemp only control contained 1-in lengths of hemp fibers. Negative control specimens consisted of high density polyethylene, a plastic which is known to be resistant to biodegradation. For a positive control, cellulose powder (Avicel PH-112 NF) was obtained from FMC Corporation, U.S.A. Blanks were also tested that contained inoculum only. The composites, negative control and pure PLA specimens were rectangles 35 mm long × 15 mm wide × 2mm thick. Ten grams of carbon content was maintained in all samples, including the powdered cellulose positive control and the hemp-only trials

Vessel: Trials were conducted in 1 L gas-tight glass bottles (Figure 7.1a). The caps were modified with a 1/8 in NPT Swagelok fittings to accommodate a silicone septum for gas sampling (Figure 7.1b). All samples and controls were tested in triplicates. To fill a bottle, about 100g of inoculum was added, and then approximately half of the

specimens to be incubated in that bottle were emplaced. The process was repeated to layer a second layer of specimens and then cover it with a layer of inoculum. In the end there were two layers of specimens and three layers (and 300 g wet weight) of inoculum, and the specimens were well buried and distributed evenly. The bottles were capped air tight (Figure 7.1c). The head space was purged with nitrogen gas, the pressure was adjusted to atmospheric pressure, after which the initial headspace concentration profile was recorded using gas chromatographer (GC) measurements. Samples were incubated in a controlled room maintained at 33±1°C. Bottles were removed as needed for measurement of gas composition and overpressure gas volume.

Figure 7.1: (a) 1 L capped glass bottles, (b) NPT Swagelok fittings, (c) Bottles with inoculum and test specimen

The ASTM protocol is based on the premise that, if anaerobic biodegradation by the digester-derived inoculum is occurring, it is likely following the same path as that in landfills and the municipal digester from which the test inoculum was sourced. That is, the inoculum could be expected to convert organic material in the mix to carbon dioxide and methane gas. This would result in an overpressure in the bottles as well as a build-up of these gases in the headspace. The overpressure was detached by measuring the flow of

gas that exited the bottle when a needle was inserted in the cap septum. The needle was attached to a digital flow meter (Agilent ADM 2000, C.A) (Figure 7.2). The flow meter records volumetric flow two times per second. The data is transmitted to a computer, where it is plotted, and the area under the curve is integrated to obtain the gas volume.

Figure 7.2: ADM2000 Agilent Technologies flow meter

The methane and carbon dioxide along with nitrogen and oxygen (negligible) were determined using an SRI 8610C GC (Figure 7.3). The SRI GC is fitted with a CTR-1 column (Alltech, Inc.) where the flow passes sequentially through a thermal conductivity detector (TCD) and then a flame ionization detector (FID). Helium carrier gas is used at a flow rate of 60 ml/min. Both, the flow and concentration data were used to calculate the mass per unit time of gaseous carbon produced from the organic fraction of the various test specimens. Gas volume and composition measurements were recorded three times a week for 50 d. This data was used to calculate the percentage biodegradation as described in the ASTM standard. Based on the mass of the sample and

the carbon content, percentage biodegradation was calculated for all the composites, and controls using the formula given below

$$Percentage\ biodegradation = \frac{mean\ C_g\ (test) - mean\ C_g\ (blank)}{C_i} * 100$$

where:

C_g = amount of gaseous carbon produced, g, and

C_i = amount of carbon in test compound added, g.

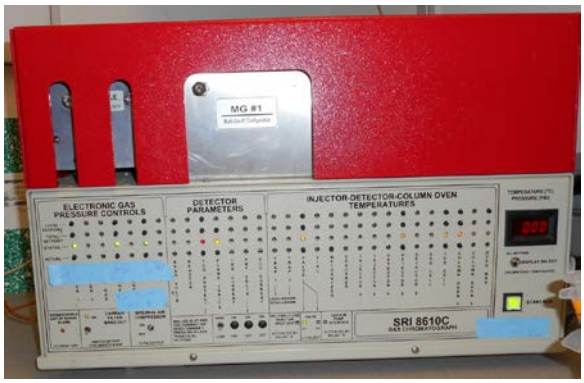

Figure 7.3: SRI 8610C gas chromatograph

Preparation for imaging: After the 50 d incubation, the specimens were removed from the bottles, washed, dried, and 10 mm × 10 mm squares were cut for microscopic investigation. The surface morphology was investigated using a JEOL JSM-6480 Scanning Electron Microscope (SEM). To improve the conductivity of the specimens, 0.5 nanometer thickness of gold was sputtered using Denton Desk IV Sputter.

7.4 Results and Discussions

The cumulative mass of carbon released through biodegradation as CO_2 and CH_4 is shown for all controls and treatments in Figure 7.4. Figure 7.5 and Figure 7.6 show this information for both the composites and controls, the composites only and the controls only, respectively, and with error bars included. The control bottles

demonstrated that when suitable substrate was present, the inoculum was capable of producing CO_2 and CH_4 as expected. The cellulose controls generated a total mass of 4.12 g C, while the blanks and negative controls generated 0.93 and 0.99 g C, respectively. Statistically, there was no evidence of composite degradation relative to the negative control or blank (Figure 7.4). A one-way ANOVA revealed that the mean total carbon yield for all samples was significantly different ($p = 0.05$) from the positive control (cellulose); but the negative control, blank, neat PLA, and all four composites were not significantly different from one another.

The rate of anaerobic biodegradability was also calculated from the evolved biogas data (Figure 7.7). While cellulose degraded 31.91% of the carbon in the biogas during the 50 d incubation, the composites showed a rate of only 1% degradation in the same time period. Pure PLA specimens showed no gas evolution, while 8.68 % of untreated hemp fiber carbon was degraded in 50 d.

The results presented here are consistent with other reports. Yagi *et al.* observed that anaerobic biodegradation of PLA at mesophilic temperatures was very slow, with gas evolution starting at 55 d and biodegradation proceeding at a rate of 2.9%/week [132]. Massardier *et al.* studied the biodegradability of various types of polymer films using the protocol of ISO Standard 14853 (Anaerobic Condition at Mesophilic Conditions), and observed no biodegradation of PLA in 28 days. Kolstad adapted ASTM Method 5511, which describes conditions similar to those used in this study and found that there was no significant degradation of PLA even after 180 d [127].

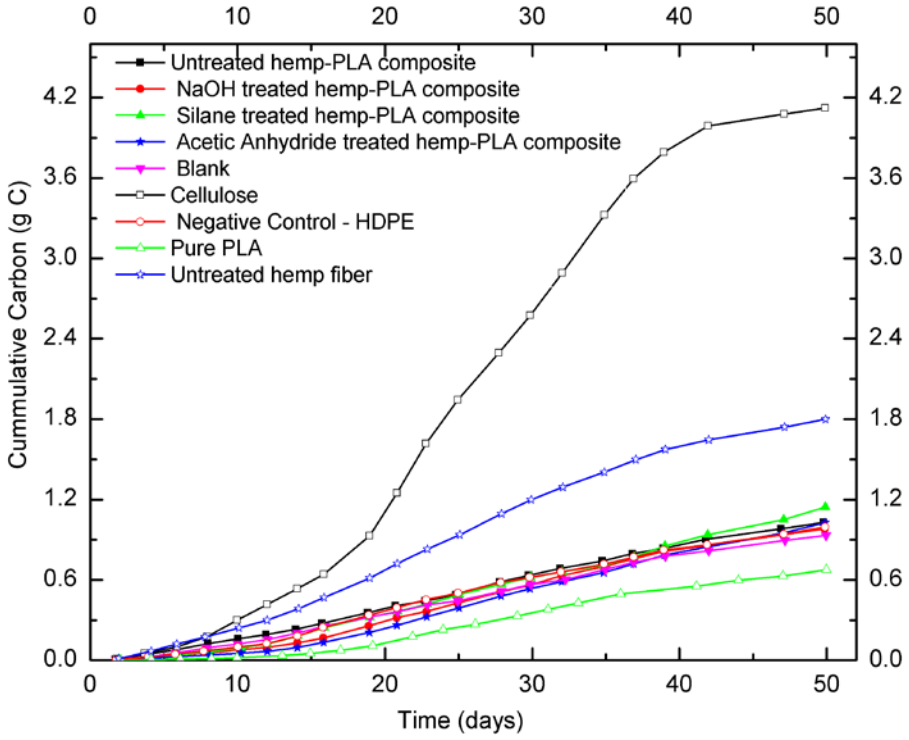

Figure 7.4: Cumulative carbon (CH_4 + CO_2) of the composites, hemp fiber, PLA, and controls

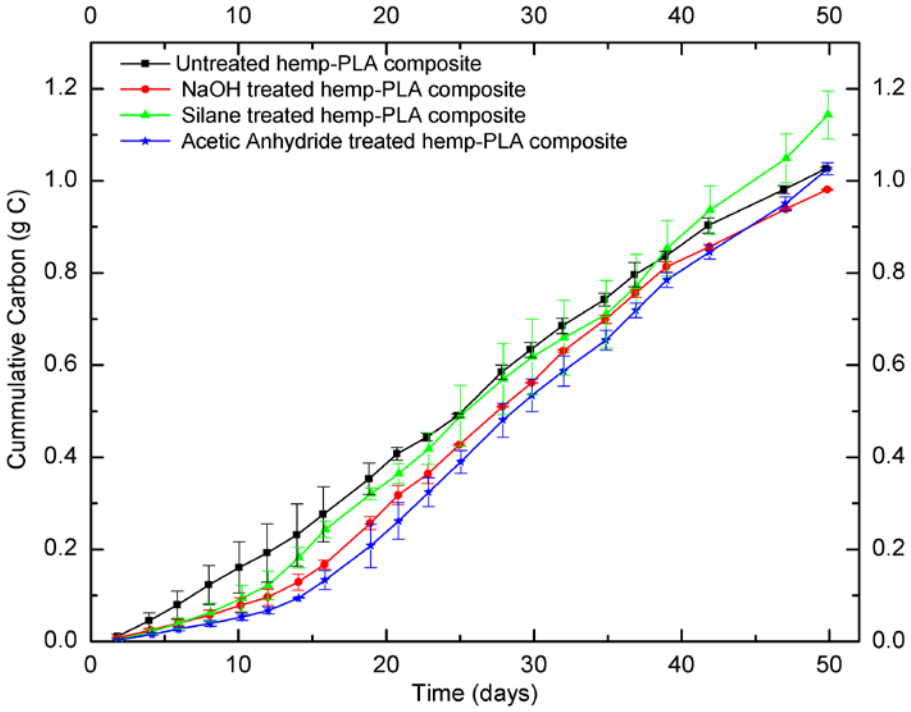

Figure 7.5: Cumulative carbon (CH_4 + CO_2) of the four composites with error bars

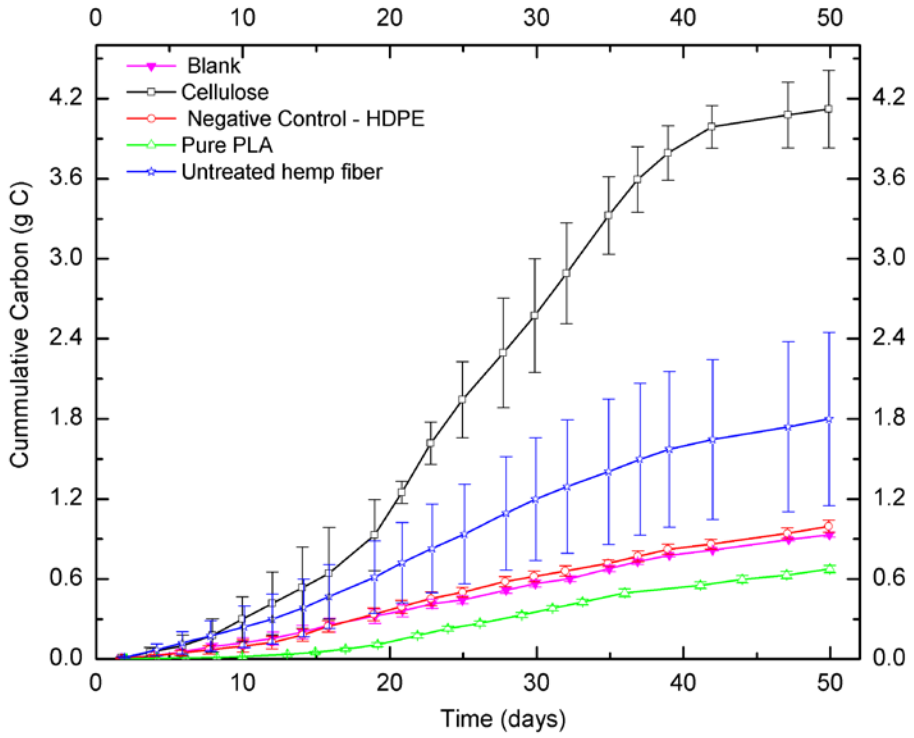

Figure 7.6: Cumulative carbon (CH_4 + CO_2) of hemp fiber, PLA, and controls

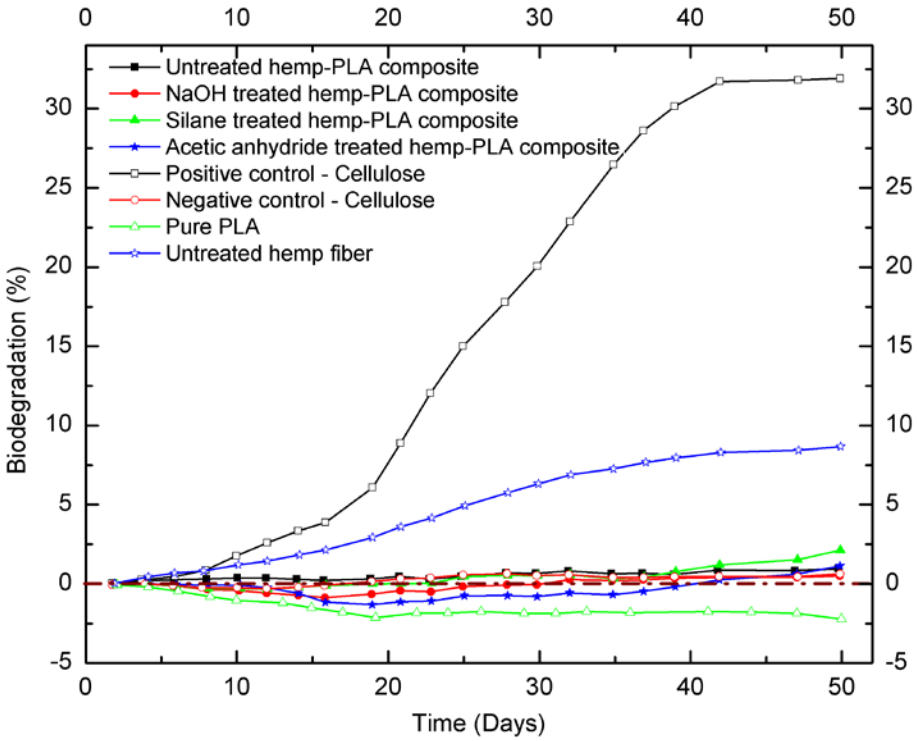

Figure 7.7: Percentage biodegradation of the composites, hemp fiber, PLA, positive and negative control

For the experimental conditions used here, the controls provided a clear indication of the sufficiency of the testing paradigm to show biodegradability if it was occurring. Although the ASTM standard called for 70% biodegradability of the positive control material, the standard was designed for thermophilic and not mesophilic conditions. The use of hemp fiber, which is known to be biodegradable, provided an additional positive control. As a lingo-cellulosic material, hemp would also be expected to be resistant to anaerobic biodegradation. Only a small spectrum of microbes can accomplish biodegradations of these materials in a landfill environment, and many of them are fungi and protozoa. Among the bacteria that can contribute to cellulose degradation are *Clostridium thermocellum* [143], and *Clostridium stercorarium* [144].

Few microbes have been identified that are capable of degrading pure PLA, and of those, only one had a temperature optimum below 60 °C, and it was an aerobe [145]. On the other hand, findings such as those reported by Yagi et al. suggest that appropriate microbes may exist in the landfill environment [132]. While temperature clearly appears to be the major environmental factor, particle size is also relevant, as Yagi *et al.* samples were ground. Also the cellulose controls used in this study were particles (~ 110μ) while, the composites, pure PLA and negative controls were introduced as rectangular specimens resulting in reduced surface area for the microbes to biodegrade these substrates. The microbes present in the incubation vessels represented a diverse mix of microbes acclimated to the substrates present in municipal wastewater. Although the relative population sizes of microbes in the mix would not be the same as those in municipal landfill waste, they likely contained sufficient diversity to response to novel substrates if they were presented.

Surface morphology changes: The SEM images of both the pure PLA and biocomposites samples showed evidence of cracking after the incubation, Figure 7.8. PLA cracking can be explained as the chain scission of the PLA molecules. Also, there was no visual difference in the degree of cracking between treated hemp-PLA composites and untreated hemp-PLA composites. Untreated hemp fiber has a cleaner surface after incubation, which is consistent with the fact that the hemp surface contains organic impurities, such as oil and wax that are readily consumed by microbes.

7.5 Conclusion

In this study, an anaerobic biodegradation method for biocomposites based on ASTM D 5511-02 was modified to simulate landfill disposal of hemp-PLA biocomposite materials and assess their biodegradability. After 50 d at 35°C, there was negligible biodegradation of the samples. There was no significant difference ($p=0.05$) among the different types of composites and biodegradability did not differ significantly from that of the blanks, negative controls, or the pure PLA samples. The surface morphology of the specimens analyzed through SEM showed cracks both in composites and PLA.

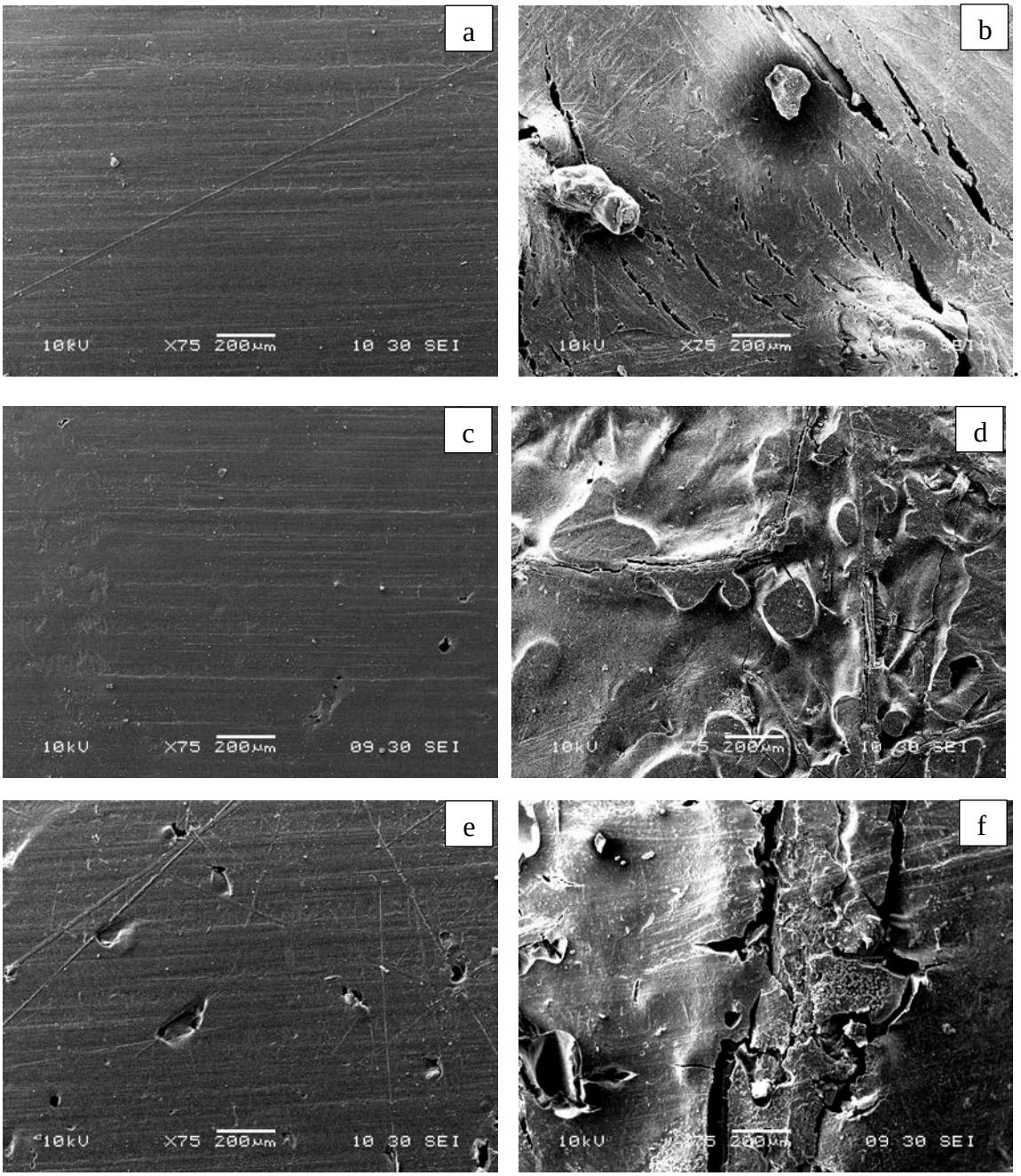

Figure 7.8: SEM pictures of composites and pure PLA, before and after 50 d of anaerobic incubation (a) untreated hemp-PLA, before (b) untreated hemp-PLA (after), (c) NaOH treated hemp-PLA, before (d) NaOH treated hemp-PLA (after), (e) Silane treated hemp-PLA, (f) Silane treated hemp-PLA (after), (g) acetic anhydride treated hemp-PLA, before (h) acetic anhydride treated hemp-PLA (after), (i) neat PLA, before (j) neat PLA (after), (k) HDPE before, (l) HDPE after, (m) untreated hemp fiber before, (n) untreated hemp fiber after.

Figure 7.8 continued

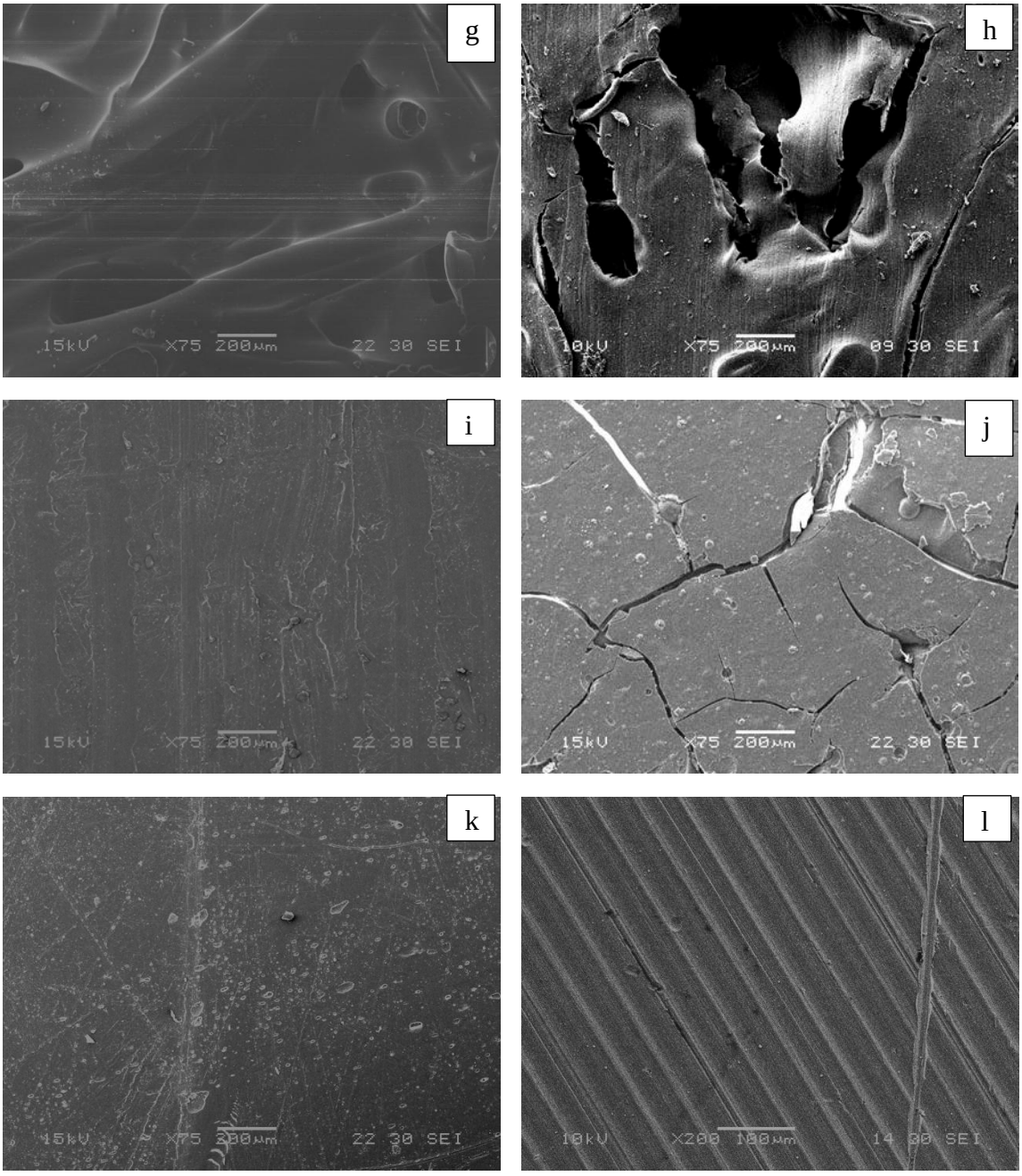

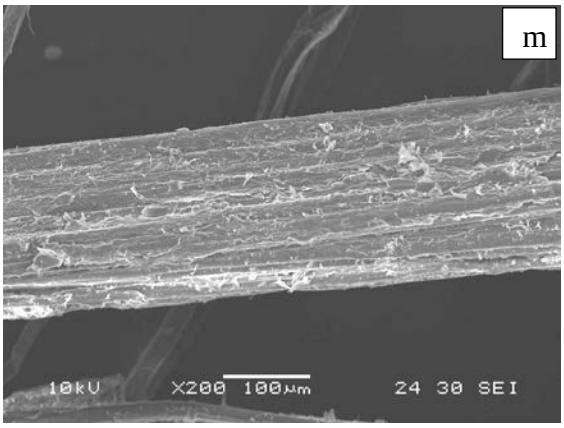
m
10kV X200 100µm 24 30 SEI

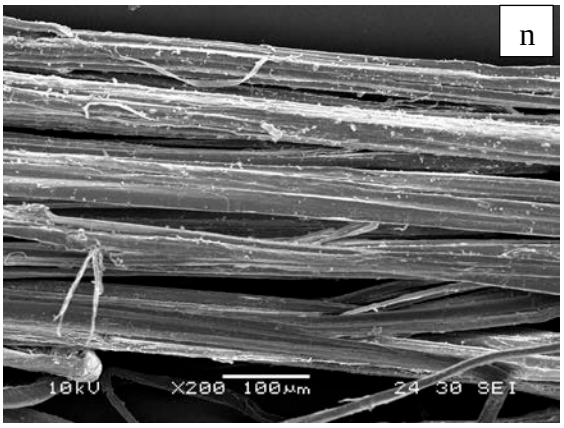
n
10kV X200 100µm 24 30 SEI

CHAPTER 8 : CONCLUSIONS AND RECOMMENDATIONS FOR FUTURE WORK

8.1 Summary

This research provided an integrated examination of the effects of surface functionalization of natural fiber on the ultimate bulk properties of natural fiber-PLA composites, including thermal stability, mechanical, thermo-mechanical behaviors and biodegradability. The surface of hemp fiber was modified using three different treatment approaches: alkali, silane, and acetic anhydride, which resulted in hydrogen bond, covalent bond, and grafting effects, respectively. Alkali treated resulted in an increased percentage of cellulose structure, silane treatment lead to the formation of covalent Si-O-Si, bonds; and acetic anhydride lead to the esterification of hydroxyl groups, resulting in the plasticization of cellulose in the hemp fiber.

The thermal stability of the composites decreased in the order: acetic anhydride > silane > alkali > untreated hemp-PLA composite. These results were confirmed by the activation energy calculations, where in 30% fiber volume fraction composites were modeled with the aid of F-W-O model. The model equation indicated that acetic anhydride had the highest activation energy among both treated and untreated composites.

The acetic anhydride and silane treated hemp-PLA composites at 30% fiber volume fraction enhanced tensile strength relative to composites made with untreated

hemp. With alkali treated hemp-PLA, the tensile strength decreased with an increase in fiber volume fraction. These trends could be explained as a result of the type of bonds that were formed due to surface functionalization. Alkali treatment resulted in hydrogen bonding which form lower energy bonds than the Si-O-Si bonds and the ester link C=O bonds formed from the other treatments. Similar trends were observed when flexural strength was compared among the composites made with hemp from various treatments. The mechanical properties of the composites in order from most to least enhanced was acetic anhydride > silane > alkali > untreated hemp-PLA composite. The experimental tensile strength was compared to values predicted by the Kelly-Tyson model. The model predicted higher strength with increase in fiber loading, but this was not a feasible. Such an increase would require an accompanying decrease in the amount of matrix, which would result in inferior fiber-matrix adhesion. The experimental results at 30% fiber volume fraction were comparatively closer to the model predicted tensile strength.

The thermo-mechanical properties of the composites tracked well with the mechancial and thermal stability of the compsoites. The 30% fiber volume fractions resulted in better stiffness and dampening coefficients of the materials. The storage modulus of the composites increased with an increase in fiber content up to 30% fiber volume fraction. The loss modulus of the composites was higher for the acetic anhydride hemp-PLA composite at 30% fiber volume fraction.

Biodegradability testing of hemp-PLA composites indicated that these composites underwent negligible biodegradation over 60 d of incubation in simulated landfill conditions. There were no significant differences among the biodegradability of composities made with hemp subjected to different treatments, and therefore no evidence

that surface funcationalization played a role in biodegradation rate. It is posible that smaller particle size might accelerate degradation of such composites in landfills, but there are many other options being considered for end of life or recycling of tehse materials. More study will be required to ensure that they fulfill the potential of bio-based materials to reduce nonbiodegradable landfill burdens and waste

In conclusion, a major finding from the study is that surface functionalization of the hemp fiber had a significant impact on the bulk properties of hemp-PLA composites since it effected the type of fiber-matrix interfacial adhesion that occurred between the fiber and the matrix. The adance in understanding the fundamental interactions involved in how fiber functionalization on bulk composite properties opens the door to the future possibility of tuning bulk properties of natural fibers composites through interface design.

8.2 Recommendations and future work

Further efforts to understand the role of interfaces on composite properties will requires additional quantitative characterization work on the interface properties of composites. Advanced techniques, such as nanoinidentation, atomic force microscopy (AFM) can be applied to help establishing an improved micromechanical modeling theory that can accurately predict bulk mechanical properties of composites by incorporating interface adhesion. In addition, it will be important to understand the interface adhesion effects on durability and long-term mechancial behaviour of composites, such as creep and fatigue. Furthermore, advances in recyclability and better accounting of a variety of life cycle cost options for natural fiber composites will aid in better designs and applications for these materials.

REFERENCES

1. Mohanty, A.K., M. Misra, and L.T. Drzal, *Surface modifications of natural fibers and performance of the resulting biocomposites: An overview*. Composite Interfaces, 2001. 8(5): p. 313-343.

2. Joshi, S.V., *Are natural fiber composites environmentally superior to glass fiber reinforced composites?* Composites Part a-Applied Science and Manufacturing, 2004. 35(3): p. 371-376.

3. Zah, R., *Curaua fibers in the automobile industry - a sustainability assessment.* Journal of Cleaner Production, 2007. 15(11-12): p. 1032-1040.

4. Li, X., L.G. Tabil, and S. Panigrahi, *Chemical treatments of natural fiber for use in natural fiber-reinforced composites: A review.* Journal of Polymers and the Environment, 2007. 15(1): p. 25-33.

5. Mukhopadhyay, S. and R. Fangueiro, *Physical Modification of Natural Fibers and Thermoplastic Films for Composites - A Review*. Journal of Thermoplastic Composite Materials, 2009. 22(2): p. 135-162.

6. Bisanda, E.T.N. and M.P. Ansell, *THE EFFECT OF SILANE TREATMENT ON THE MECHANICAL AND PHYSICAL-PROPERTIES OF SISAL-EPOXY COMPOSITES.* Composites Science and Technology, 1991. 41(2): p. 165-178.

7. Castro, C., *Determination of optimal alkaline treatment conditions for fique fiber bundles as reinforcement of composites materials.* Revista Tecnica De La Facultad De Ingenieria Universidad Del Zulia, 2007. 30(2): p. 136-142.

8. Li, Y. and K.L. Pickering, *Hemp fibre reinforced composites using chelator and enzyme treatments.* Composites Science and Technology, 2008. 68(15-16): p. 3293-3298.

9. Amar K. Mohanty, M.M., Lawrence T. Drzal, ed. *natural fibers, biopolymers, and biocomposites*. 2005, CRC Press.

10. Akil, H.M., *Kenaf fiber reinforced composites: A review*. Materials & Design, 2011. 32(8-9): p. 4107-4121.

11. Roger M.Rowell, R.A.Y., Judith K. Rowell, ed. *Paper and Composites for Agro-Based Resources*. 1997, Lewis Publishers, CRC Press, Inc.

12. Adler, E., *Lignin chemistry—past, present and future.* Wood Science and Technology, 1977. 11(3): p. 169-218.

13. O'Sullivan, A., *Cellulose: the structure slowly unravels.* Cellulose, 1997. 4(3): p. 173-207.

14. Sakurada, I., Y. Nukushina, and T. Ito, *Experimental determination of the elastic modulus of crystalline regions in oriented polymers.* Journal of Polymer Science, 1962. 57(165): p. 651-660.

15. Lorna J. Gibson, M.F.A.a.B.A.H., *CELLULAR MATERIALS in Nature and medicine*. 2010, New York: Cambridge University Press.

16. Z.H. Gao, J.Y.G., X-M. Wang, Z.G. Li, X.D. Bai, *FTIR and XPS study of the reaction of phenyl isocyanate and cellulose with different moisture contents.* Pigment & Resin Technology, 2005. 34(5): p. 282-289.

17. Kelly, A., ed. *Concise encyclopedia of composite materials*. 1st ed. 1989, Pergamon Press.

18. T. Kent Kirk, R.L.F., *Enzymatic "Combustion": The microbial degradation of lignin.* Annual Review of Microbiology, 1987. 41: p. 465-501.

19. Summerscales, J., *A review of bast fibres and their composites. Part 1 - Fibres as reinforcements.* Composites Part A: Applied Science and Manufacturing, 2010. 41(10): p. 1329-1335.

20. Earleywine, M., *Understanding Marijuana - A New Look at the Scientific Evidence*. 2002, New York: Oxford University Press, Inc.

21. Struik, P.C.A., S.; Bullard, M.J.; Stutterheim, N.C.; Venturi, G.; Cromack, H.T.H., *Agronomy of fibre hemp (Cannabis sativa L.) in Europe.* Industrial Crops and Products, 2000. 11(2-3): p. 107-118.

22. Alden, D.M., J.L.R. Proops, and P.W. Gay, *Industrial hemp's double dividend: a study for the USA.* Ecological Economics, 1998. 25(3): p. 291-301.

23. Paul, A. and S. Thomas, *Electrical properties of natural-fiber-reinforced low density polyethylene composites: A comparison with carbon black and glass-fiber-filled low density polyethylene composites.* Journal of Applied Polymer Science, 1997. 63(2): p. 247-266.

24. Bledzki, A.K.a.G., J., *Composites Reinforced with Cellulose Based Fibers.* Progress in Polymer Science, 1999. 24: p. 221-274.

25. Frederick TW, N.W., *Natural fibers plastics and composites*. 2004, Kluwer Academic Publishers: New York.

26. Singh, B.P., ed. *Industrial Crops and Uses*. 2010, CABI International: Cambridge, MA.

27. Auras, R., B. Harte, and S. Selke, *An Overview of Polylactides as Packaging Materials.* Macromolecular Bioscience, 2004. 4(9): p. 835-864.

28. Gatenholm, P. and A. Mathiasson, *Biodegradable natural composites. II. Synergistic effects of processing cellulose with PHB.* Journal of Applied Polymer Science, 1994. 51(7): p. 1231-1237.

29. Yoshito Ikada, H.T., *Biodegradable polyesters for medical and ecological applications.* Macromol. Rapid Commun, 2000. 21: p. 117-132.

30. Mohanty, S., S.K. Verma, and S.K. Nayak, *Dynamic mechanical and thermal properties of MAPE treated jute/HDPE composites.* Composites Science and Technology, 2006. 66(3-4): p. 538-547.

31. Van de Velde, K. and P. Kiekens, *Biopolymers: overview of several properties and consequences on their applications.* Polymer Testing, 2002. 21(4): p. 433-442.

32. Witzke, D.R., *Introduction to properties, engineering, and prospects of polylactide polymers*, in *Chemical Engineering*. 1997, Michigan State University: East Lansing.

33. Rafael Auras, L.-T.L., Susan E. M. Selke, & Hideto Tsuji, ed. *POLY (LACTIC ACID) synthesis, structures, properties, processing, and applcaition*. ed. R.F.G.a.D. Nwabunma. 2010, John Wiley & Sonc, Inc.: Hoboken, New Jersey.

34. Park, S.-D., M. Todo, and K. Arakawa, *Effect of annealing on the fracture toughness of poly(lactic acid).* Journal of Materials Science, 2004. 39(3): p. 1113-1116.

35. Han, S.O., *Understanding the Reinforcing Mechanisms in Kenaf Fiber/PLA and Kenaf Fiber/PP Composites: A Comparative Study.* International Journal of Polymer Science, 2012. 2012: p. 8.

36. Nishino, T., *Kenaf reinforced biodegradable composite.* Composites Science and Technology, 2003. 63(9): p. 1281-1286.

37. Ochi, S., *Mechanical properties of kenaf fibers and kenaf/PLA composites.* Mechanics of Materials, 2008. 40(4–5): p. 446-452.

38. Huda, M.S., *Effect of fiber surface-treatments on the properties of laminated biocomposites from poly(lactic acid) (PLA) and kenaf fibers.* Composites Science and Technology, 2008. 68(2): p. 424-432.

39. Serizawa, S., K. Inoue, and M. Iji, *Kenaf-fiber-reinforced poly(lactic acid) used for electronic products.* Journal of Applied Polymer Science, 2006. 100(1): p. 618-624.

40. Oksman, K., M. Skrifvars, and J.F. Selin, *Natural fibres as reinforcement in polylactic acid (PLA) composites.* Composites Science and Technology, 2003. 63(9): p. 1317-1324.

41. Bax, B. and J. Müssig, *Impact and tensile properties of PLA/Cordenka and PLA/flax composites.* Composites Science and Technology, 2008. 68(7–8): p. 1601-1607.

42. Shanks, R.A., A. Hodzic, and D. Ridderhof, *Composites of poly(lactic acid) with flax fibers modified by interstitial polymerization.* Journal of Applied Polymer Science, 2006. 99(5): p. 2305-2313.

43. Kumar, R., M.K. Yakubu, and R.D. Anandjiwala, *Biodegradation of flax fiber reinforced poly lactic acid.* Express Polymer Letters, 2010. 4(7): p. 423-430.

44. Raj, G., *Role of Polysaccharides on Mechanical and Adhesion Properties of Flax Fibres in Flax/PLA Biocomposite.* International Journal of Polymer Science, 2011. 2011.

45. Plackett, D., *Biodegradable composites based on l-polylactide and jute fibres.* Composites Science and Technology, 2003. 63(9): p. 1287-1296.

46. Yu, T., Y. Li, and J. Ren, *Preparation and properties of short natural fiber reinforced poly(lactic acid) composites.* Transactions of Nonferrous Metals Society of China, 2009. 19: p. S651-S655.

47. Hongwei Ma and Chang Whan Joo, *Structure and mechanical properties of jute—polylactic acid biodegradable composites.* Journal of Composite Materials, 2011. 45(14): p. 1451-1460.

48. Zhaoqian Li, X.Z., and Chonghua Pei, *Effect of Sisal Fiber Surface Treatment on Properties of Sisal Fiber Reinforced Polylactide Composites.* International Journal of Polymer Science, 2011. 2011.

49. Yu, T., *Effect of fiber surface-treatments on the properties of poly(lactic acid)/ramie composites.* Composites Part A: Applied Science and Manufacturing, 2010. 41(4): p. 499-505.

50. Kimura Teruo, K.M., Matsuo Tatsuki, Matsubara Hirokazu, Sakobe Tadayuki *Compression Molding and Mechanical Properties of Green-Composite Based on Ramie/PLA Non-Twisted Commingled Yarn.* Journal of the Society of Materials Science, 2004. 53(7): p. 776-781.

51. van den Oever, M.J.A., B. Beck, and J. Mussig, *Agrofibre reinforced poly(lactic acid) composites: Effect of moisture on degradation and mechanical properties.* Composites Part a-Applied Science and Manufacturing, 2010. 41(11): p. 1628-1635.

52. Shumao, L., *Influence of ammonium polyphosphate on the flame retardancy and mechanical properties of ramie fiber-reinforced poly(lactic acid) biocomposites.* Polymer International, 2010. 59(2): p. 242-248.

53. Bledzki, A.K., A. Jaszkiewicz, and D. Scherzer, *Mechanical properties of PLA composites with man-made cellulose and abaca fibres.* Composites Part A: Applied Science and Manufacturing, 2009. 40(4): p. 404-412.

54. Lee, S.H. and S.Q. Wang, *Biodegradable polymers/bamboo fiber biocomposite with bio-based coupling agent.* Composites Part a-Applied Science and Manufacturing, 2006. 37(1): p. 80-91.

55. Tokoro, R., *How to improve mechanical properties of polylactic acid with bamboo fibers.* Journal of Materials Science, 2008. 43(2): p. 775-787.

56. Lee, S.-H., T. Ohkita, and K. Kitagawa, *Eco-composite from poly(lactic acid) and bamboo fiber*, in *Holzforschung*. 2004. p. 529.

57. Huda, M.S., *Effect of chemical modifications of the pineapple leaf fiber surfaces on the interfacial and mechanical properties of laminated biocomposites.* Composite Interfaces, 2008. 15(2-3): p. 169-191.

58. Hu, R. and J.-K. Lim, *Fabrication and Mechanical Properties of Completely Biodegradable Hemp Fiber Reinforced Polylactic Acid Composites.* Journal of Composite Materials, 2007. 41(13): p. 1655-1669.

59. Masirek, R., *Composites of poly(L-lactide) with hemp fibers: Morphology and thermal and mechanical properties.* Journal of Applied Polymer Science, 2007. 105(1): p. 255-268.

60. Graupner, N., *Improvement of the Mechanical Properties of Biodegradable Hemp Fiber Reinforced Poly(lactic acid) (PLA) Composites by the Admixture of Man-made Cellulose Fibers.* Journal of Composite Materials, 2009. 43(6): p. 689-702.

61. Islam, M.S., K.L. Pickering, and N.J. Foreman, *Influence of alkali treatment on the interfacial and physico-mechanical properties of industrial hemp fibre reinforced polylactic acid composites.* Composites Part A: Applied Science and Manufacturing, 2010. 41(5): p. 596-603.

62. Islam, M.S., K.L. Pickering, and N.J. Foreman, *Influence of accelerated ageing on the physico-mechanical properties of alkali-treated industrial hemp fibre*

reinforced poly(lactic acid) (PLA) composites. Polymer Degradation and Stability, 2010. 95(1): p. 59-65.

63. Sawpan, M.A., K.L. Pickering, and A. Fernyhough, *Improvement of mechanical performance of industrial hemp fibre reinforced polylactide biocomposites.* Composites Part A: Applied Science and Manufacturing, 2011. 42(3): p. 310-319.

64. Sawpan, M.A., K.L. Pickering, and A. Fernyhough, *Effect of fibre treatments on interfacial shear strength of hemp fibre reinforced polylactide and unsaturated polyester composites.* Composites Part a-Applied Science and Manufacturing, 2011. 42(9): p. 1189-1196.

65. Yew, G.H., *Water absorption and enzymatic degradation of poly(lactic acid)/rice starch composites.* Polymer Degradation and Stability, 2005. 90(3): p. 488-500.

66. Yew, G.H., *Natural Weathering of Poly (Lactic Acid): Effects of Rice Starch and Epoxidized Natural Rubber.* Journal of Elastomers and Plastics, 2009. 41(4): p. 369-382.

67. Bledzki, A.K. and A. Jaszkiewicz, *Mechanical performance of biocomposites based on PLA and PHBV reinforced with natural fibres - A comparative study to PP*. Composites Science and Technology, 2010. 70(12): p. 1687-1696.

68. Huda, M.S., *Wood-fiber-reinforced poly(lactic acid) composites: Evaluation of the physicomechanical and morphological properties.* Journal of Applied Polymer Science, 2006. 102(5): p. 4856-4869.

69. Pilla, S., *Polylactide-pine wood flour composites.* Polymer Engineering & Science, 2008. 48(3): p. 578-587.

70. Huda, M.S., *A Study on Biocomposites from Recycled Newspaper Fiber and Poly(lactic acid).* Industrial & Engineering Chemistry Research, 2005. 44(15): p. 5593-5601.

71. LiuLiu, *Biodegradable Composites from Sugar Beet Pulp and Poly(lactic acid).* Journal of Agricultural and Food Chemistry, 2005. 53(23): p. 9017-9022.

72. Ganster, J., H.P. Fink, and M. Pinnow, *High-tenacity man-made cellulose fibre reinforced thermoplastics – Injection moulding compounds with polypropylene and alternative matrices.* Composites Part A: Applied Science and Manufacturing, 2006. 37(10): p. 1796-1804.

73. Valadez-Gonzalez, A., *Effect of fiber surface treatment on the fiber-matrix bond strength of natural fiber reinforced composites.* Composites Part B-Engineering, 1999. 30(3): p. 309-320.

74. Mwaikambo, L.Y. and M.P. Ansell, *The effect of chemical treatment on the properties of hemp, sisal, jute and kapok for composite reinforcement.* Angewandte Makromolekulare Chemie, 1999. 272: p. 108-116.

75. Albano, C., *Thermal stability of blends of polyolefins and sisal fiber.* Polymer Degradation and Stability, 1999. 66(2): p. 179-190.

76. Felix, J.M., P. Gatenholm, and H.P. Schreiber, *CONTROLLED INTERACTIONS IN CELLULOSE-POLYMER COMPOSITES .1. EFFECT ON MECHANICAL-PROPERTIES.* Polymer Composites, 1993. 14(6): p. 449-457.

77. George, J., S.S. Bhagawan, and S. Thomas, *Thermogravimetric and dynamic mechanical thermal analysis of pineapple fibre reinforced polyethylene composites.* Journal of Thermal Analysis, 1996. 47(4): p. 1121-1140.

78. Shokoohi, S., A. Arefazar, and R. Khosrokhavar, *Silane coupling agents in polymer-based reinforced composites: A review.* Journal of Reinforced Plastics and Composites, 2008. 27(5): p. 473-485.

79. Bilba, K. and M.A. Arsene, *Silane treatment of bagasse fiber for reinforcement of cementitious composites.* Composites Part a-Applied Science and Manufacturing, 2008. 39(9): p. 1488-1495.

80. Sinha, E. and S. Panigrahi, *Effect of Plasma Treatment on Structure, Wettability of Jute Fiber and Flexural Strength of its Composite.* Journal of Composite Materials, 2009. 43(17): p. 1791-1802.

81. Na Lu, S.M.B., *Effect of Physical and Chemical Surface Treatment on the Thermal Stability of Hemp Fibers as Reinforcement in Composite Structures.* Applied Mechanics and Materials 2011. 71-78: p. 616-620.

82. Gulati, D. and M. Sain, *Fungal-modification of natural fibers: A novel method of treating natural fibers for composite reinforcement.* Journal of Polymers and the Environment, 2006. 14(4): p. 347-352.

83. Schirp, A., *Production and characterization of natural fiber-reinforced thermoplastic composites using wheat straw modified with the fungus Pleurotus ostreatus.* Journal of Applied Polymer Science, 2006. 102(6): p. 5191-5201.

84. Lu, N. and S. Oza, *Thermal stability and thermo-mechanical properties of hemp-high density polyethylene composites: Effect of two different chemical modifications.* Composites Part B: Engineering, 2013. 44(1): p. 484-490.

85. Lu, N. and S. Oza, *A comparative study of the mechanical properties of hemp fiber with virgin and recycled high density polyethylene matrix.* Composites Part B: Engineering, 2013. 45(1): p. 1651-1656.

86. Mishra, S., *Studies on mechanical performance of biofibre/glass reinforced polyester hybrid composites.* Composites Science and Technology, 2003. 63(10): p. 1377-1385.

87. Paul, A., K. Joseph, and S. Thomas, *Effect of surface treatments on the electrical properties of low-density polyethylene composites reinforced with short sisal fibers.* Composites Science and Technology, 1997. 57(1): p. 67-79.

88. Tserki, V., *A study of the effect of acetylation and propionylation surface treatments on natural fibres.* Composites Part a-Applied Science and Manufacturing, 2005. 36(8): p. 1110-1118.

89. Hill, C.A.S., H. Khalil, and M.D. Hale, *A study of the potential of acetylation to improve the properties of plant fibres.* Industrial Crops and Products, 1998. 8(1): p. 53-63.

90. Rong, M.Z., *The effect of fiber treatment on the mechanical properties of unidirectional sisal-reinforced epoxy composites.* Composites Science and Technology, 2001. 61(10): p. 1437-1447.

91. Sreekala, M.S., *Oil palm fibre reinforced phenol formaldehyde composites: Influence of fibre surface modifications on the mechanical performance.* Applied Composite Materials, 2000. 7(5-6): p. 295-329.

92. Nair, K.C.M., S. Thomas, and G. Groeninckx, *Thermal and dynamic mechanical analysis of polystyrene composites reinforced with short sisal fibres.* Composites Science and Technology, 2001. 61(16): p. 2519-2529.

93. Sreekala, M.S., M.G. Kumaran, and S. Thomas, *Water sorption in oil palm fiber reinforced phenol formaldehyde composites.* Composites Part a-Applied Science and Manufacturing, 2002. 33(6): p. 763-777.

94. Mishra, S., *Graft copolymerization of acrylonitrile on chemically modified sisal fibers.* Macromolecular Materials and Engineering, 2001. 286(2): p. 107-113.

95. Agrawal, R., *Activation energy and crystallization kinetics of untreated and treated oil palm fibre reinforced phenol formaldehyde composites.* Materials Science and Engineering a-Structural Materials Properties Microstructure and Processing, 2000. 277(1-2): p. 77-82.

96. Van de Weyenberg, I., *Influence of processing and chemical treatment of flax fibres on their composites.* Composites Science and Technology, 2003. 63(9): p. 1241-1246.

97. Cantero, G., *Effects of fibre treatment on wettability and mechanical behaviour of flax/polypropylene composites.* Composites Science and Technology, 2003. 63(9): p. 1247-1254.

98. Gassan, J. and A.K. Bledzki, *The influence of fiber-surface treatment on the mechanical properties of jute-polypropylene composites.* Composites Part a-Applied Science and Manufacturing, 1997. 28(12): p. 1001-1005.

99. Keener, T.J., R.K. Stuart, and T.K. Brown, *Maleated coupling agents for natural fibre composites.* Composites Part a-Applied Science and Manufacturing, 2004. 35(3): p. 357-362.

100. A.K. Bledzki, V.E.S., O. Faruk, *Rapra Review Reports*, in *Natural and wood fiber reinforcement in polymers* R.T.L. Sally Humphreys, Editor. 2002.

101. Ragoubi, M., *Impact of corona treated hemp fibres onto mechanical properties of polypropylene composites made thereof.* Industrial Crops and Products, 2010. 31(2): p. 344-349.

102. Morales, J., *Plasma modification of cellulose fibers for composite materials.* Journal of Applied Polymer Science, 2006. 101(6): p. 3821-3828.

103. Buschle-Diller, G., C. Fanter, and F. Loth, *Structural Changes in Hemp Fibers as a Result of Enzymatic Hydrolysis with Mixed Enzyme Systems.* Textile Research Journal, 1999. 69(4): p. 244-251.

104. Kalia, S., B.S. Kaith, and I. Kaur, *Pretreatments of Natural Fibers and their Application as Reinforcing Material in Polymer Composites-A Review*. Polymer Engineering and Science, 2009. 49(7): p. 1253-1272.

105. Aziz, S.H. and M.P. Ansell, *The effect of alkalization and fibre alignment on the mechanical and thermal properties of kenaf and hemp bast fibre composites: Part 1 - polyester resin matrix.* Composites Science and Technology, 2004. 64(9): p. 1219-1230.

106. Arbelaiz, A., *Mechanical properties of flax fibre/polypropylene composites. Influence of fibre/matrix modification and glass fibre hybridization.* Composites Part a-Applied Science and Manufacturing, 2005. 36(12): p. 1637-1644.

107. International, A., *ASTM E 1131 "Standard Test Method for Compositional Analysis by Thermogravimetry"*. 2008, ASTM International: PA.

108. International, A., *ASTM C 1557-03 "Standard test method for tensile strength and Young's modulus of fibers"*. 2008, ASTM International: PA.

109. International, A., *ASTM D 3039/D3039M "Standard Test Method for Tensile Properties of Polymer Matrix Composite Materials"*. 2008: PA.

110. International, A., *ASTM D790 - 10 Standard Test Methods for Flexural Properties of Unreinforced and Reinforced Plastics and Electrical Insulating Materials* 2010: West Conshohocken, PA.

111. *Rule of Mixtures*. [cited 2013 2 Jan]; Available from: http://pas.ce.wsu.edu/CE537-1/Lectures/Rule%20of%20Mixtures.pdf.

112. Sgriccia, N., M.C. Hawley, and M. Misra, *Characterization of natural fiber surfaces and natural fiber composites.* Composites Part A: Applied Science and Manufacturing, 2008. 39(10): p. 1632-1637.

113. U.S.D.A, F.S. *Thermal degradartion of wood components: a review of the literature*. 1970 [cited 2013 2 Jan]; Available from: http://www.fpl.fs.fed.us/documnts/fplrp/fplrp130.pdf.

114. Yao, F., *Thermal decomposition kinetics of natural fibers: Activation energy with dynamic thermogravimetric analysis.* Polymer Degradation and Stability, 2008. 93(1): p. 90-98.

115. Alvarez, V.A. and A. Vázquez, *Thermal degradation of cellulose derivatives/starch blends and sisal fibre biocomposites.* Polymer Degradation and Stability, 2004. 84(1): p. 13-21.

116. Mukherjee, T. and N. Kao, *PLA Based Biopolymer Reinforced with Natural Fibre: A Review*. Journal of Polymers and the Environment, 2011. 19(3): p. 714-725.

117. Yao, F., *Rice straw fiber-reinforced high-density polyethylene composite: Effect of fiber type and loading.* Industrial Crops and Products, 2008. 28(1): p. 63-72.

118. R.T.Sanderson. *Chemical bonds and bond energy*. 1976; Available from: http://www.cem.msu.edu/~reusch/OrgPage/bndenrgy.htm.

119. Friedman, H.L., *Kinetics of thermal degradation of char-forming plastics from thermogravimetry. Application to a phenolic plastic.* Journal of Polymer Science Part C: Polymer Symposia, 1964. 6(1): p. 183-195.

120. Flynn J H, W.L.A., *General treatment of thermogravimetry of polymers.* Journal of Research of the National Bureauu of Standards - A-Physics and Chemistry, 1966. 70A(6): p. 4878-523.

121. Ozawa, T., *A modified method for kinetic analysis of thermoanalytical data.* Journal of Thermal Analysis, 1976. 9(3): p. 369-373.

122. Kissinger, H.E., *Reaction Kinetics in Differential Thermal Analysis.* Analytical Chemistry, 1957. 29(11): p. 1702-1706.

123. Ouajai, S. and R.A. Shanks, *Composition, structure and thermal degradation of hemp cellulose after chemical treatments.* Polymer Degradation and Stability, 2005. 89(2): p. 327-335.

124. Sawpan, M.A., K.L. Pickering, and A. Fernyhough, *Flexural properties of hemp fibre reinforced polylactide and unsaturated polyester composites.* Composites Part A: Applied Science and Manufacturing, 2012. 43(3): p. 519-526.

125. Associates, F., *Life cycle inventory of five products produced from polylactide (PLA) and petroleum-based resins*. 2006, Athena Sustainable Materials Institute.

126. Suh, Y.-J. and P. Rousseaux, *An LCA of alternative wastewater sludge treatment scenarios.* Resources, Conservation and Recycling, 2002. 35(3): p. 191-200.

127. Kolstad, J.J., *Assessment of anaerobic degradation of Ingeo™ polylactides under accelerated landfill conditions.* Polymer Degradation and Stability, 2012. 97(7): p. 1131-1141.

128. Ho, K.-L., *Degradation of Polylactic Acid (PLA) Plastic in Costa Rican Soil and Iowa State University Compost Rows.* Journal of environmental polymer degradation, 1999. 7(4): p. 173-177.

129. Vargas, L.F., *Effect of electron beam treatments on degradation kinetics of polylactic acid (PLA) plastic waste under backyard composting conditions.* Packaging Technology and Science, 2009. 22(2): p. 97-106.

130. Kim, M.C. and T. Masuoka, *Degradation properties of PLA and PHBV films treated with CO2-plasma.* Reactive and Functional Polymers, 2009. 69(5): p. 287-292.

131. Metters, A.T., C.N. Bowman, and K.S. Anseth, *A Statistical Kinetic Model for the Bulk Degradation of PLA-b-PEG-b-PLA Hydrogel Networks.* The Journal of Physical Chemistry B, 2000. 104(30): p. 7043-7049.

132. Yagi, H., *Anaerobic biodegradation tests of poly(lactic acid) and polycaprolactone using new evaluation system for methane fermentation in anaerobic sludge.* Polymer Degradation and Stability, 2009. 94(9): p. 1397-1404.

133. Kale, G., *Biodegradability of polylactide bottles in real and simulated composting conditions.* Polymer Testing, 2007. 26(8): p. 1049-1061.

134. Shogren, R.L., *Biodegradation of starch/polylactic acid/poly(hydroxyester-ether) composite bars in soil.* Polymer Degradation and Stability, 2003. 79(3): p. 405-411.

135. Teramoto, N., *Biodegradation of aliphatic polyester composites reinforced by abaca fiber.* Polymer Degradation and Stability, 2004. 86(3): p. 401-409.

136. Yussuf, A.A., I. Massoumi, and A. Hassan, *Comparison of Polylactic Acid/Kenaf and Polylactic Acid/Rise Husk Composites: The Influence of the Natural Fibers on the Mechanical, Thermal and Biodegradability Properties.* Journal of Polymers and the Environment, 2010. 18(3): p. 422-429.

137. Ohkita, T. and S.H. Lee, *Thermal degradation and biodegradability of poly (lactic acid)/corn starch biocomposites.* Journal of Applied Polymer Science, 2006. 100(4): p. 3009-3017.

138. Wu, C.S., *Renewable resource-based composites of recycled natural fibers and maleated polylactide bioplastic: Characterization and biodegradability.* Polymer Degradation and Stability, 2009. 94(7): p. 1076-1084.

139. Iovino, R., *Biodegradation of poly(lactic acid)/starch/coir biocomposites under controlled composting conditions.* Polymer Degradation and Stability, 2008. 93(1): p. 147-157.

140. Petinakis, E., *Biodegradation and thermal decomposition of poly(lactic acid)-based materials reinforced by hydrophilic fillers.* Polymer Degradation and Stability, 2010. 95(9): p. 1704-1707.

141. Pradhan, R., *Compostability and biodegradation study of PLA-wheat straw and PLA-soy straw based green composites in simulated composting bioreactor.* Bioresource Technology, 2010. 101(21): p. 8489-8491.

142. Kendall, J.L.H.N.Y.L.A. *Integrated temperature and gas analysis at a municipal solid waste landfill*. Available from: http://digitalcommons.calpoly.edu/cgi/viewcontent.cgi?article=1137&context=cenv_fac.

143. Pérez, J., *Biodegradation and biological treatments of cellulose, hemicellulose and lignin: an overview.* International Microbiology, 2002. 5(2): p. 53-63.

144. Leschine, S.B., *Cellulose degradtion in anaerobic environments.* Annual Review of Microbiology, 1995. 49: p. 399-426.

145. Sukkhum, S. and V. Kitpreechavanich, *New Insight into Biodegradation of Poly (L-Lactide), Enzyme Production and Characterization*. Progress in Molecular and Environmental Bioengineering - From Analysis and Modeling to Technology Applications. 2011.

APPENDIX A: PHOTOGRAHPIC IMAGES OF TENSILE TESTED SPECIMENS

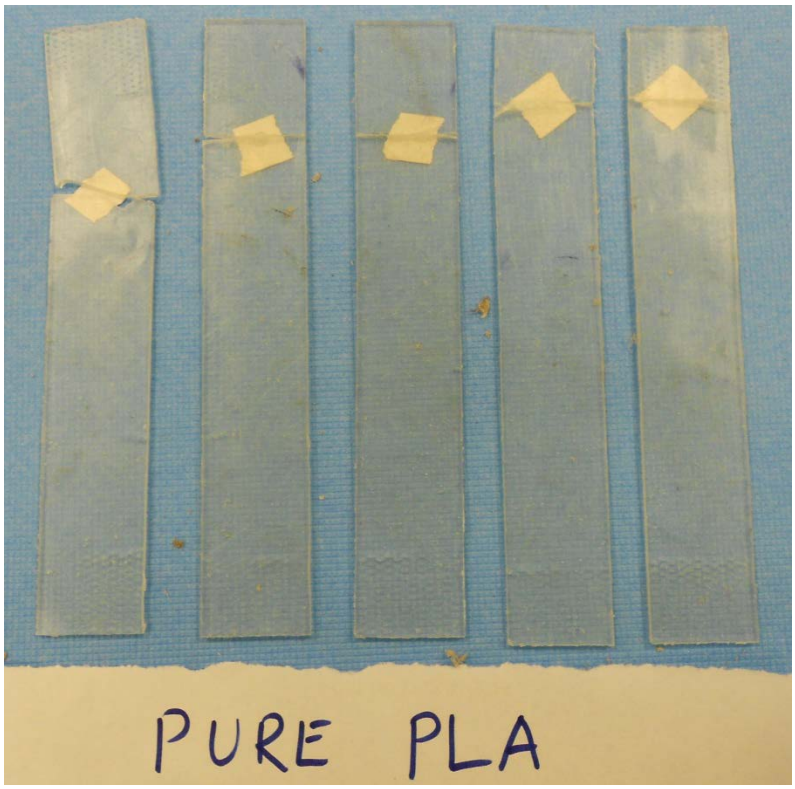

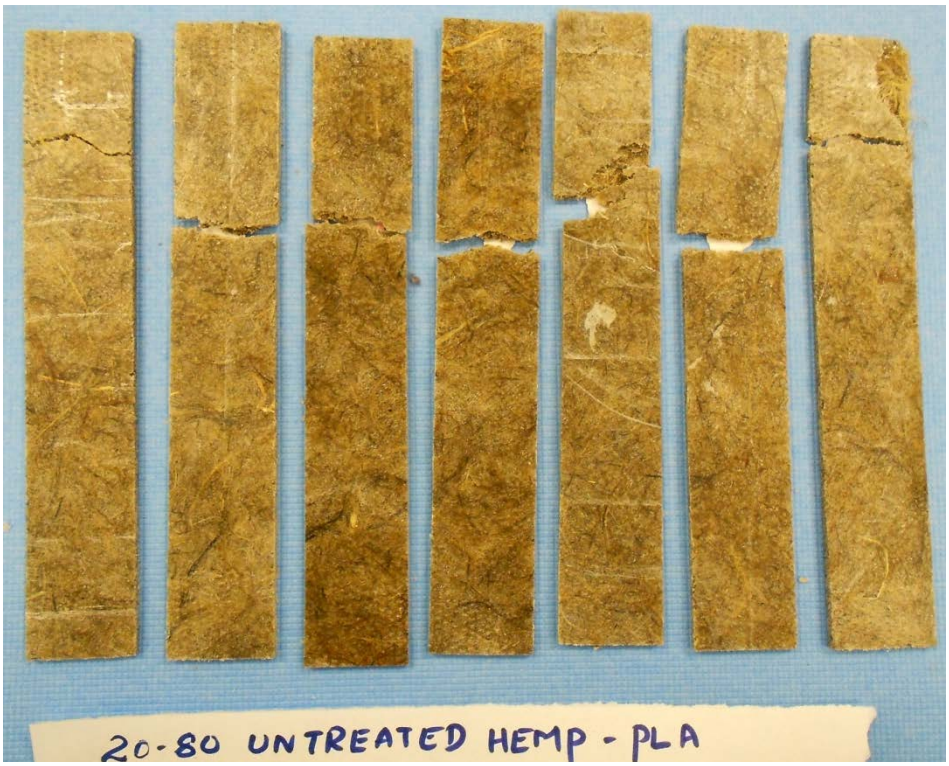


30-70 UNTREATED HEMP- PLA

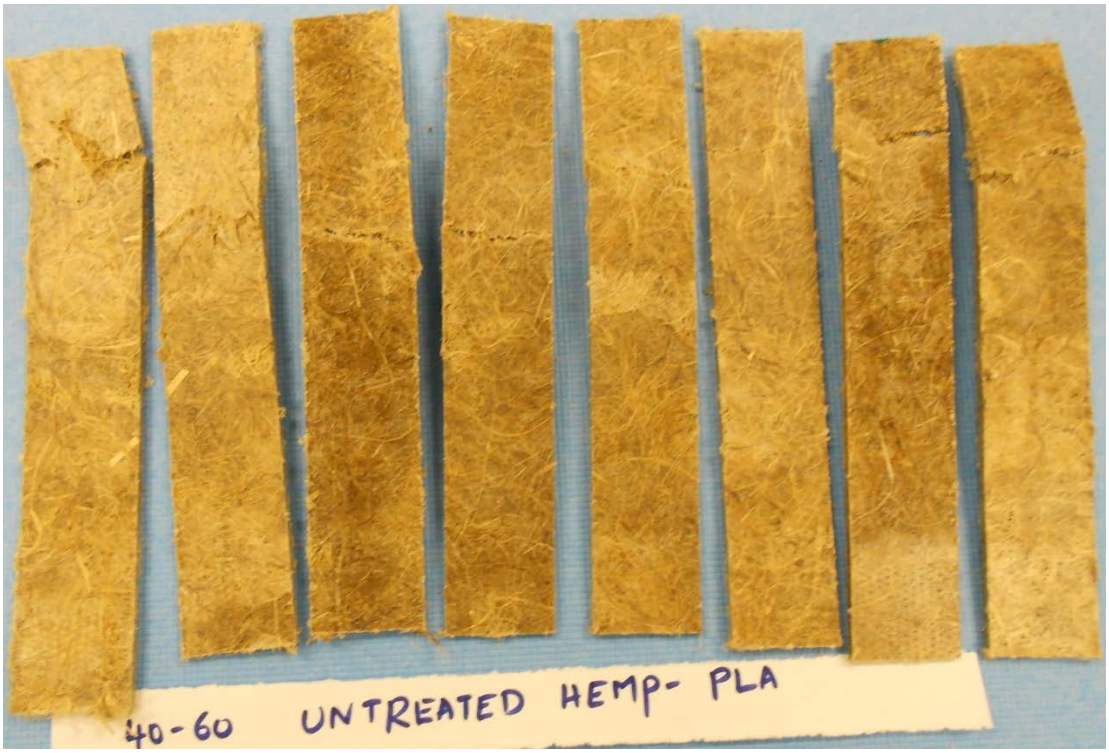
40-60 UNTREATED HEMP- PLA

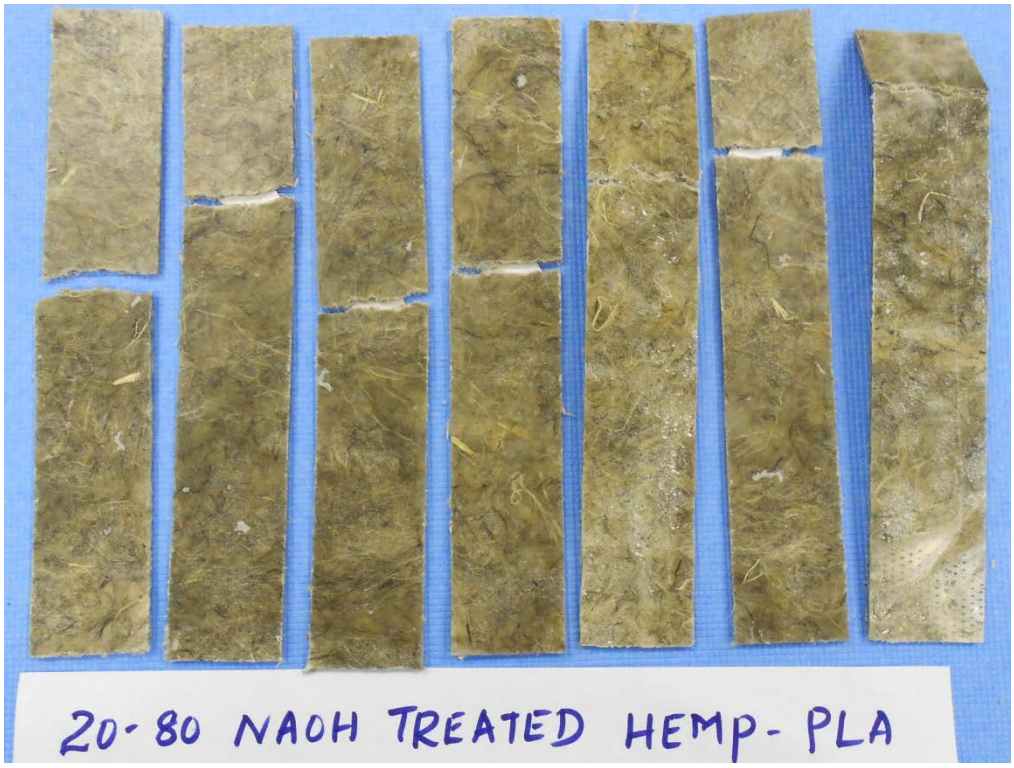
20-80 NAOH TREATED HEMP-PLA


30-70 NAOH TREATED HEMP-PLA


40-60 NaOH TREATED HEMP-PLA


20-80 SILANE TREATED HEMP-PLA


30-70 SILANE TREATED HEMP-PLA

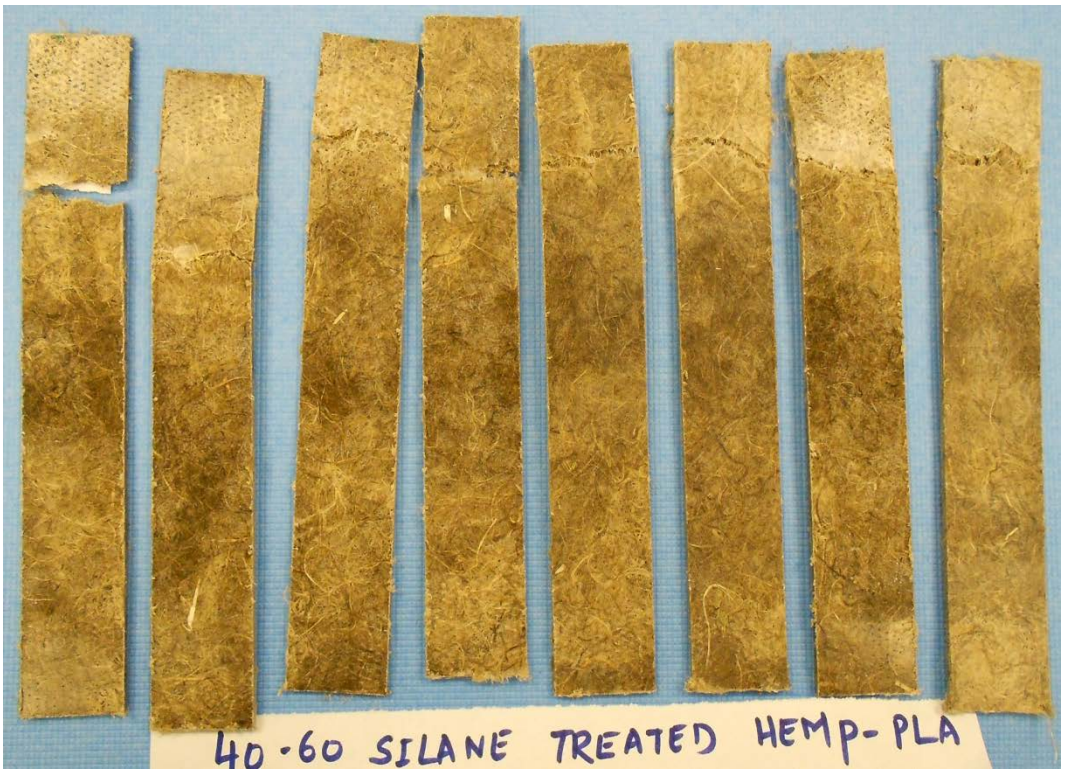
40-60 SILANE TREATED HEMP-PLA


20-80 ACETIC ANHYRIDE HEMp-PLA

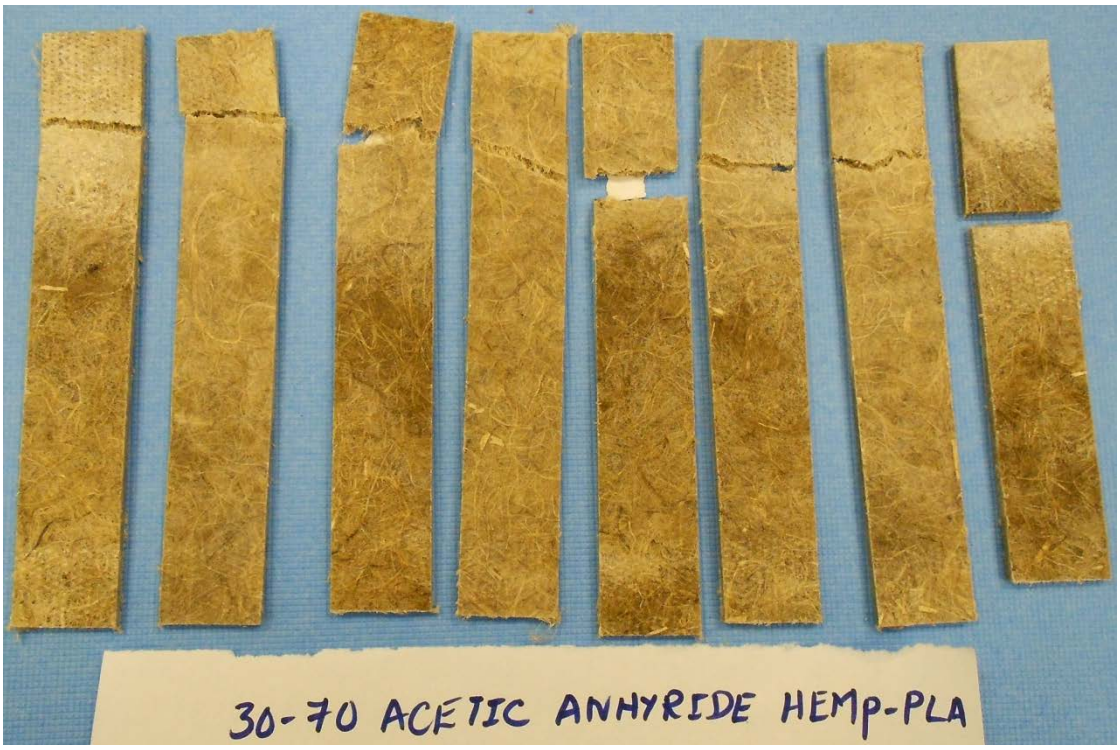
30-70 ACETIC ANHYRIDE HEMp-PLA

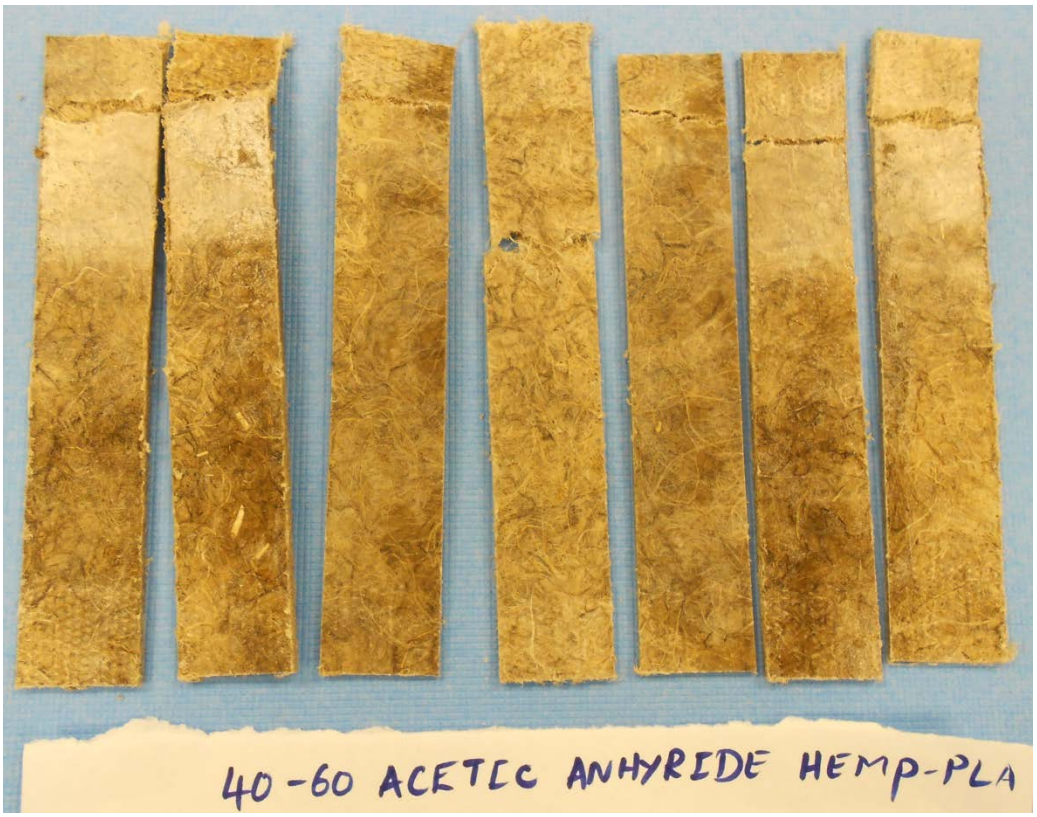
40-60 ACETIC ANHYRIDE HEMP-PLA

APPENDIX B: STRESS-STRAIN CURVES FOR ALL THE TENSILE TESTED SPECIMENS

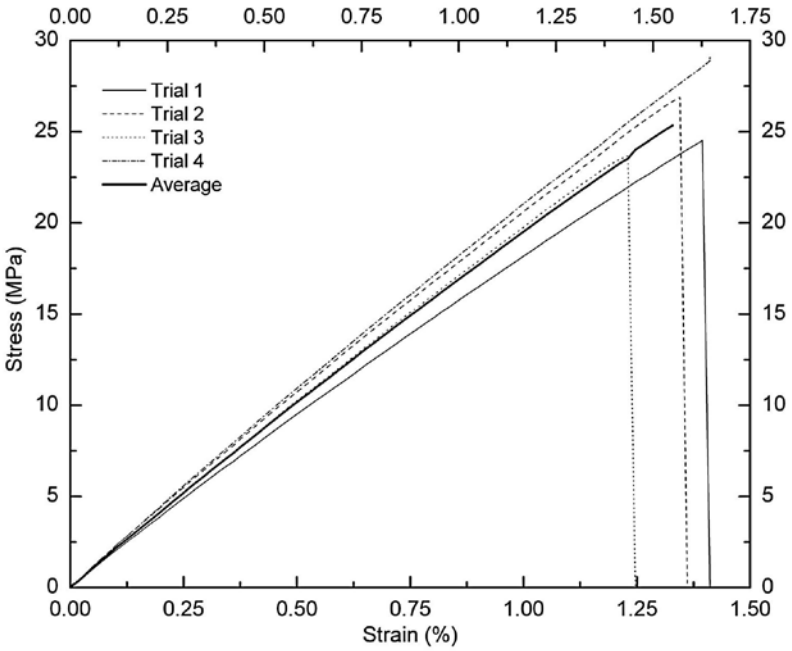

Stress strain curves of pure PLA specimens

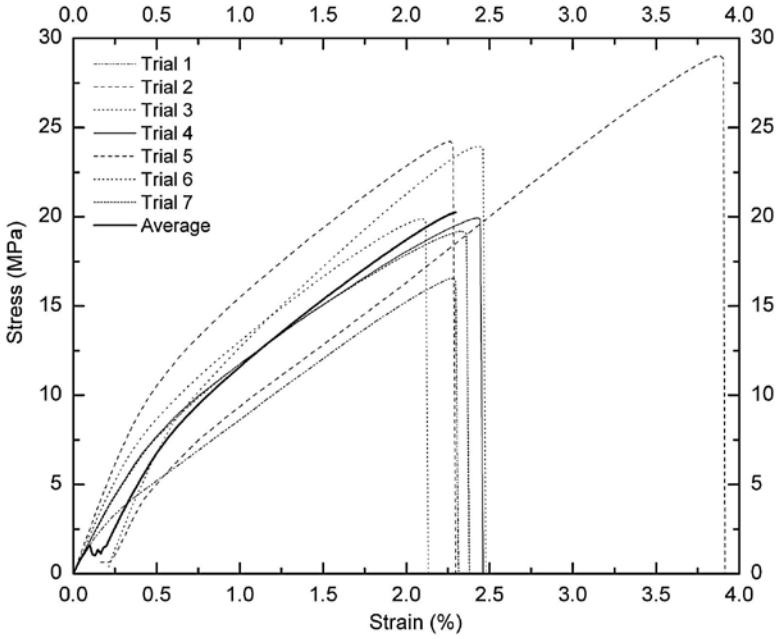

Stress strain curves for 20-80 untreated hemp-PLA composite specimens

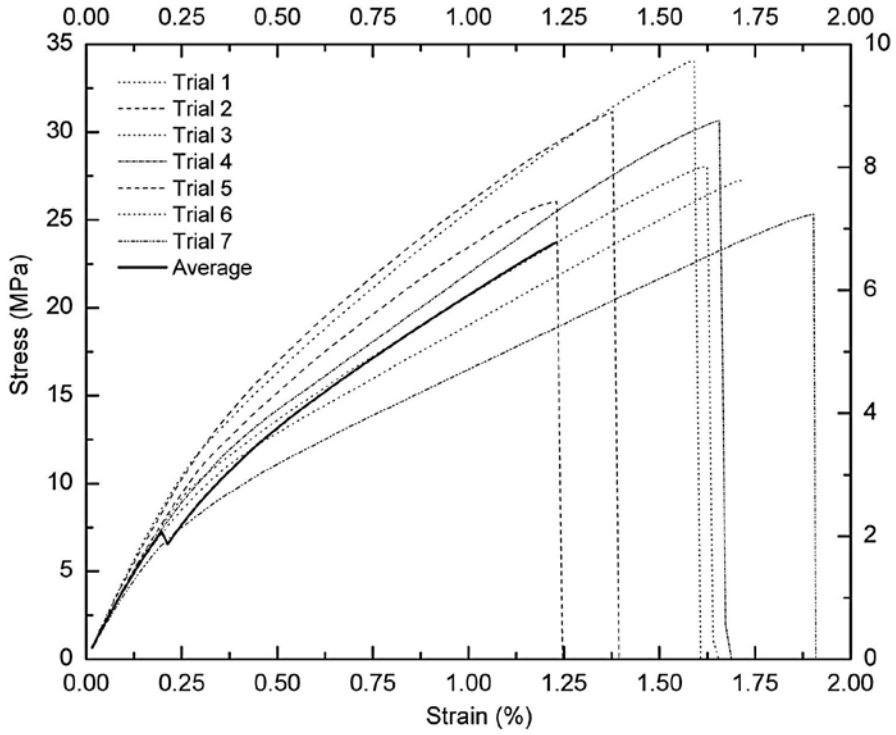

Stress strain curves for 30-70 untreated hemp-PLA composite specimens

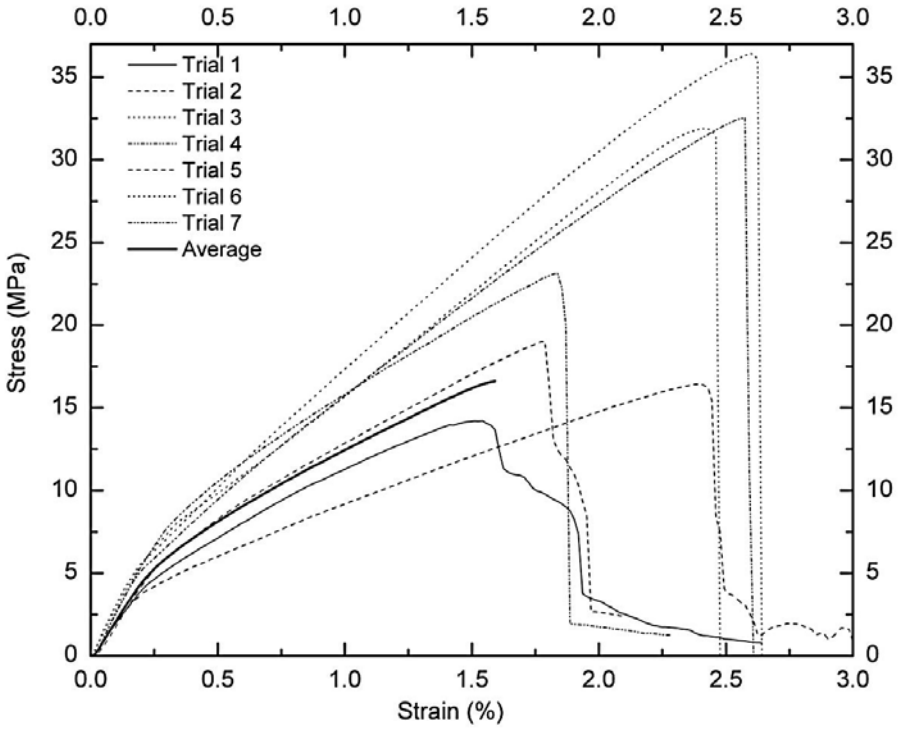

Stress strain curves for 40-60 untreated hemp-PLA composite specimens

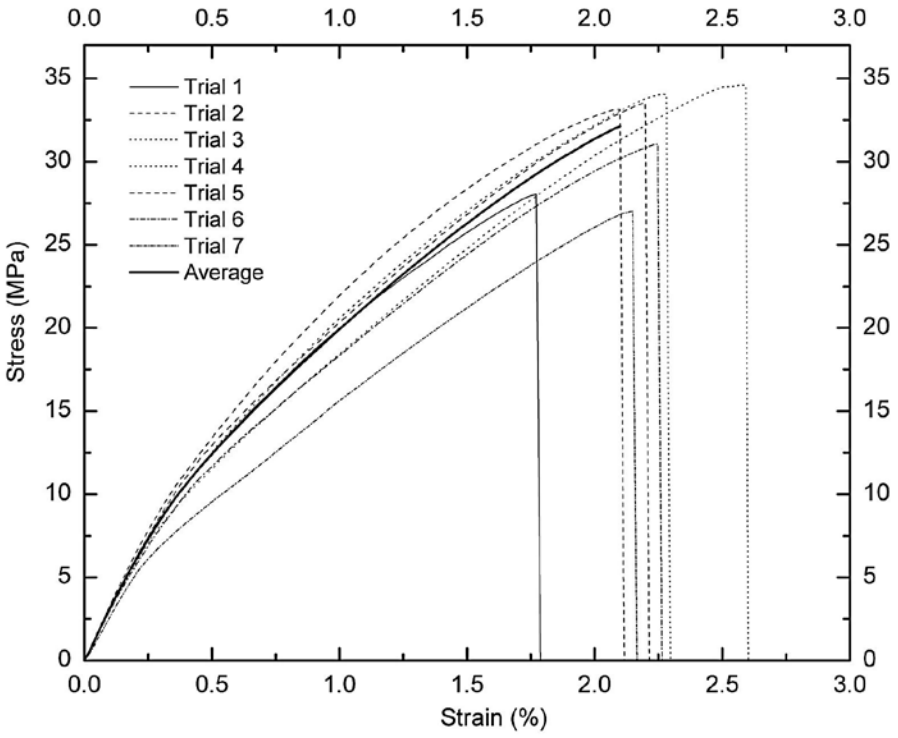

Stress strain curves for 20-80 NaOH treated hemp-PLA composite specimens

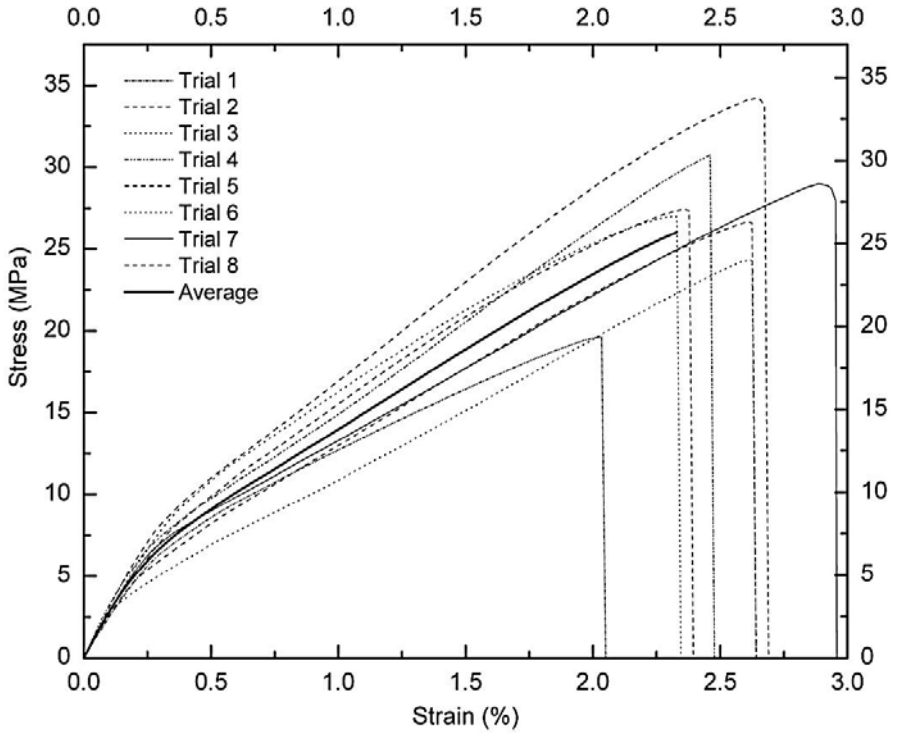

Stress strain curves for 30-70 NaOH treated hemp-PLA composite specimens

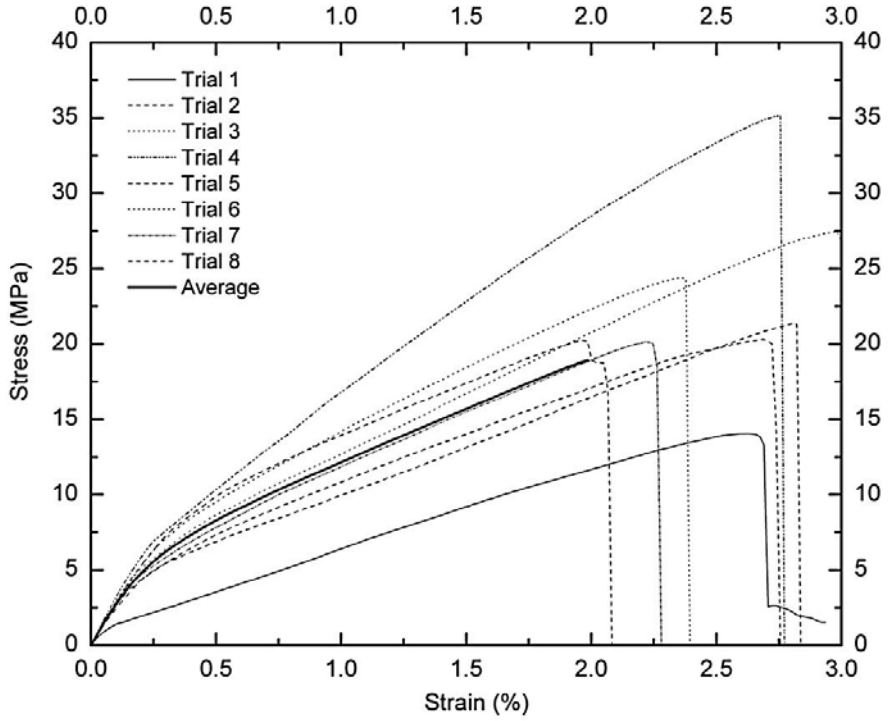

Stress strain curves for 40-60 NaOH treated hemp-PLA composite specimens

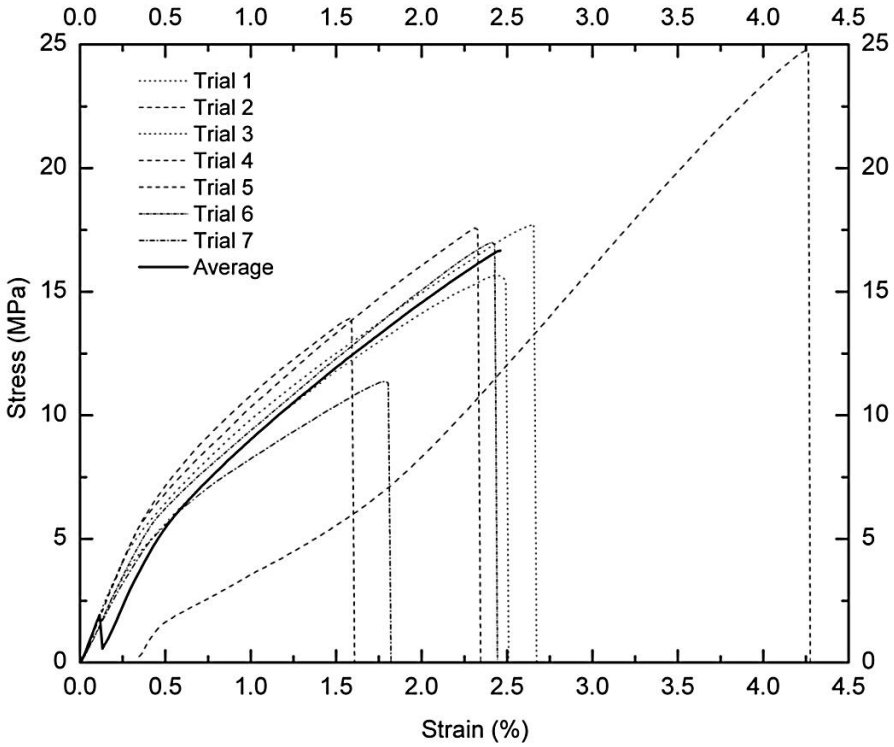

Stress strain curves for 20-80 Silane treated hemp-PLA composite specimens

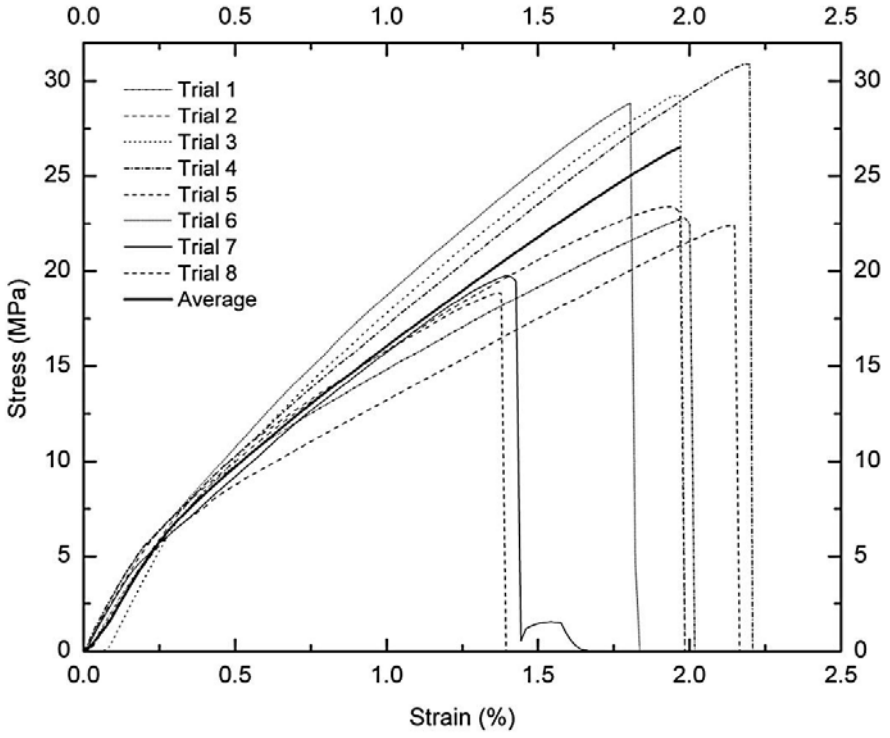

Stress strain curves for 30-70 Silane treated hemp-PLA composite specimens

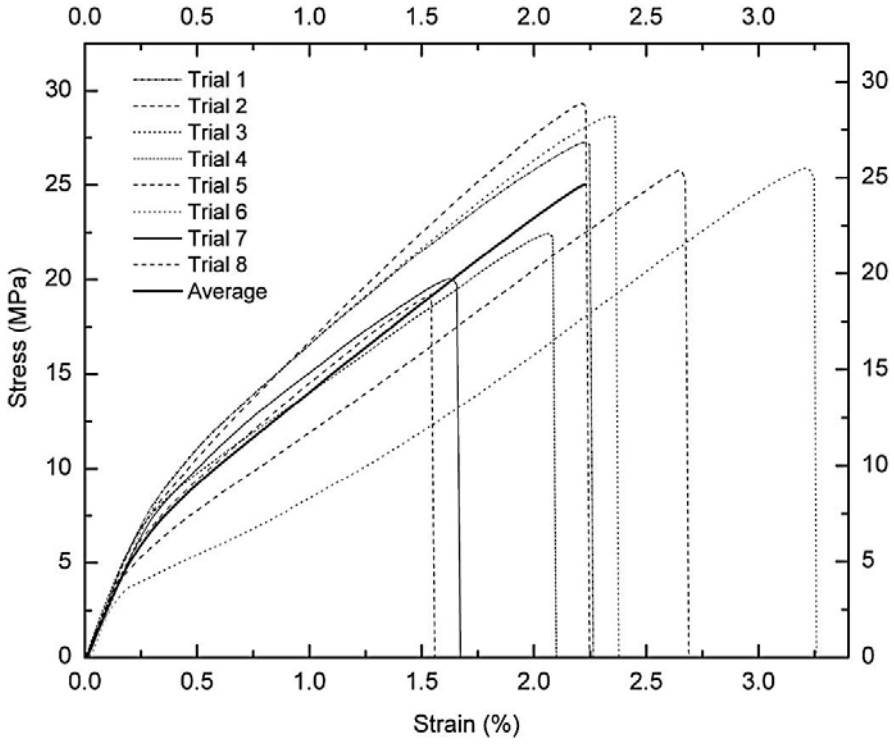

Stress strain curves for 40-60 Silane treated hemp-PLA composite specimens

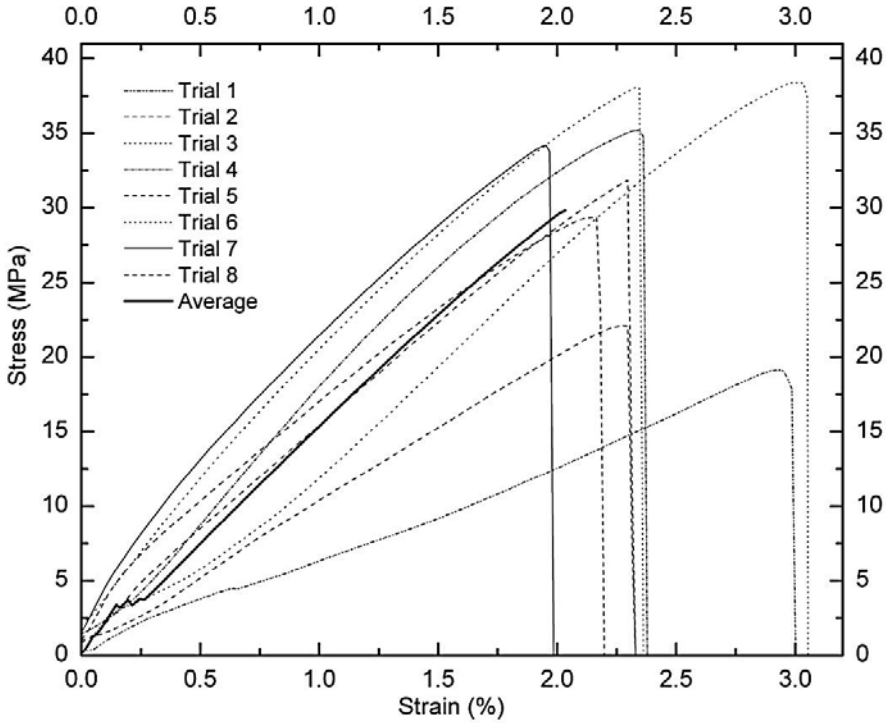

Stress strain curves for 20-80 acetic anhydride treated hemp-PLA composite specimens

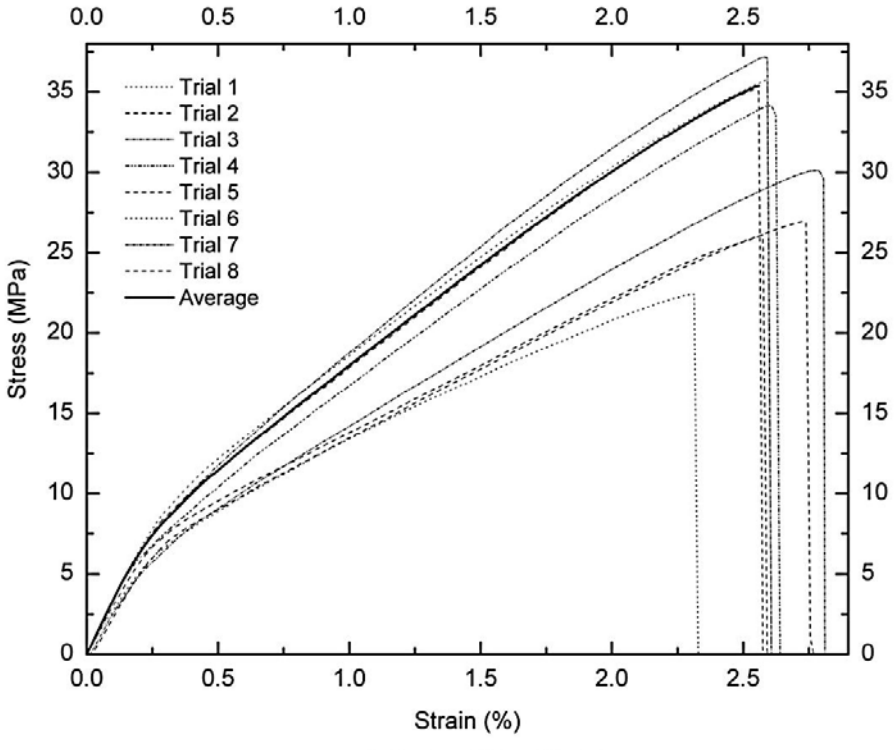

Stress strain curves for 30-70 acetic anhydride treated hemp-PLA composite specimens

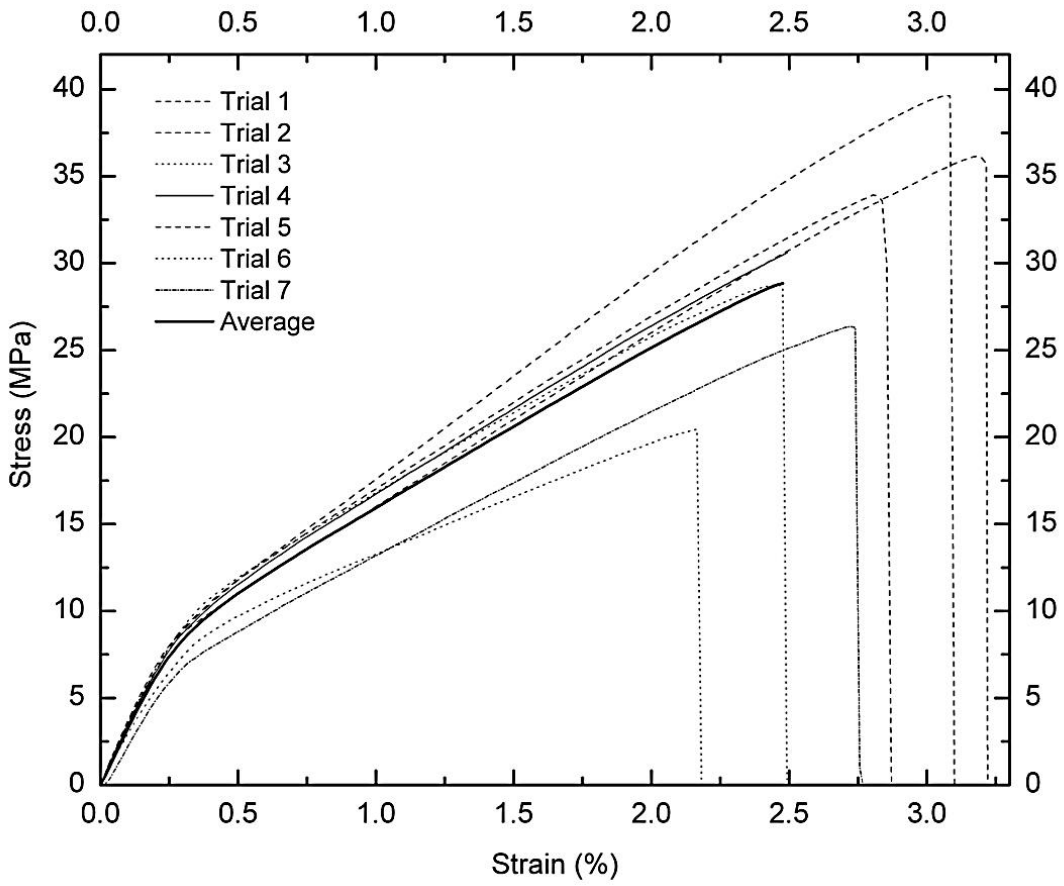

Stress strain curves for 40-60 acetic anhydride treated hemp-PLA composite specimens

APPENDIX C: PHOTOGRAHPIC IMAGES OF FLEXURAL TESTED SPECIMENS

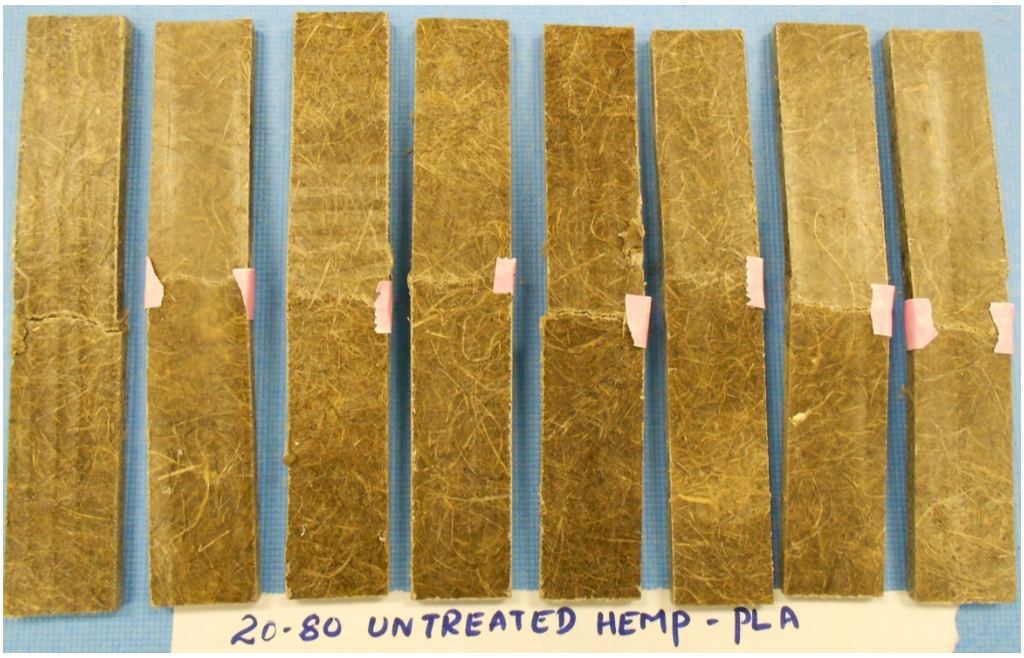

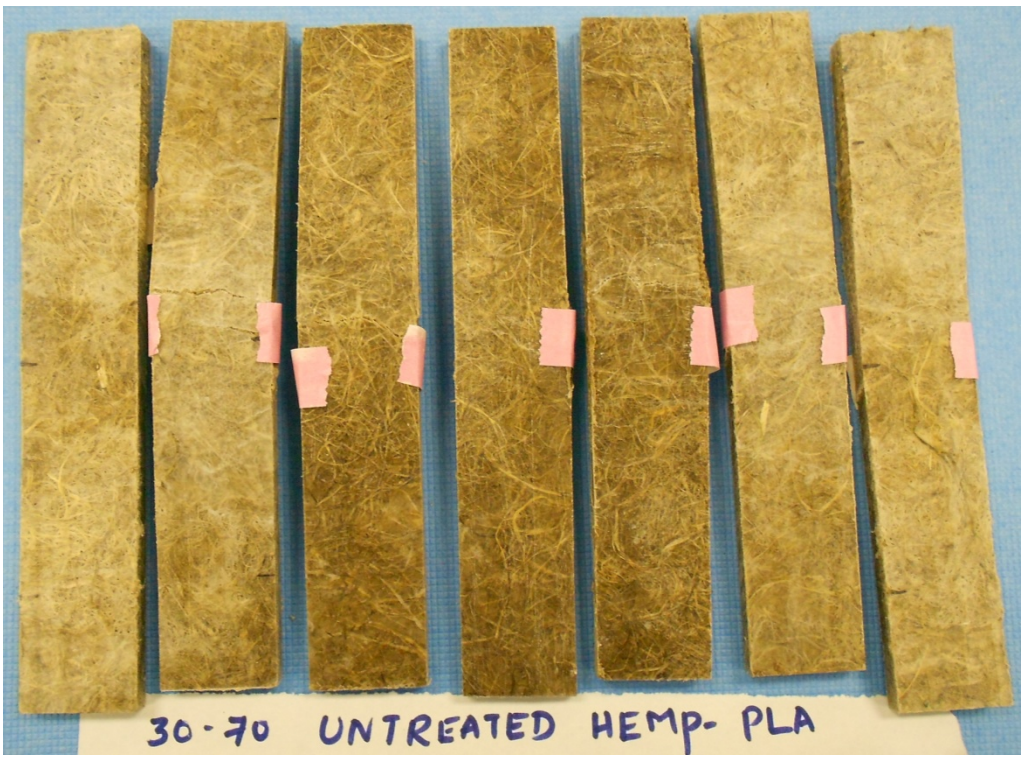

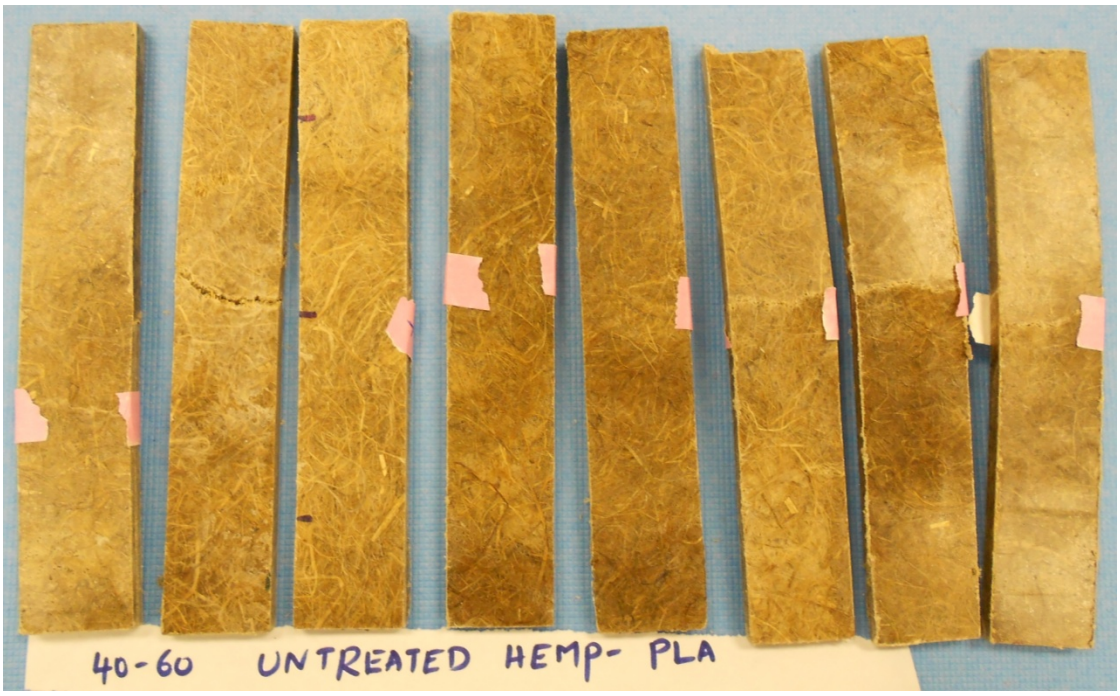
40-60 UNTREATED HEMP- PLA

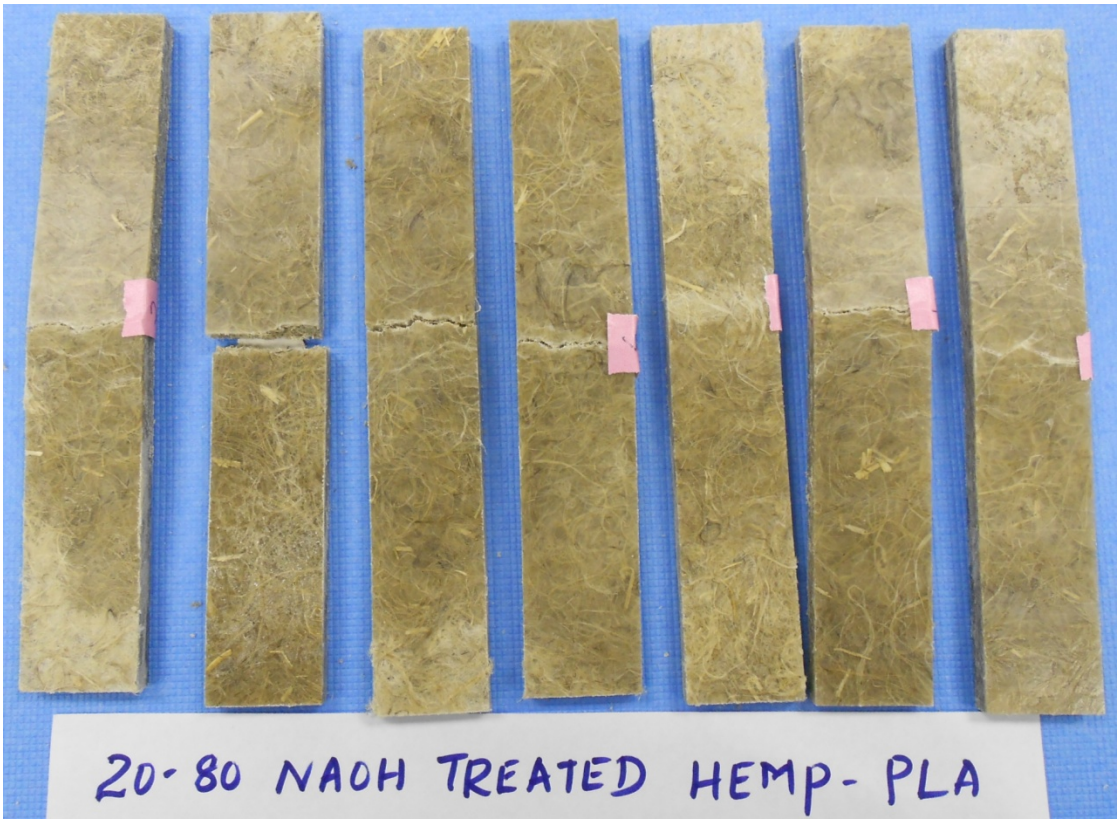
20-80 NAOH TREATED HEMP- PLA

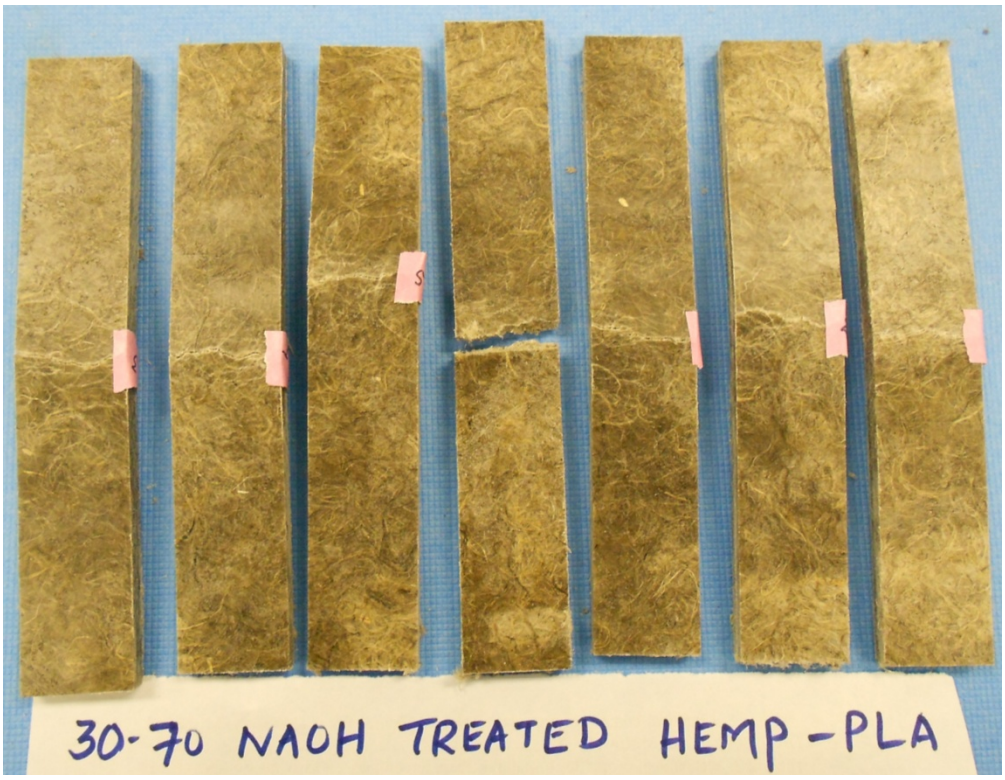
30-70 NAOH TREATED HEMP-PLA


40-60 NAOH TREATED HEMP-PLA


20-80 SILANE TREATED HEMP-PLA


30-70 SILANE TREATED HEMP-PLA

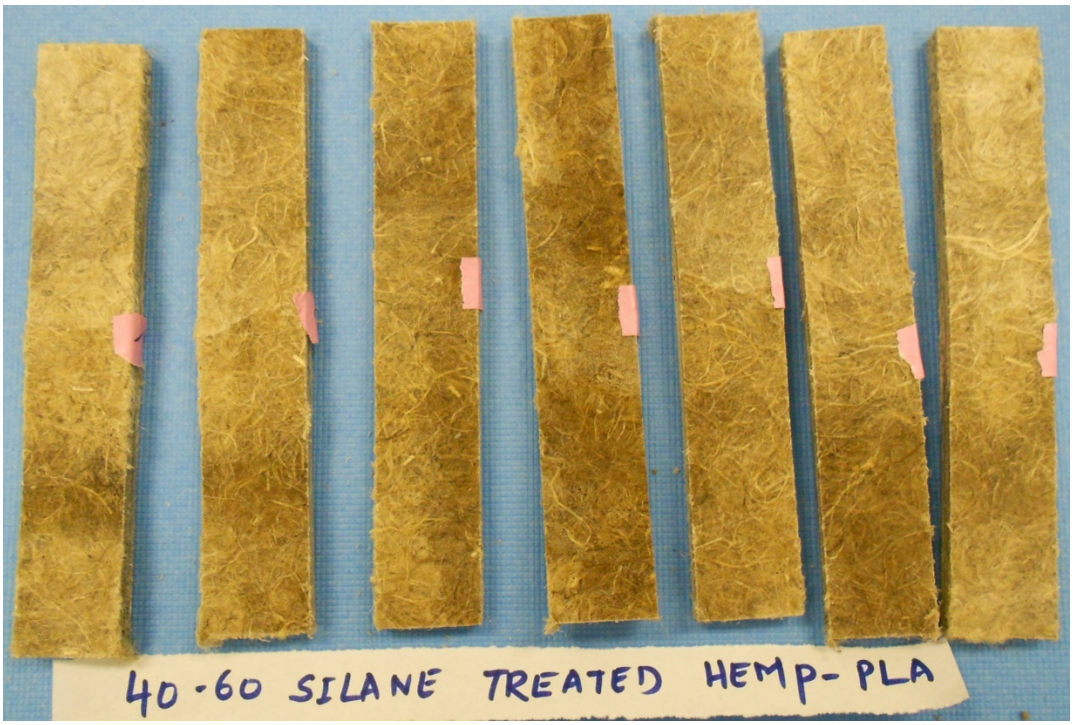
40-60 SILANE TREATED HEMP-PLA

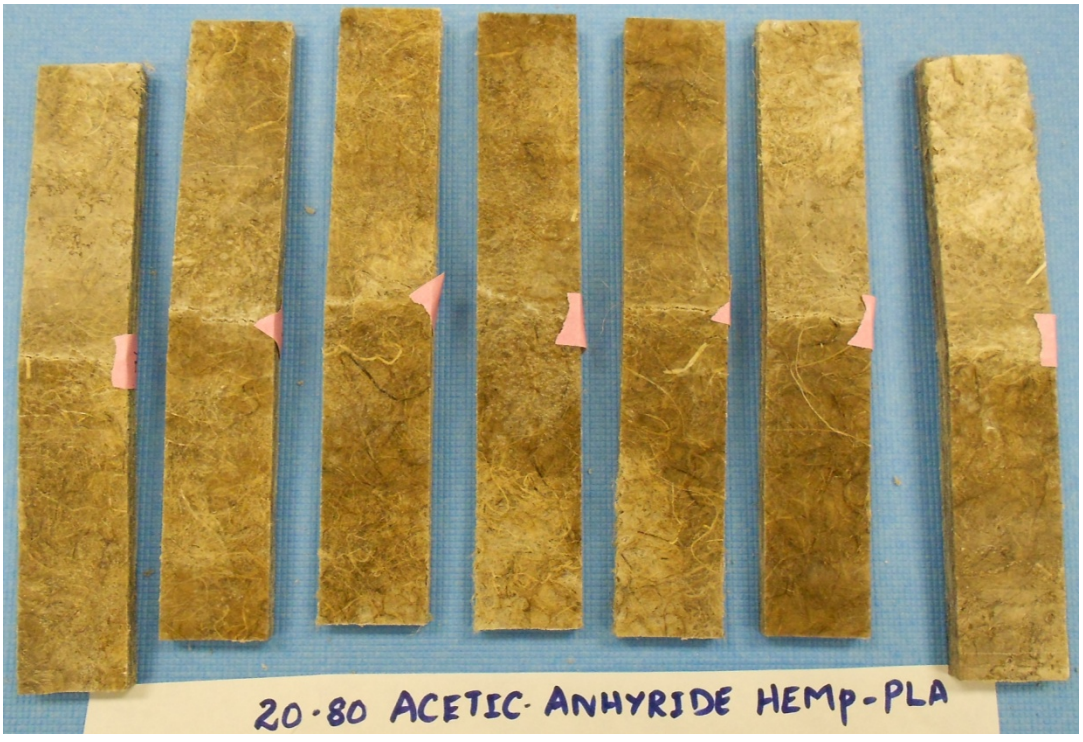
20-80 ACETIC ANHYRIDE HEMP-PLA

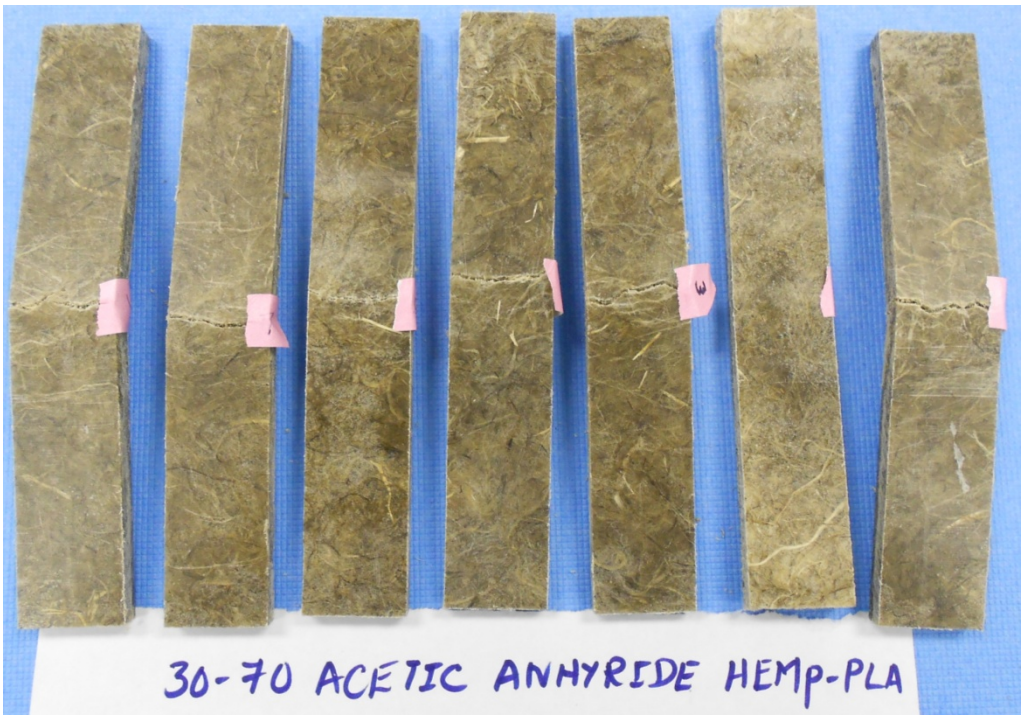

**** The pink tape on the specimen marks the point where fracture was observed.

APPENDIX D: STRESS-STRAIN CURVES FOR ALL THE FLEXURAL TESTED SPECIMENS

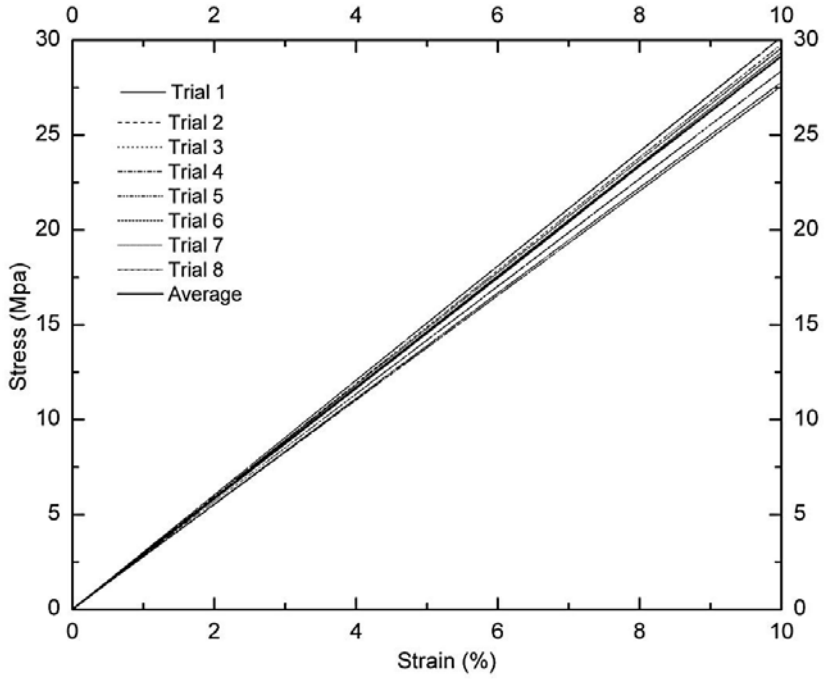

Stress strain curves for 20-80 untreated hemp-PLA composite specimens

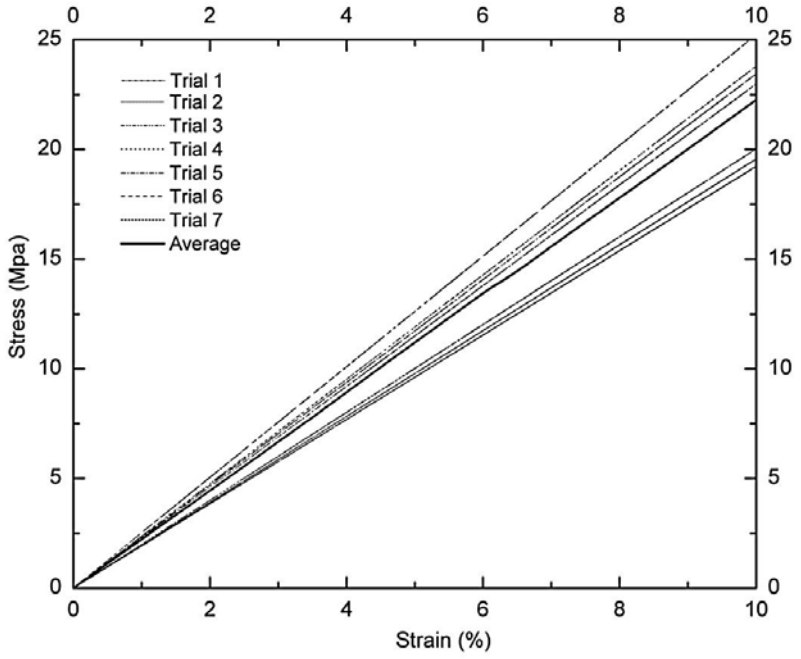

Stress strain curves for 30-70 untreated hemp-PLA composite specimens

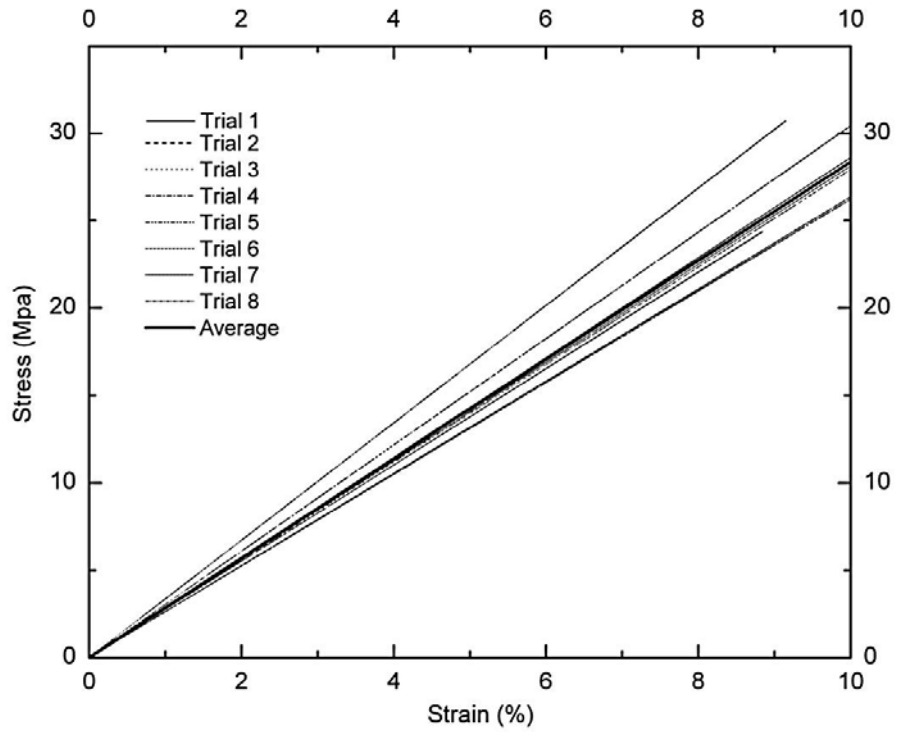

Stress strain curves for 40-60 untreated hemp-PLA composite specimens

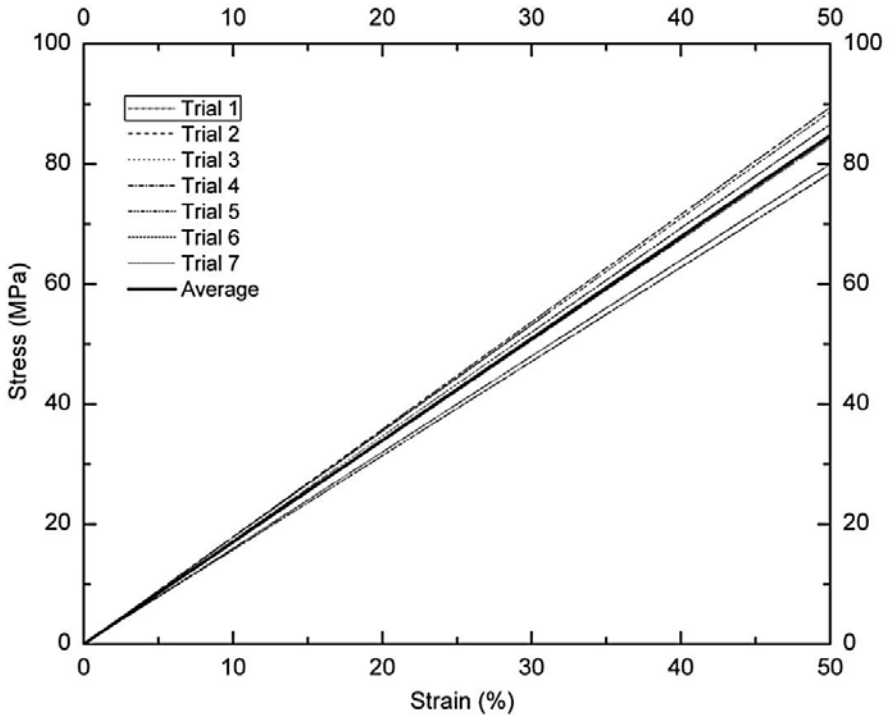

Stress strain curves for 20-80 NaOH treated hemp-PLA composite specimens

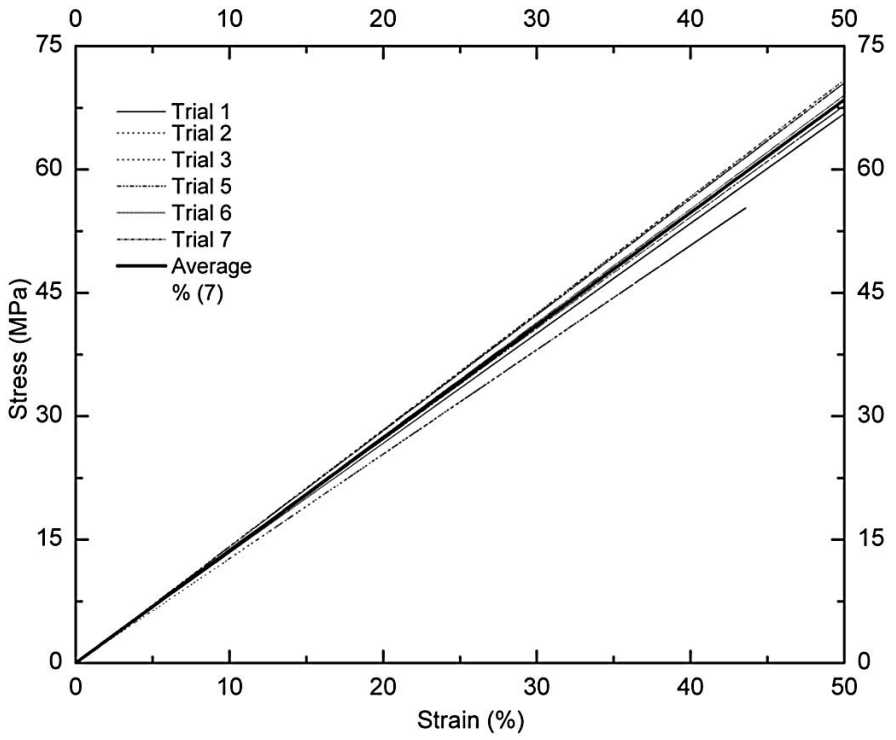

Stress strain curves for 30-70 NaOH treated hemp-PLA composite specimens

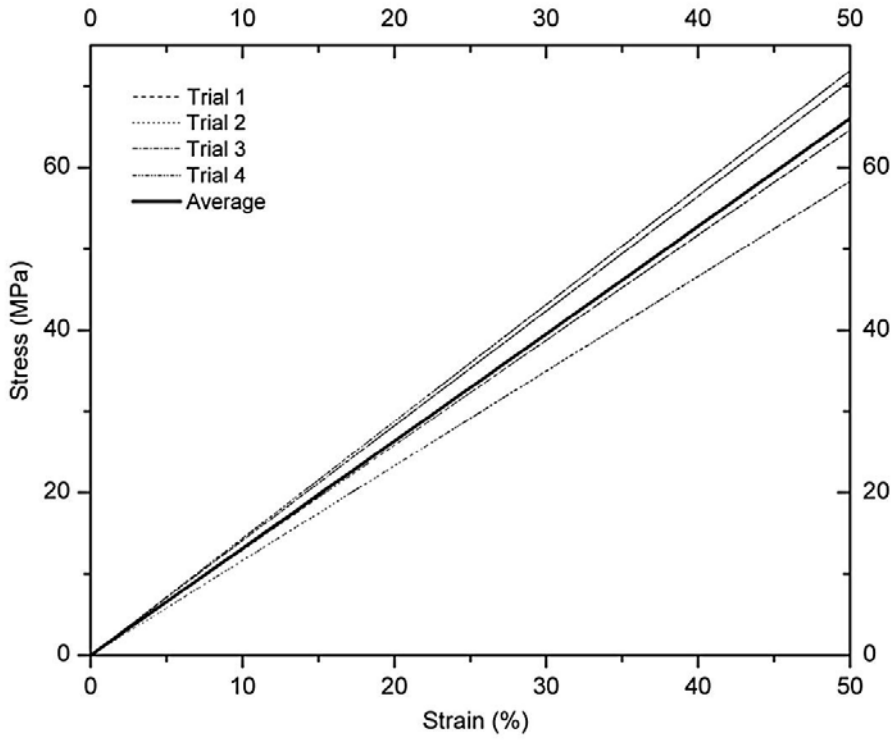

Stress strain curves for 40-60 NaOH treated hemp-PLA composite specimens

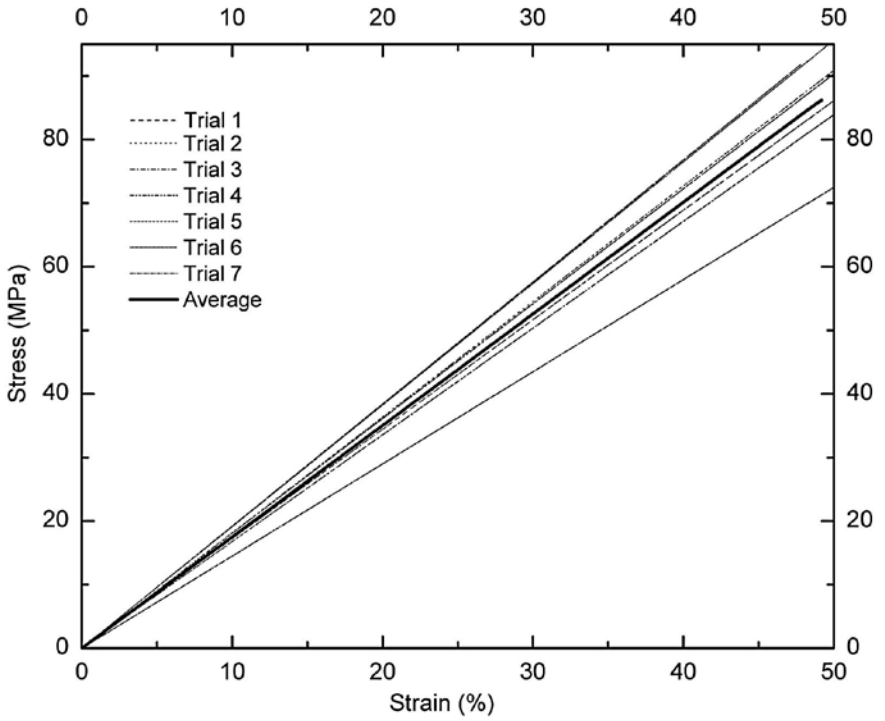

Stress strain curves for 20-80 Silane treated hemp-PLA composite specimens

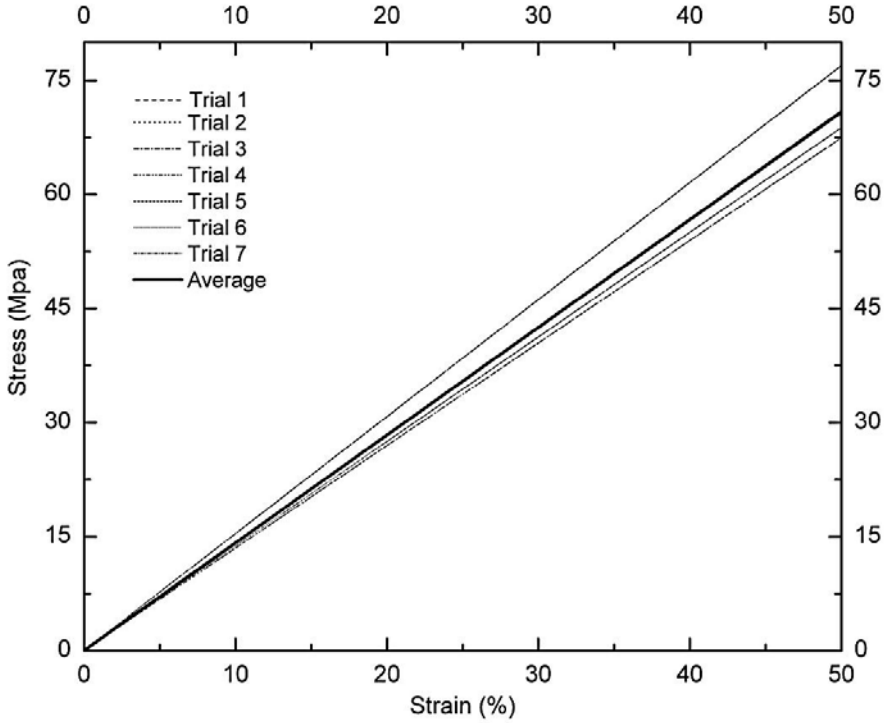

Stress strain curves for 30-70 Silane treated hemp-PLA composite specimens

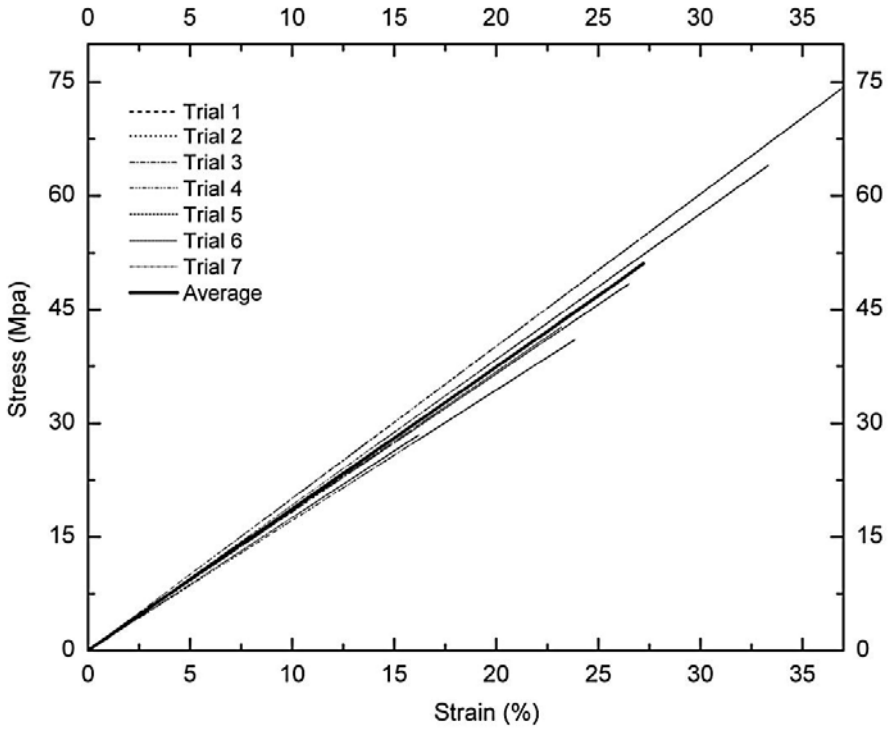

Stress strain curves for 40-60 Silane treated hemp-PLA composite specimens

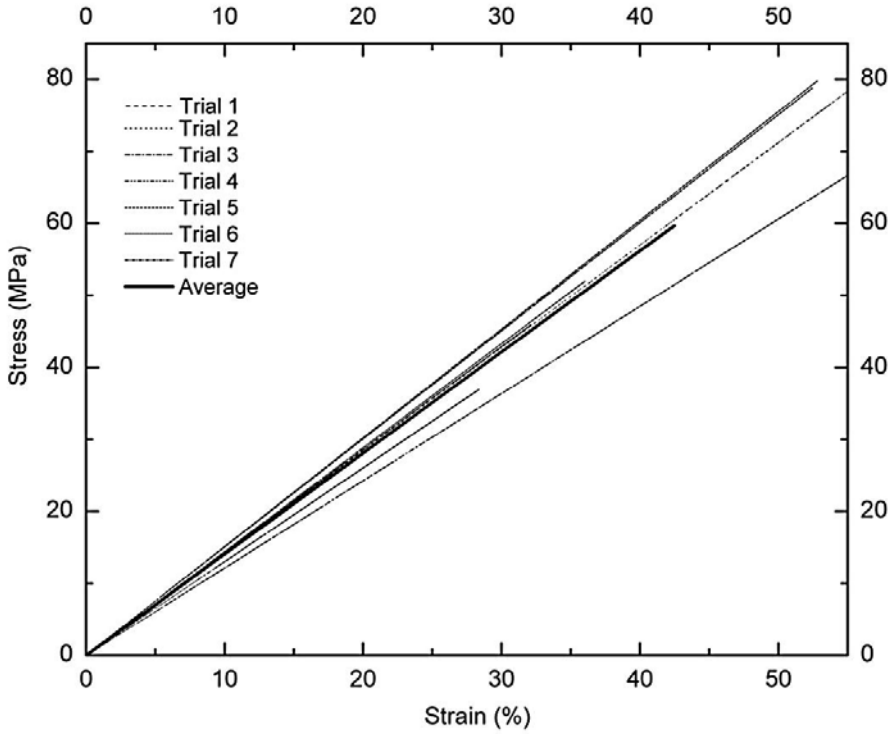

Stress strain curves for 20-80 Acetic anhydride treated hemp-PLA composite specimens

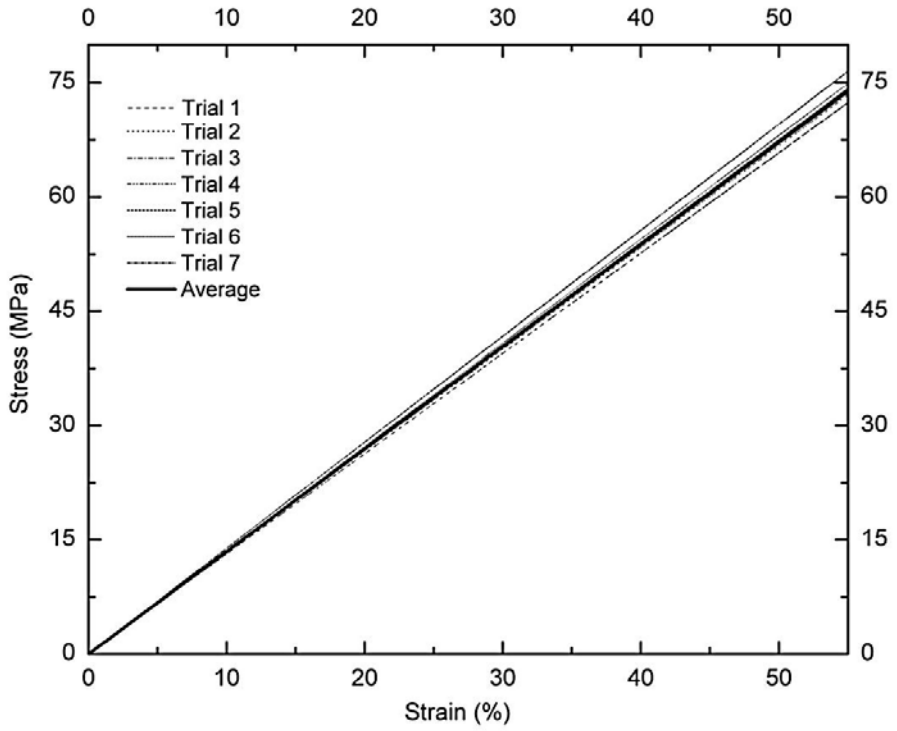

Stress strain curves for 30-70 Acetic anhydride treated hemp-PLA composite specimens

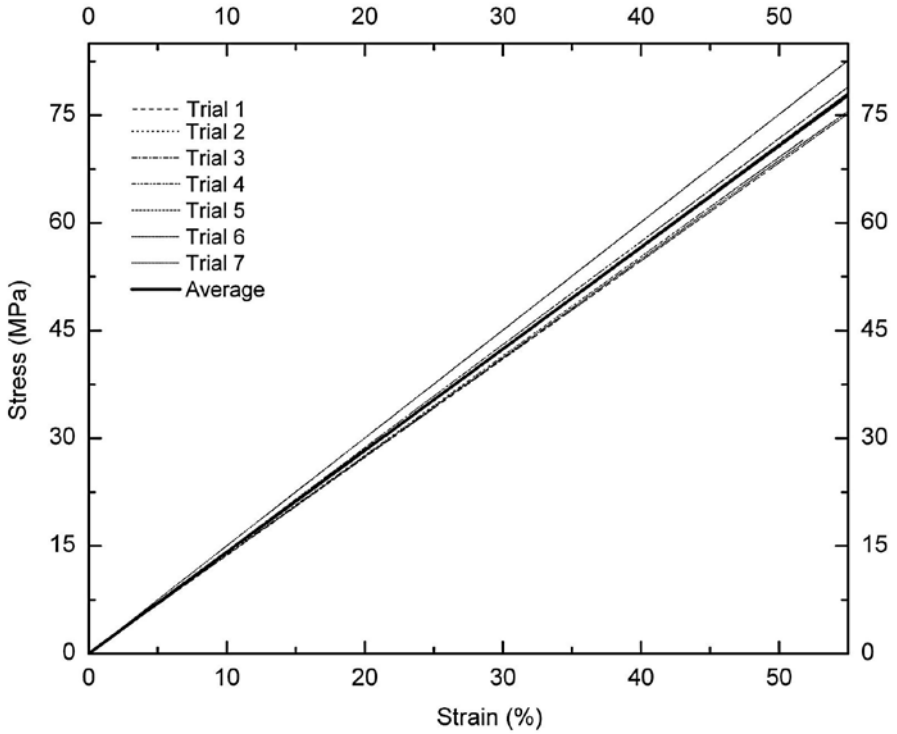

Stress strain curves for 40-60 Acetic anhydride treated hemp-PLA composite specimens

APPENDIX E: STRESS-STRAIN CURVES FOR ALL SINGLE FIBER TESTED SPECIMENS

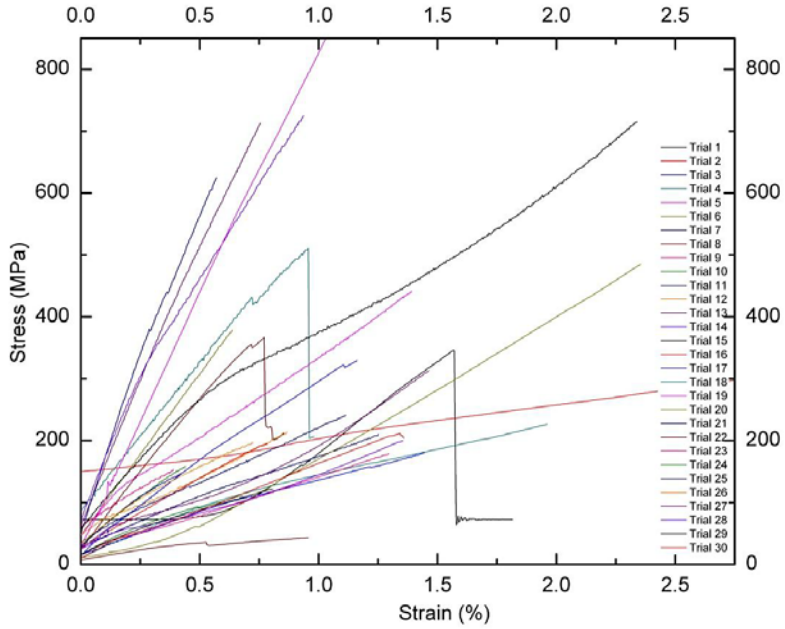

Stress-strain curves for untreated hemp fiber specimens

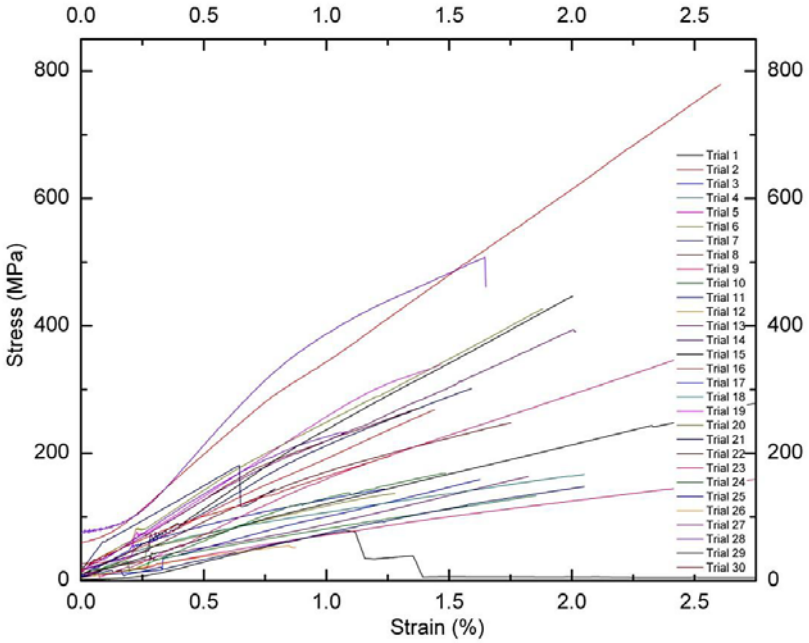

Stress-strain curves for NaOH treated hemp fiber specimens

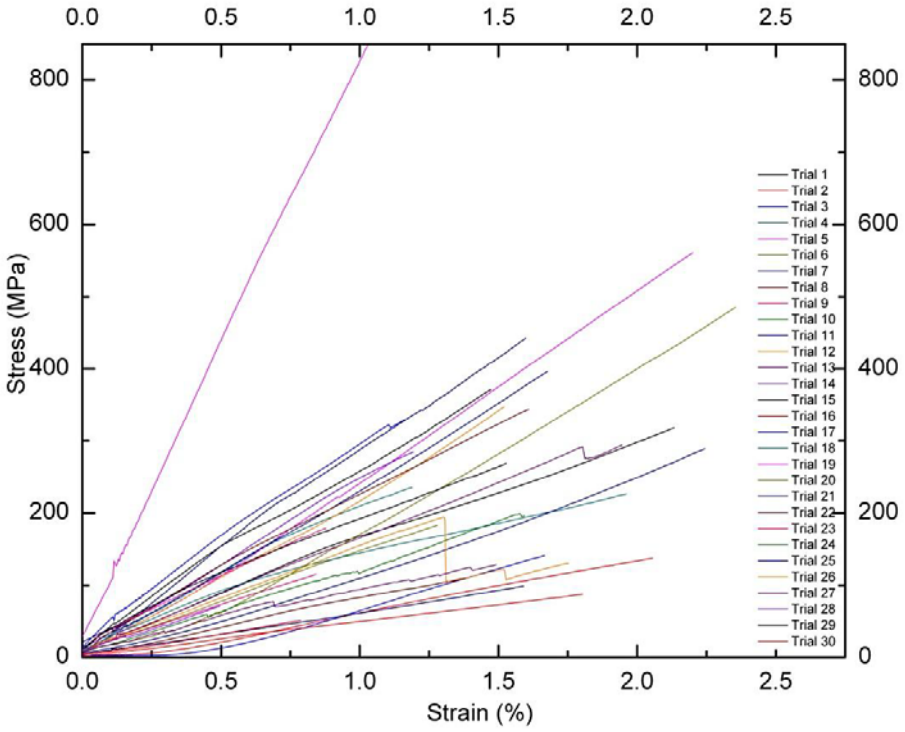

Stress-strain curves for silane treated hemp fiber specimens

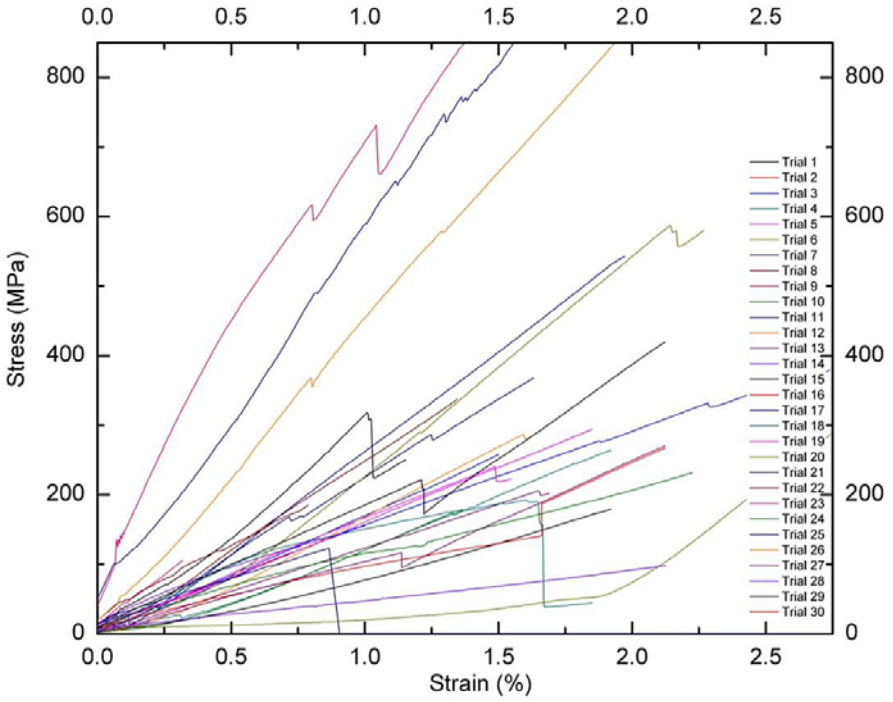

Stress-strain curves for acetic anhydride treated hemp fiber specimens